






This is to certify that the
thesis entitled

A STUDY OF THE VIBRATIONAL SPECTRA OF THE PARTIALLY
DEUTERATED POLYCRYSTALLINE ETHYLENES

presented by
Richard G. Whitfield

has been accepted towards fulfillment
of the requirements for
PH.D. degree in Chemistry


Major professor

Date September 26, 1977

A STUDY OF THE VIBRATIONAL SPECTRA OF THE
PARTIALLY DEUTERATED POLYCRYSTALLINE ETHYLENES

By

Richard G. Whitfield

A DISSERTATION

Submitted to

Michigan State University

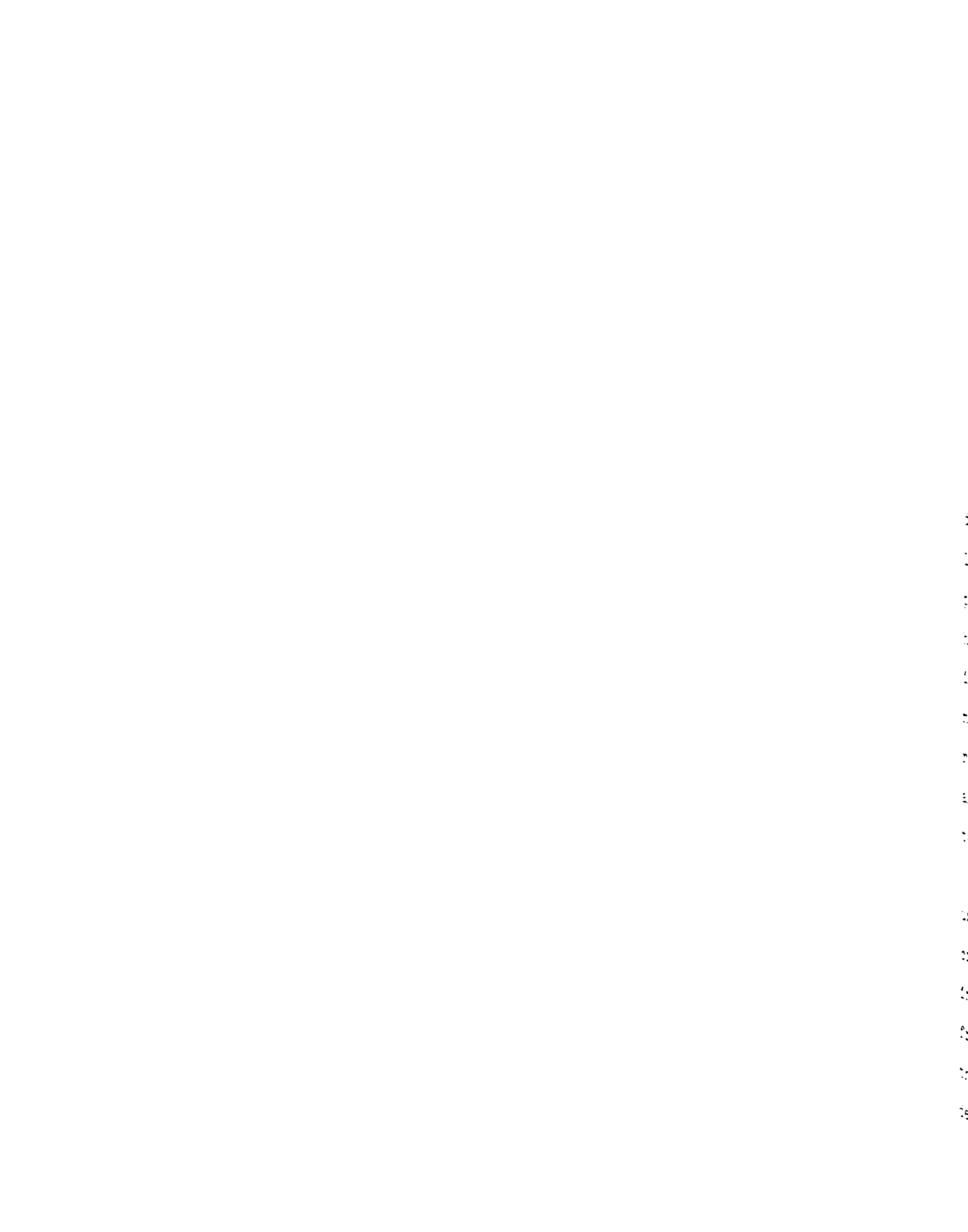
in partial fulfillment of the requirements

for the degree of

DOCTOR OF PHILOSOPHY

Department of Chemistry

1977



ABSTRACT

A STUDY OF THE VIBRATIONAL SPECTRA OF THE
PARTIALLY-DEUTERATED POLYCRYSTALLINE ETHYLENES

By

Richard G. Whitfield

The mid-infrared and Raman spectra of the partially-deuterated ethylenes: C_2H_3D , *cis*- $C_2H_2D_2$, *trans*- $C_2H_2D_2$, 1,1- $C_2H_2D_2$ and C_2HD_3 , and of dilute mixed crystals of the partially-deuterated ethylenes in C_2H_4 and in one another have been observed in order to gain more insight into the intermolecular force field of ethylene and those of molecular crystals in general. Information concerning the retention of the symmetry of the parent (C_2H_4) crystal as an "effective" symmetry in the partially-deuterated crystals has also been obtained.

Various sets of atom-atom interaction potentials were used to calculate the lattice frequencies of the C_2H_4 crystal using recent single crystal x-ray data. The best interaction potential was used to calculate the lattice frequencies of the partially-deuterated ethylenes, assuming the crystal structure and symmetry is unchanged by the deuteration. By comparing the observed and calculated

frequencies, it was determined that the lattice modes of these crystals can be described in the virtual-crystal limit. Consistent with the virtual-crystal theory, mutual exclusion was retained for the lattice modes of these disordered solids and slight changes in the relative intensities of the observed librations were noted. An attempt to observe the missing optically active translation of C_2H_4 in the far-infrared is described. It is suggested to be at 35 cm^{-1} .

The dilute-mixed crystal spectra were observed to determine the number of energetically-inequivalent orientations which exist for the partially-deuterated ethylenes in a lattice site; this reveals information concerning the "effective" site symmetry of the host, and was determined to be C_1 in every case, consistent with the predictions of the virtual-crystal approximations. A comparison of the spectra of the partially-deuterated ethylenes in a C_2H_4 host and in each other indicates that the intermolecular interactions of the crystal are myopic; that is, the number of orientational components and the energies of these components are independent of the isotopic nature of the host crystal.

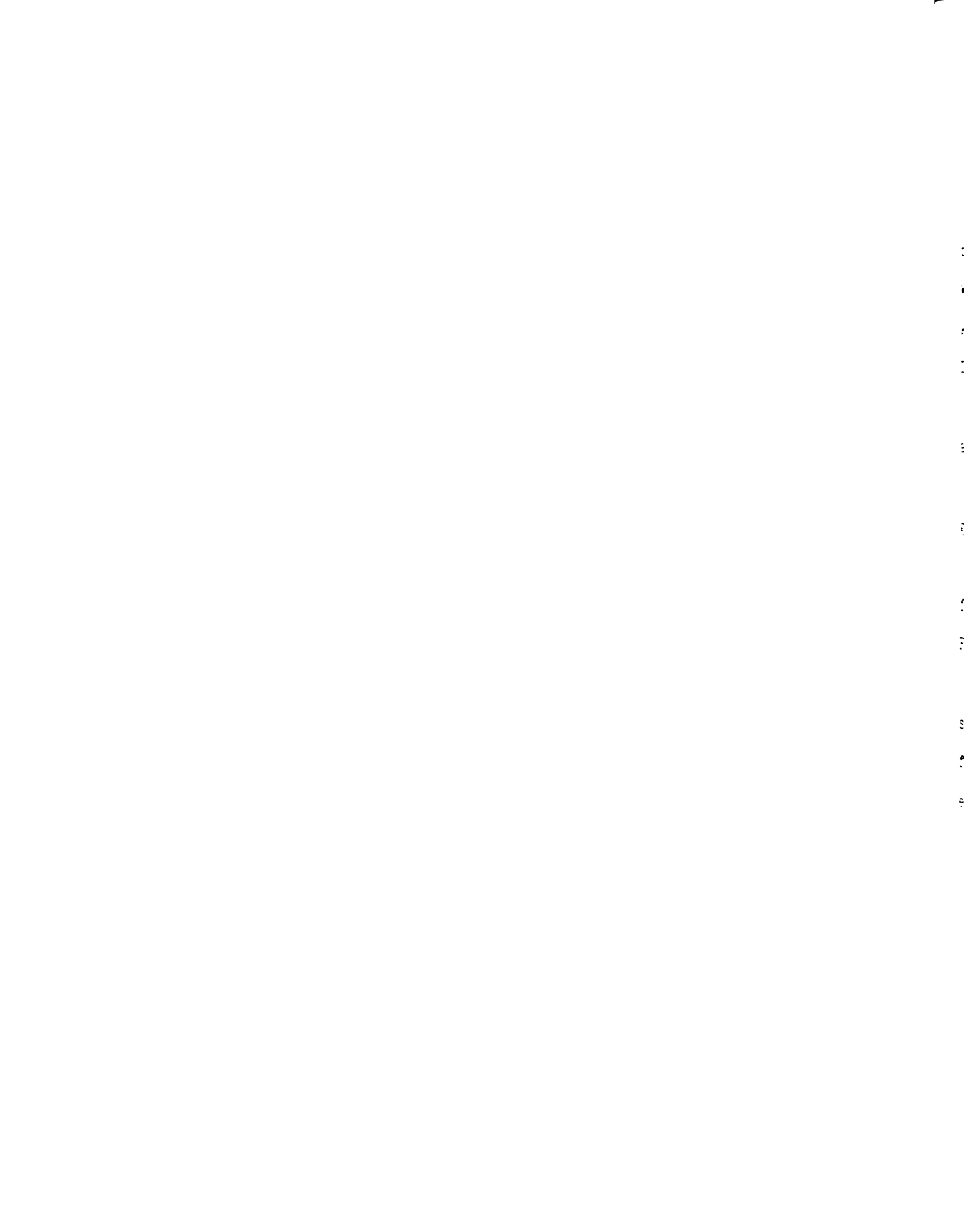
Due to the "effective" C_1 site symmetry, the internal modes of cis-ethylene- d_2 and 1,1-ethylene- d_2 can be treated in the pure crystal exciton formalism and are quite similar to the internal mode spectra of C_2H_4 and C_2D_4 . However,

the internal modes of ethylene-d₁, trans-ethylene-d₂ and ethylene-d₃ must be treated as mixed-crystal modes. The coherent potential approximation was used to calculate the band structures of the internal modes of these "mixed" crystals, and the computational results were used to assist in the assignment of the components of the C₂H₃D, trans-C₂H₂D₂, and C₂HD₃ bands. The assignments of ν_4 and ν_8 of C₂HD₃ have been switched. This assignment interchange is supported by observed static field energy shifts in the crystal, and by the calculated potential energy distributions of these modes. Mutual exclusion was observed for the internal modes of trans-C₂H₂D₂; this further supports the concept of "effective" C₁ site symmetry for the partially-deuterated ethylene crystals.

to

Pat

. . . to grow in our love and understanding of each
other, our fellow man, and God.



ACKNOWLEDGMENTS

I want to first thank my wife, Pat, for her loving patience and understanding without which this work would have never been completed, and my son, Ricky, for keeping her distracted during the preparation of this Dissertation.

I also want to thank my parents for their interest and understanding during the course of my education.

The interest and advice of Dr. Leroi during my graduate career is greatly appreciated.

I wish to acknowledge the financial support received from Michigan State University and the National Science Foundation.

Finally, I wish to thank my fellow group members, students, faculty and staff of the Department of Chemistry for making my stay here a very pleasant and memorable experience.

Page 1
Page 2
Page 3
Page 4
Page 5
Page 6
Page 7
Page 8
Page 9
Page 10

Page 11
Page 12
Page 13
Page 14
Page 15

Page 16

TABLE OF CONTENTS

Chapter	Page
LIST OF TABLES	vi
LIST OF FIGURES.	ix
I. INTRODUCTION	1
II. GENERAL THEORY	5
A. The Vibrations of Molecular Crystals	5
B. The Crystal Structure of Ethylene	8
C. Theoretical Treatments of Molecular-Crystal Vibrations	14
Calculation of the Crystal- Vibrational Frequencies.	14
The Exciton Formalism.	20
D. The Orientational Effect-Crystals of the Partially-Deuterated Ethylenes.	28
III. EXPERIMENTAL	34
IV. THE LATTICE VIBRATIONS OF THE PARTIALLY-DEUTERATED ETHYLENES	41
A. Phonons in Disordered Solids	41
B. The Potential Function of Ethylene	45
C. The Librations of the Partially- Deuterated Ethylenes	51
D. Conclusions.	64
V. PROBING THE SITE SYMMETRY OF THE PARTIALLY- DEUTERATED ETHYLENES VIA THE ORIENTATIONAL EFFECT	66

Chapter	Page
A. Theory	66
B. Experimental	69
C. Conclusions.	100
VI. THE INTERNAL MODES OF THE PARTIALLY- DEUTERATED ETHYLENES	102
A. Introduction	102
B. The Internal Modes of cis-C ₂ H ₂ D ₂ and 1,1-C ₂ H ₂ D ₂	106
C. Excitons of Binary Mixed Molecular Crystals-The Coherent Potential Approximation.	121
D. The Internal Modes of C ₂ H ₃ D, trans- C ₂ H ₂ D ₂ and C ₂ HD ₃	
E. Comparison of the Internal Modes of the Polycrystalline Ethylenes.	155
F. Conclusions.	164
VII. DISCUSSION AND SUGGESTIONS FOR FUTURE WORK	166
APPENDIX A	170
APPENDIX B	191
APPENDIX C	199
REFERENCES	202

LIST OF TABLES

Table		Page
1	Lattice parameters ^a and orientation matrix ^b for the ethylene crystal	9
2	Structural parameters for free ethylene molecule and molecule in crystal	11
3	Correlation table for solid ethylene	12
4	Partially-deuterated ethylenes- Analytical data.	35
5	Nonbonded-potential parameters, where $V_{1j} = B \exp(-Cr) - Ar^{-6} + Er^{-1}$	46
6	The observed and calculated lattice frequencies (cm^{-1}) of solid ethylene	48
7	The observed and calculated lattice frequencies (cm^{-1}) of solid ethylene-d ₄	49
8	The calculated and observed librational frequencies of the ethylenes.	56
9	The crystal normal coordinates of the librations of the isotopic ethylene crystals.	58
10	Perturbation strengths of the ethylene librations.	62

Table	Page	
11	The number of orientational components for the partially-deuterated ethylenes in a C_1 or C_1 site	68
12	Observed frequencies of C_2H_3D funda- mentals in 1% C_2H_3D/C_2H_4	70
13	Observed frequencies of cis- $C_2H_2D_2$ fundamentals in 1% cis- $C_2H_2D_2/C_2H_4$	71
14	Observed frequencies of trans- $C_2H_2D_2$ fundamentals in 1% trans- $C_2H_2D_2/C_2H_4$. . .	72
15	Observed frequencies of 1,1- $C_2H_2D_2$ fundamentals in 1% 1,1- $C_2H_2D_2/C_2H_4$	73
16	Observed frequencies of C_2HD_3 funda- mentals in 1% C_2HD_3/C_2H_4	74
17	Observed frequencies of C_2H_3D funda- mentals in 4% $C_2H_3D/cis-C_2H_2D_2$	92
18	Observed frequencies of C_2H_3D funda- mentals in 1% $C_2H_3D/trans-C_2H_2D_2$	93
19	Observed frequencies of C_2H_3D funda- mentals in 4% $C_2H_3D/1,1-C_2H_2D_2$	94
20	Observed frequencies of C_2H_3D funda- mentals in 1% C_2H_3D/C_2HD_3	95
21	Observed frequencies of 1,1- $C_2H_2D_2$ fundamentals in 1,1- $C_2H_2D_2/C_2HD_3$	96
22	Observed frequencies of C_2HD_3 funda- mentals in 1% C_2HD_3/C_2H_3D	97

Table	Page	
23	Calculated harmonic C-13 shifts (cm^{-1}) from the C-12 frequencies	104
24	Internal fundamental frequencies (cm^{-1}) of cis- $\text{C}_2\text{H}_2\text{D}_2^a$	108
25	Internal fundamental frequencies (cm^{-1}) of 1,1- $\text{C}_2\text{H}_2\text{D}_2^*$	110
26	Orientalional Splittings (cm^{-1}) of $\text{C}_2\text{H}_3\text{D}$, trans- $\text{C}_2\text{H}_2\text{D}_2$ and C_2HD_3^a	129
27	Internal fundamental frequencies (cm^{-1}) of $\text{C}_2\text{H}_3\text{D}^*$	132
28	Internal fundamental frequencies (cm^{-1}) of trans- $\text{C}_2\text{H}_2\text{D}_2^*$	134
29	Internal fundamental frequencies (cm^{-1}) of C_2HD_3^*	136
30	Potential-energy distribution and calculated frequencies of the out- of-plane vibrations of C_2HD_3	157
31	Gas-to-mixed crystal shifts of the ethylenes (cm^{-1}) ^a	160
32	Bandwidths of the ethylenes (cm^{-1}).	163

LIST OF FIGURES

Figure		Page
1	The crystal structure of ethylene (from Reference 23)	9
2	The structure of an arbitrary exciton band of ethylene.	26
3	The molecular structure and point group symmetries of the ethylenes	29
4	The orientations of C_2H_3D in C_2H_4 (C_2HD_3 in C_2D_4)	31
5	The Raman lattice region of C_2H_3D , $1,1-C_2H_2D_2$ and C_2HD_3 . The peaks marked with an asterisk are laser fluorescence lines.	52
6	The Raman lattice region of cis- $C_2H_2D_2$, $1,1-C_2H_2D_2$ and trans- $C_2H_2D_2$. The peak marked with an asterisk is a laser fluorescence line	53
7	The highest frequency Raman lattice modes of $1,1-C_2H_2D_2$	54
8	The calculated librational frequencies versus the number of deuteriums	60
9	The observed librational frequencies versus the number of deuteriums. The D_2 frequencies are the mean of the	

Figure	Page
	cis-C ₂ H ₂ D ₂ , 1,1-C ₂ H ₂ D ₂ and trans- C ₂ H ₂ D ₂ values 61
10	Part of the infrared spectrum of 10% C ₂ H ₃ D/C ₂ H ₄ ; ν ₁ , ν ₄ and ν ₃ of C ₂ H ₃ D 76
11	Part of the infrared spectrum of 1% C ₂ H ₃ D/C ₂ H ₄ ; ν ₇ and ν ₁₂ of C ₂ H ₃ D 77
12	Part of the infrared spectrum of 1% cis-C ₂ H ₂ D ₂ /C ₂ H ₄ ; ν ₁ , ν ₇ and ν ₁₀ of cis-C ₂ H ₂ D ₂ 78
13	Part of the infrared spectrum of 1% trans-C ₂ H ₂ D ₂ /C ₂ H ₄ ; ν ₄ and ν ₁₂ of trans-C ₂ H ₂ D ₂ 79
14	Part of the Raman spectrum of 1% trans-C ₂ H ₂ D ₂ /C ₂ H ₄ ; ν ₁ and ν ₃ of trans-C ₂ H ₂ D ₂ 80
15	Part of the infrared spectrum of 1% 1,1-C ₂ H ₂ D ₂ /C ₂ H ₄ ; ν ₁ , ν ₇ and ν ₁₂ of 1,1-C ₂ H ₂ D ₂ 81
16	Part of the infrared spectrum of 1% C ₂ HD ₃ /C ₂ H ₄ ; ν ₅ , ν ₄ and ν ₁₂ of C ₂ HD ₃ . . . 82
17	Part of the Raman spectrum of 4% C ₂ H ₃ D/cis-C ₂ H ₂ D ₂ ; ν ₃ and ν ₁₂ of C ₂ H ₃ D. The peak marked with an asterisk is assigned as ν ₃ of

Figures	Page
	trans-C ₂ H ₂ D ₂ 84
18	Part of the infrared spectrum of 4% C ₂ H ₃ D/cis-C ₂ H ₂ D ₂ ; ν_1 , ν_4 and ν_3 of C ₂ H ₃ D. The peak marked with an asterisk is assigned as ν_4 of trans-C ₂ H ₂ D ₂ 85
19	Part of the infrared spectrum of 1% C ₂ H ₃ D/trans-C ₂ H ₂ D ₂ ; ν_7 and ν_{12} of C ₂ H ₃ D 86
20	Part of the infrared spectrum of 4% C ₂ H ₃ D/1,1-C ₂ H ₂ D ₂ ; ν_1 , ν_4 and ν_3 of C ₂ H ₃ D 87
21	Part of the Raman spectrum of 4% C ₂ H ₃ D/1,1-C ₂ H ₂ D ₂ ; ν_3 and ν_7 of C ₂ H ₃ D 88
22	Part of the infrared spectrum of 1% C ₂ H ₃ D/C ₂ HD ₃ ; ν_7 and ν_{12} of C ₂ H ₃ D 89
23	Part of the infrared spectrum of 1,1-C ₂ H ₂ D ₂ /C ₂ HD ₃ ; ν_1 , ν_7 and ν_{12} of 1,1-C ₂ H ₂ D ₂ 90
24	Part of the infrared spectrum of 1% C ₂ HD ₃ /C ₂ H ₃ D; ν_4 and ν_8 of C ₂ HD ₃ 91

Figure	Page
25	Internal modes of cis-C ₂ H ₂ D ₂ ; ν_3 and ν_{12} . The peak marked with an asterisk is attributed to C-13 substituted molecules. 114
26	Internal modes of cis-C ₂ H ₂ D ₂ ; ν_{10} and ν_9 . The peak marked with an asterisk is attributed to C-13 substituted molecules 116
27	Internal modes of 1,1-C ₂ H ₂ D ₂ ; ν_1 and ν_2 . The peak marked with an asterisk is attributed to H ₂ ¹² C = ¹³ CD ₂ 117
28	Internal modes of 1,1-C ₂ H ₂ D ₂ ; ν_4 and ν_{10} . The peak marked with an asterisk is attributed to H ₂ ¹³ C= ¹² CD ₂ 118
29	Mixed crystal exciton band structure. 122
30	Internal modes of C ₂ H ₃ D; ν_{12} and ν_{10} . The peak marked with an asterisk is attributed to H ₂ ¹² C = ¹³ CHD 138
31	Internal modes of C ₂ H ₃ D; ν_3 and ν_4 139
32	Internal modes of trans-C ₂ H ₂ D ₂ ; ν_1 and ν_{12} 140

Figure		Page
33	Internal modes of trans-C ₂ H ₂ D ₂ ; ν ₅ and ν ₄	141
34	ν ₈ , trans-C ₂ H ₂ D ₂ , calculated and observed Raman band. The peak marked with an asterisk is attributed to C-13 substituted molecules.	142
35	ν ₇ , trans-C ₂ H ₂ D ₂ , calculated and observed infrared band.	143
36	ν ₁ region of C ₂ HD ₃ in the infrared and Raman spectra	144
37	ν ₆ region of C ₂ HD ₃ in the infrared and Raman spectra	145



CHAPTER I

INTRODUCTION

It has been known for several decades that information concerning the symmetry and the intermolecular-force field of a molecular crystal can be obtained from a study of its vibrational spectrum.¹⁻³ The amount of experimental and theoretical work in this area has increased tremendously since the first papers on the subject were published by Hornig⁴ and by Winston and Halford⁵ in the late 1940's. This increase was triggered by the availability of laser sources for Raman spectroscopy and by the tremendous increase in the sophistication of far-infrared instrumentation. Much of the initial work involved attempts to develop a qualitative understanding of the vibrational spectra. The first attempt at a quantitative interpretation was reported in 1962 when Dows attempted to calculate the vibrational spectrum of the ethylene crystal.⁶ The early work in vibrational spectroscopy of molecular crystals has been reviewed by Dows⁷ (internal modes) and Schnepf⁸ (lattice modes). The more recent work in this area has been discussed by Bailey,⁹ Pawley¹⁰ and by Schnepf and Jacobi.¹¹

Many researchers have concentrated their efforts on the study of molecular crystals of simple aliphatic hydrocarbons, such as acetylene,¹² ethylene¹³ and ethane,¹⁴

2

3

4

5

6

7

8

9

10

11

12

13

14

15

16

17

18

19

20

21

22

23

24

25

26

27

28

and on the simple aromatic hydrocarbons, such as benzene¹⁵ and naphthalene,¹⁶ in order to develop a more quantitative understanding of the intermolecular forces of the solids. These simple hydrocarbons are particularly attractive for study because they usually crystallize with two or four molecules per unit cell, and only three types of atom-atom interactions need be considered. This greatly simplifies the model calculations which are done to aid in the understanding of the vibrational spectrum of a molecular crystal.

Crystalline ethylene has evoked the interest of molecular spectroscopists since the mid-infrared spectrum was reported by Dows in 1962,^{6,17} who pointed out that the molecules in the unit cell could be oriented in two different ways in the crystal with the same resultant spectroscopic activity and pattern. Later the far-infrared^{18,19} and Raman²⁰ spectra of ethylene were reported, but no additional evidence for either crystal structure was indicated. In 1973, Elliott and Leroi reported the Raman spectrum of ethylene and ethylene-d₄,¹³ and were able to determine which intermolecular force field parameters for hydrocarbon crystals best fit the observed librational frequencies of ethylene. By means of oriented gas model intensity calculations, they determined that only one of Dows' two proposed crystal structures properly predicted the observed relative

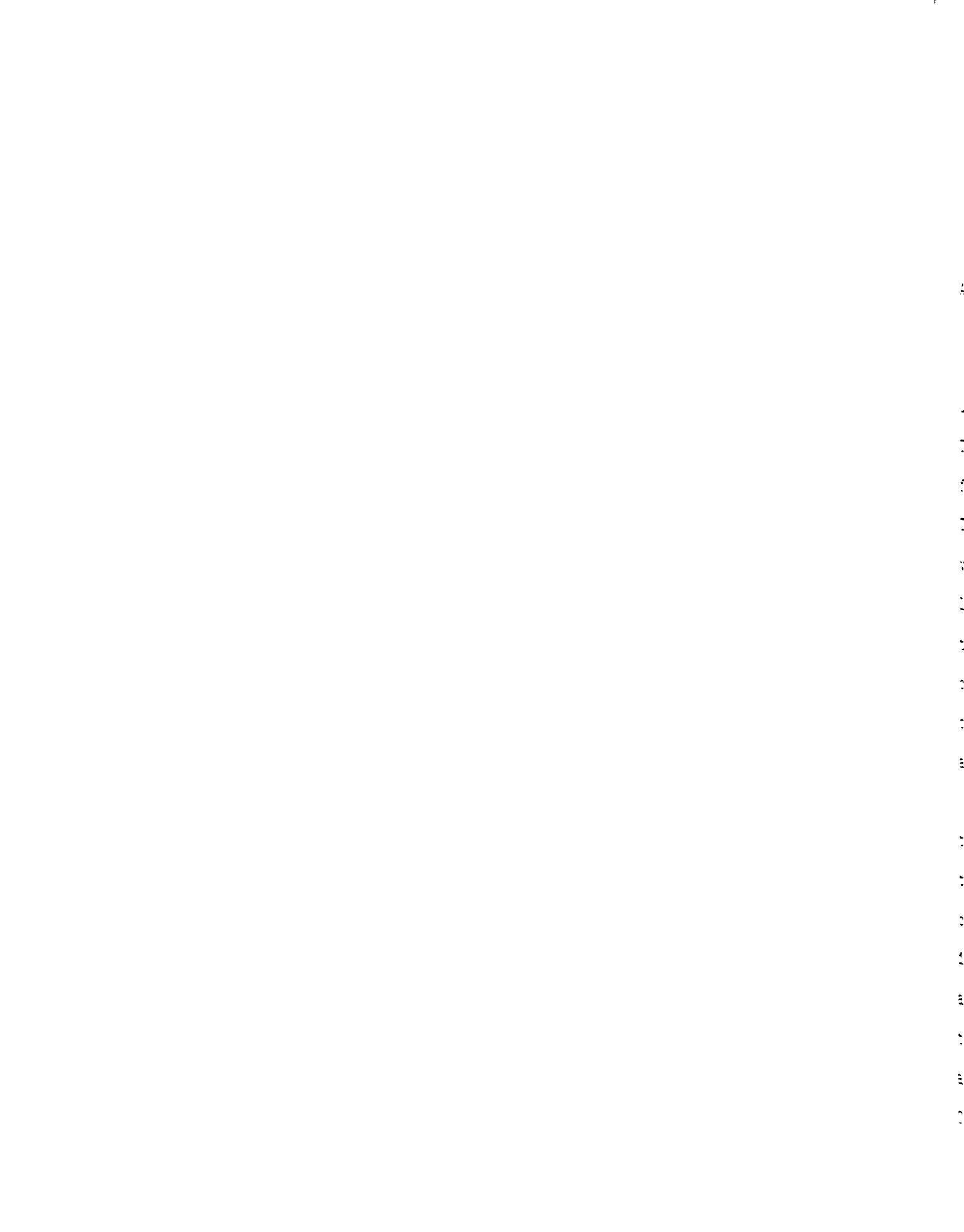


intensities. This determination has recently been confirmed by X-ray²¹ and neutron-diffraction^{22,23} experiments.

This study of the vibrational spectra of the partially-deuterated ethylene crystals; $-d_1$, $asym-d_2$, $cis-d_2$, $trans-d_2$ and $-d_3$, has been conducted to gain more insight into the intermolecular force field of ethylene and those of molecular crystals in general. Information concerning the retention of the symmetry of the parent (C_2H_4) crystal as an "effective" symmetry in the partially-deuterated crystals has also been obtained. This provides some understanding of the effects of perturbations, due to disorder in the crystals, on the intermolecular-force fields of molecular crystals. The retention of symmetry enables interpretation of the spectra of some of the partially-deuterated ethylenes on the basis of pure-crystal theories, while a mixed-crystal treatment is required for the others.

Duncan et al. have recently measured the mid-infrared spectrum of polycrystalline ethylene- $1,1-d_2$ to determine the C-13 isotopic shifts.²⁴ The C-13 shifts were used in a determination of the intramolecular force field of ethylene. This is the only previous vibrational study of a partially-deuterated ethylene crystal of which this author is aware. The only previous vibrational study on an entire series of isotopic crystals of which this

author is aware involved the partially-deuterated benzene crystals; however, orientational and resonance effects precluded a general interpretation of the experimental spectra.²⁵⁻²⁷



CHAPTER II

GENERAL THEORY

A. The Vibrations of Molecular Crystals

The vibrational motions of molecular crystals are usually classified as either internal or external modes. The internal vibrations are essentially those of the free molecule, subject to solid state interactions. The external or lattice modes are entirely solid state vibrations, and are characterized by their low frequency. Lattice vibrations can be further classified into translations, which arise from changes in the position of the centers of gravity of the molecules, or librations, which originate from the torsional motions of the molecules about their centers of gravity.

This separation of the internal and external vibrations of the crystal can usually be accomplished because the intermolecular forces - the forces between the molecules in the crystal - are usually much weaker than the intramolecular forces - the forces between the atoms of a given molecule. This difference in the magnitude of the forces is often used as a criterion for defining a molecular crystal as opposed to an atomic crystal. Coupling between the internal and external vibrations



can often be ignored if the lowest internal frequency is much higher than the highest lattice frequency.

A molecular crystal has $3LpN$ degrees of freedom, where L is the number of unit cells, p is the number of molecules in the unit cell, and N is the number of atoms per molecule. Therefore, if the translational symmetry of the crystal lattice is ignored, the vibrational spectra would be expected to consist of $3pN$ bands each consisting of L closely spaced frequencies. If the translational symmetry of the crystal is accounted for, the $\underline{k} = 0$ selection rule is introduced where \underline{k} is the wave vector of a vibrational excitation traveling through the crystal with wave-like character. This selection rule greatly simplifies the optical spectrum since \underline{k} must be zero for a molecular crystal vibration to be observed via infrared or Raman spectroscopy; this arises because the interaction of a vibrational excitation with a photon requires a conservation of momentum. Therefore, the value of the wave vector of the vibrational excitation must be of the same order as that of the probing radiation.

The vibrational excitations of a molecular crystal may be classified as either phonons or excitons. The lattice vibrations, which are delocalized excitations in the crystal, are referred to as phonons, and the internal vibrations, which are localized, are usually classified as excitons because they can be conveniently



treated theoretically in the same formalism as electronic excitons. Since the phonons are delocalized, they are quite dependent on \underline{k} whereas the localized excitons are only slightly dependent on \underline{k} .¹

In order that $\underline{k} = 0$, the displacements of corresponding atoms in different unit cells must be precisely in phase and thus the $\underline{k} = 0$ selection rule reduces the number of vibrational degrees of freedom that need be considered to $3pN$. Three of these degrees of freedom are the acoustic modes, whose frequencies are zero at $\underline{k} = 0$. (The acoustic modes correspond to the pure translation of the entire lattice in space.) The other degrees of freedom are accounted for by the librations ($3p$), translations ($3p-3$) and the internal vibrations $(3N-6)p$, assuming a non-linear molecule. Therefore, if no degeneracies are present, the internal region would consist of $3N-6$ vibrations, each showing p components usually referred to as Davydov or factor-group components.

The symmetry of the crystal can be used to predict the number and activity of the vibrational modes of a molecular solid. Lattice dynamicists are often concerned with several types of symmetry groups in the crystal. These include the space group, the unit cell or factor-group, and the site-group symmetries of the lattice. The space group entirely describes the symmetry relations among the molecules in the lattice, including

the translational symmetry. The space-group symmetry minus the translational symmetry is the unit-cell symmetry which describes the symmetry relations of the molecules in the unit cell. The site group describes the symmetry of the static field in which the molecules in the crystal interact. A correlation^{28,29} of the free-molecule symmetry with the site and unit cell symmetries provides information concerning the activity and number of Davydov components of the molecular-crystal modes.

B. The Crystal Structure of Ethylene

The crystal structure of ethylene has been the subject of some question since an early X-ray investigation³¹ which reported the carbon positions and lattice parameters. Recent neutron-diffraction studies^{22,23} on powdered samples of C_2D_4 and a single crystal X-ray²¹ study of C_2H_4 have determined solid ethylene to be monoclinic, under normal pressures, with space group $P12_1/n1$ (C_{2h}^5) with two molecules per unit cell occupying sites of C_1 symmetry. The crystal structure of ethylene is shown in Figure 1. Table 1 lists the lattice parameters and the orientational matrix for an ethylene molecule centered at the origin and initially oriented with the C=C bond along the crystallographic x-axis and the hydrogens in the xz-plane. a, b and c correspond with Figure 1. α , β and γ are the angles

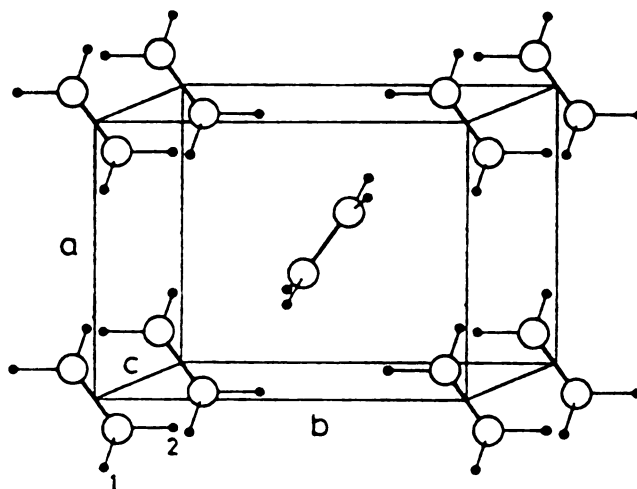


Figure 1. The crystal structure of ethylene (from Reference 23).

Table 1. Lattice parameters^a and orientation matrix^b for the ethylene crystal.

$a = 4.626\text{\AA}$	$b = 6.620\text{\AA}$	$c = 4.067\text{\AA}$
$\alpha = 90^\circ$	$\beta = 94.39^\circ$	$\gamma = 90^\circ$

	x	y	z
a	0.8002	-0.5965	0.0665
b	-0.5448	-0.6752	0.4972
c	0.2517	0.4340	0.8651

^aFrom Reference 21.

^bSee text.

between b and c, a and c, and between a and b, respectively. The orientation matrix arises from rotations about the x, y and z axes by angles of -57.3° , 36.6° and 4.8° , respectively. The bond lengths, bond angles, and the changes caused by deuteration of the free molecule, and of the molecule in the crystal, are given in Table 2. H(1) and H(2) correspond to the hydrogens labeled 1 and 2 in Figure 1. The δ 's are the reductions in bond lengths caused by deuteration.

An orientationally disordered phase (II) of solid ethylene, which occurs at high pressure, has recently been discovered by Ligthart²³ using nuclear magnetic resonance spectroscopy. However, the current investigation is not concerned with the vibrational spectra of this phase.

The correlation table for solid ethylene (phase I) is given in Table 3. Twelve doublets, six of which are Raman active and six of which are infrared active, are predicted for the internal modes. Six Raman-active librations and three infrared-active translations are expected in the lattice region. The vibrational spectra of ethylene and ethylene-d₄ have been found to be consistent with these predictions, except that only two of the three infrared-active translations have been observed.^{13,17,19}

Table 2. Structural parameters for free ethylene molecule and molecule in crystal.

	Gas ^a	Crystal ^b
r(C=C)	1.3384Å	1.314Å
r(C-H(1))	1.0870Å	0.992Å
r(C-H(2))	1.0870Å	1.021Å
α(H(1)-C-H(2))	117.37°	116.8°
α(H(1)-C=C)	121.32°	121.2°
α(H(2)-C=C)	121.32°	122.0°
δr(C-H) [H-D]	0.0016Å	
δr(C=C) [H-D]	0.00012Å per D	
δα(H-C-H) [H ₂ -D ₂]	0.0°	

^aGas values and δ's from Reference 30.

^bFrom Reference 21.

Table 3. Correlation table for solid ethylene.

	Molecular-Point Group D_{2h}	Site Group C_1	Factor Group C_{2h}^a
ν_1, ν_2, ν_3	$3A_g$	$6A_g$	$6A_g$ R
ν_5, ν_6	$2B_{1g}$		$6B_g$ R
ν_8	$1B_{2g}$		
(Internal Modes)			
ν_4	$1A_u$	$6A_u$	$6A_u$ IR
ν_7	$1B_{1u}$		$6B_u$ IR
ν_9, ν_{10}	$2B_{2u}$		
ν_{11}, ν_{12}	$2B_{3u}$		

Table 3. Continued.

	Molecular-Point Group D_{2h}	Site Group C_1	Factor Group C_{2h}^a
	(External Modes)		
(R_z)	$1B_{1g}$	$3A_g$	$3A_g$ R
(R_y)	$1B_{2g}$		$3B_g$ R
(R_x)	$1B_{3g}$		
(T_z)	$1B_{1u}$	$3A_u$	$3A_u$ IR (1-acoustic)
(T_y)	$1B_{2u}$		$3B_u$ IR (2-acoustic)
(T_x)	$1B_{3u}$		

^aR and IR indicate Raman and infrared activity, respectively.

1

2

3

4

5

6

7

8

9

10

11

12

13

14

15

16

17

18

19

20

21

22

23

24

25

26

27

28

C. Theoretical Treatments of Molecular-Crystal Vibrations

In the next two sections, theoretical descriptions of the vibrations of molecular crystals are discussed. The first section is a semiclassical treatment which follows closely the work of Taddei, et al.³² This was used to calculate the external frequencies of the ethylenes as discussed in Chapter IV. The second section will review the vibrational exciton formalism^{7,15,33,34} for pedagogical reasons. This will aid in the discussion of the experimental data for both pure and dilute-mixed crystals of the partially-deuterated ethylenes.

A coherent-potential calculation will also be utilized for the internal modes of some of the partially-deuterated ethylenes. However, this is discussed in Appendix B and in Chapter VI along with the internal mode data.

Calculation of the Crystal-Vibrational Frequencies

The potential energy, V , of a molecular crystal is described as a sum of the intramolecular potential, V_0 and the intermolecular potential, V_e ,

$$V = V_0 + V_e. \quad (1)$$

The infinitesimal linear displacements of the atoms for

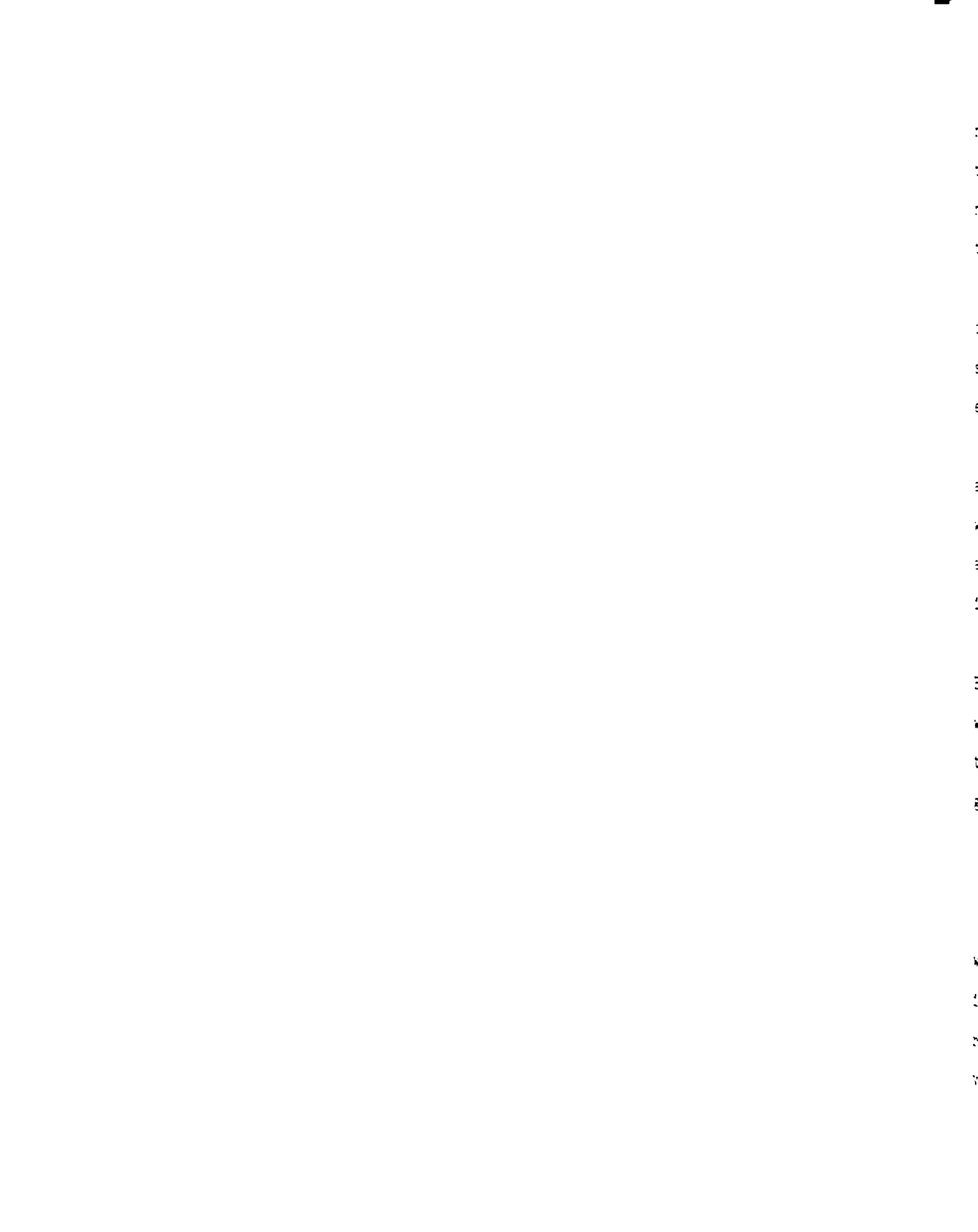
a crystal large enough to fulfill the cyclic boundary conditions are described in terms of the normal coordinates of the molecule and the external displacement coordinates. The external displacement coordinates are the Eckart-mass weighted translational and torsional coordinates.

As usual in the vibrational problem, the potential energy is expanded in a Taylor series about the equilibrium configuration in terms of the internal and external coordinates,

$$V = \frac{1}{2} \sum_{\alpha\mu} \left[\sum_n^{3N-6} (\partial^2 V_0 / \partial Q_{\alpha\mu n}^2)_0 Q_{\alpha\mu n}^2 + \sum_{\beta\nu} \sum_{\ell m}^{3N} (\partial^2 V_e / \partial Q_{\alpha\mu\ell} \partial Q_{\beta\nu m})_0 Q_{\alpha\mu\ell} Q_{\beta\nu m} \right], \quad (2)$$

where μ, ν label the molecule in the unit cell, α, β the unit cell and ℓ, m, n the internal and external coordinates. The first $(3N-6)$ coordinates are the internal coordinates for a non-linear molecule, where N is the number of atoms in the molecule, and the last 6 coordinates are the external coordinates.

The force field of the free molecule may be assumed for V_0 if the equilibrium configuration of the molecule is not deformed severely in the crystal. However, V_0 , in principle, should be the intramolecular potential



relative to the molecule in the site, and uncoupled to the other molecules in the crystal. It should also be noted that the second derivative of V_0 is with respect to the internal normal modes only.

The form of V_e will be specified later. The second derivative of the intermolecular potential is with respect to both the internal normal coordinates and the external coordinates.

The first derivatives of the potential have been assumed to be zero. These terms may be excluded only when the interaction terms between the intramolecular and intermolecular potentials are actually negligible and if V_e has a minimum for the observed crystal structure.

The problem may now be simplified by expressing Equation (2) in terms of the symmetry coordinates $Q_{\nu m}(\underline{k})$, which belong to the irreducible representation of the translational group. These symmetry coordinates are given as follows:

$$Q_{\nu m}(\underline{k}) = L^{-1/2} \sum_{\beta} Q_{\beta \nu m} \exp(2\pi i \underline{k} \cdot \underline{r}_{\beta}), \quad (3)$$

where L is the number of unit cells in the crystal, \underline{r}_{β} is a vector connecting the β^{th} cell with an arbitrary reference cell which will be labeled 1, and \underline{k} is the wave vector.

The potential energy in terms of these symmetry

coordinates becomes,

$$V = \frac{1}{2} \sum_{\underline{k}} \sum_{\mu} \left[\sum_{\ell} \lambda_{\ell} Q_{\mu\ell}^*(\underline{k}) Q_{\mu\ell}(\underline{k}) \right. \\ \left. + \sum_{\nu} \sum_{\ell m} F_{\mu\ell}^{\nu m}(\underline{k}) Q_{\mu\ell}^*(\underline{k}) Q_{\nu m}(\underline{k}) \right] \quad (4)$$

where,

$$F_{\mu\ell}^{\nu m}(\underline{k}) = \sum_{\beta} (\partial^2 V_e / \partial Q_{1\mu\ell} \partial Q_{\beta\nu m})_0 \exp(-2\pi i \underline{k} \cdot \underline{r}_{\beta}) \quad (5)$$

The frequencies of the crystal normal modes $\nu(\underline{k})$ can be calculated by solving the secular equation:

$$|F_{\mu\ell}^{\nu m}(\underline{k}) - [\lambda(\underline{k}) - \lambda_{\ell}] \delta_{\mu\nu} \delta_{\ell m}| = 0 \quad (6)$$

where $\lambda(\underline{k}) = 4\pi^2 \nu^2(\underline{k})$ and $\lambda_{\ell} = 4\pi^2 \nu_{\ell}^2$. The ν_{ℓ} 's are the frequencies of the free molecule.

The form of the intermolecular potential, V_e , must be specified in order to evaluate $F_{\mu\ell}^{\nu m}(\underline{k})$. When only pairwise interactions are considered,

$$V_e = \frac{1}{2} \sum_{\alpha\beta} \sum_{\mu\nu} V_{\alpha\mu}^{\beta\nu}, \quad (7)$$

where $V_{\alpha\mu}^{\beta\nu}$ is the pairwise interaction between the μ^{th} molecule in the α^{th} unit cell and the ν^{th} molecule in

the β^{th} unit cell.

Therefore, in terms of Equation (7),

$$F_{\mu\ell}^{\nu m}(\underline{k}) = \sum_{\substack{\beta \\ \beta \neq 1 \\ \text{if } \mu=\nu}} \exp(-2\pi i \underline{k} \cdot \underline{r}_{\beta}) \left(\frac{\partial^2 V_{1\mu}^{\beta\nu}}{\partial Q_{1\mu\ell} \partial Q_{\beta\nu m}} \right)_0 \quad (8)$$

$$+ \delta_{\mu\nu} \sum_{\substack{\beta \\ \beta \neq 1 \\ \text{if } \mu=\tau}} \sum_{\tau} \left(\frac{\partial^2 V_{1\mu}^{\beta\tau}}{\partial Q_{1\mu\ell} \partial Q_{1\mu\tau}} \right)_0.$$

The molecule-molecule interactions are usually expressed as a sum of atom-atom interactions,

$$V_e = \frac{1}{2} \sum_{\alpha\beta} \sum_{\mu\nu} \sum_{ij} V_{\alpha\mu i}^{\beta\nu j} (r_{\alpha\mu i}^{\beta\nu j}), \quad (9)$$

where i labels the atoms belonging to molecule $\alpha\mu$, and j the atoms belonging to molecule $\beta\nu$. $r_{\alpha\mu i}^{\beta\nu j}$ is the interatomic distance between atoms i and j . In terms of the atom-atom potentials the second derivatives in Equation (8) are given by,

$$\left(\frac{\partial^2 V_{1\mu}^{\beta\nu}}{\partial Q_{1\mu\ell} \partial Q_{\beta\nu m}} \right)_0 = \sum_{ij} \left\{ \left(\frac{\partial^2 V_{ij}}{\partial r_{ij}^2} \right)_0 \left(\frac{\partial r_i}{\partial Q_{1\mu\ell}} \cdot \frac{\partial r_{ij}}{\partial r_i} \right) \right. \quad (10)$$

$$\left. \left(\frac{\partial r_j}{\partial Q_{\beta\nu m}} \cdot \frac{\partial r_{ij}}{\partial r_j} \right) + \left(\frac{\partial V_{ij}}{\partial r_{ij}} \right)_0 \left[\left(\frac{\partial r_i}{\partial Q_{1\mu\ell}} \cdot \frac{\partial r_{ij}}{\partial r_i} \right) \left(\frac{\partial r_j}{\partial Q_{\beta\nu m}} \cdot \frac{\partial r_{ij}}{\partial r_j} \right) \right] \right\}$$

where for simplicity, $V_{\alpha\mu 1}^{\beta\nu j}$ and $r_{\alpha\mu 1}^{\beta\nu j}$ have been replaced by V_{1j} and r_{1j} , respectively. Taddei et al.^{32,35,36} have pointed out that traditionally the second term in the above equation has been ignored. They have calculated the lattice frequencies of benzene with and without this term. The inclusion of this term caused a 2% to 15% reduction in the calculated lattice frequencies, showing the effect of this term is not negligible. It has therefore been included in the calculation of the ethylene lattice frequencies.

The solution of the above secular equation (Equation (6)) will give the frequencies of the crystal normal modes over the entire Brillouin region. However, k selection rules make it possible to observe only the optically-active vibrations, that is vibrations with $k = 0$, via infrared spectroscopy and Raman scattering. It should be noted that k arises from the translational symmetry of the crystal; therefore if the translational symmetry is destroyed it may no longer be a "good" quantum number.

The intermolecular potential is usually specified as the sum of molecule-molecule pairwise interactions which are expressed as a sum of atom-atom interactions. The atom-atom interaction potential for hydrocarbons is expressed as,

$$V_{ij} = A \exp(-Br_{ij}) - Cr_{ij}^{-6} \quad (11)$$

where r_{ij} is the interatomic distance between atom i of molecule α and atom j of a molecule other than α in the crystal. A , B and C are the potential constants which are obtained by refinement to other crystal properties such as heats of sublimation and crystal lattice energies.

The actual calculation of the crystal frequencies of the ethylenes were done using program TBON, a computer program written by Taddei and Bonadeo.

The Exciton Formalism

As stated above, this discussion of the exciton formalism is included to aid in a qualitative discussion of the splittings and shifts of modes in the solid state in comparison to those of the free molecule. This will also assist in the explanation of the orientational effect in the next section.

In the tight-binding limit, that is where the excited states are expressed in terms of localized excitations, the Hamiltonian for the excited states of a perfect crystal may be written as a sum of a one-site Hamiltonian, H^0 , and an intersite Hamiltonian, H^1 ,

$$H = H^0 + H^1 \quad (12)$$

where,

$$H^0 = \sum_{n=1}^N \sum_{\alpha=1}^{\sigma} H_{n\alpha}^0 \quad (13)$$

and

$$H^1 = \sum_{n\alpha \neq n'\alpha'} V_{n\alpha, n'\alpha'} \quad (14)$$

In Equations (13) and (14) n specifies the unit cell and α the site in the unit cell which is assumed to be interchange equivalent. Interchange equivalence indicates the existence of symmetry operations in the unit cell group not included in the site group which interchange the molecules in the unit cell. The $V_{n\alpha, n'\alpha'}$ terms represent the pairwise interactions of the molecules in the crystal.

$H_{n\alpha}^0$ may be considered to be the free-molecule Hamiltonian, the Hamiltonian of the distorted molecule in some averaged field of all the other molecules, or the Hamiltonian of the molecule whose nuclear framework has been distorted to match that of the molecule in the crystal. To facilitate the discussion of the orientational effect in the next section, $H_{n\alpha}^0$ is chosen to be the Hamiltonian of the free molecule. The eigenfunctions of the Hamiltonian are designated as $\psi_{n\alpha}^f$ where f designates the excited vibrational state of the crystal.

The zeroth-order crystal states, $\phi_{n\alpha}^f$, represent a localized excitation on the molecule at site $n\alpha$,

$$\phi_{n\alpha}^f = \psi_{n\alpha}^f \prod_{n'\alpha' \neq n\alpha} \psi_{n'\alpha'}^0 \quad (15)$$

It is assumed that the various f states do not mix or are premixed and that the localized excitation functions are orthogonal,

$$\langle \phi_{n\alpha}^f | \phi_{n'\alpha'}^{f'} \rangle = \delta_{nn'} \delta_{\alpha\alpha'} \delta_{ff'} \quad (16)$$

The translational symmetry of the crystal is accounted for by forming extended exciton states,

$$\phi_{\alpha}^f(\underline{k}) = L^{-1/2} \sum_{n=1}^L \exp(i\underline{k} \cdot \underline{R}_{n\alpha}) \phi_{n\alpha}^f \quad (17)$$

where $\underline{R}_{n\alpha}$ indicates the position of the α^{th} molecule in the n^{th} unit cell,

$$\underline{R}_{n\alpha} = \underline{r}_n + \underline{I}_{\alpha} \quad (18)$$

Here, \underline{r}_n is the vector from an arbitrary crystal origin to the origin of the n^{th} unit cell and \underline{I}_{α} is the vector from the origin of the unit cell to the molecule in the α^{th} site.

The \underline{k} -dependent general matrix element is,

$$\langle \phi_{\alpha}^f(\underline{k}) | H | \phi_{\alpha}^f(\underline{k}) \rangle = (\epsilon^f + D^f) \delta_{\alpha\alpha'} + L_{\alpha\alpha'}^f(\underline{k}) \quad (19)$$

where

$$\epsilon^f = \langle \phi_{n\alpha}^f | H_{n\alpha}^0 | \phi_{n\alpha}^f \rangle = \langle \psi_{n\alpha}^f | H_{n\alpha}^0 | \psi_{n\alpha}^f \rangle \quad (20)$$

is the \underline{k} -independent free molecule excitation energy, and

$$D^f = \langle \phi_{n\alpha}^f | H^1 | \phi_{n\alpha}^f \rangle = \sum_{n\alpha \neq n'\alpha'} \langle \psi_{n\alpha}^f \psi_{n'\alpha'}^0 | V_{n\alpha, n'\alpha'} | \psi_{n\alpha}^f \psi_{n'\alpha'}^0 \rangle \quad (21)$$

is the \underline{k} independent contribution to the environmental shift. The \underline{k} -dependent term has both a diagonal part,

$$L_{\alpha\alpha}^f(\underline{k}) = \sum_{n\alpha \neq n'\alpha'} \exp[i\underline{k}(\underline{R}_{n\alpha} - \underline{R}_{n'\alpha'})] \langle \phi_{n\alpha}^f | V_{n\alpha, n'\alpha'} | \phi_{n'\alpha'}^f \rangle \quad (22)$$

which represents the interactions of the translationally-equivalent molecules, and off-diagonal parts,

$$L_{\alpha\alpha'}^f(\underline{k}) = \sum_{n\alpha, n'\alpha'} \exp[i\underline{k}(\underline{R}_{n\alpha} - \underline{R}_{n'\alpha'})] \langle \phi_{n\alpha}^f | V_{n\alpha, n'\alpha'} (1 - \delta_{\alpha\alpha'}) | \phi_{n'\alpha'}^f \rangle, \quad (23)$$

which represent the interactions of the translationally-inequivalent molecules in the crystal.

The energies for a particular value of \underline{k} are found

by solving a $\sigma \times \sigma$ secular equation. For the ethylene crystal, where $\sigma = 2$, the crystal energies are given by,³⁴

$$E^f(\underline{k})^\pm = \epsilon^f + D^f + \frac{1}{2}[L_{\alpha\alpha}^f(\underline{k}) + L_{\alpha'\alpha'}^f(\underline{k})] \quad (24)$$

$$\pm \left\{ \left(\frac{1}{4} \right) [L_{\alpha\alpha}^f(\underline{k}) - L_{\alpha'\alpha'}^f(\underline{k})]^2 + |L_{\alpha\alpha'}^f(\underline{k})|^2 \right\}^{1/2},$$

where $E^f(0)^+$ and $E^f(0)^-$ are the energies of the two Davydov components for the internal vibration f . For $\underline{k} = 0$, $L_{\alpha\alpha}^f(\underline{k}) = L_{\alpha'\alpha'}^f(\underline{k}) \equiv L_{\alpha\alpha}^f$. Therefore,

$$E^{f\pm} = \epsilon^f + D^f + L_{\alpha\alpha}^f \pm L_{\alpha\alpha'}^f. \quad (25)$$

The terms of the right side of Equation (25) may be equated to the different contributions to the band structure of ethylene. D^f is the static field term and involves no resonance interaction among the molecules in the crystal. $L_{\alpha\alpha}^f$ is the resonance contribution caused by interaction of translationally-equivalent molecules and $L_{\alpha\alpha'}^f$ is the resonance contribution caused by interaction of translationally-inequivalent molecules in the crystal.

The static and resonance terms can be separated experimentally by observing the spectra of isotopic dilute mixed crystals. The complete separation of these terms is referred to as the ideal-mixed crystal; that is, there



exist no resonance interactions between the molecules in the crystal. The ideal-mixed crystal is most nearly achieved if the following requirements are fulfilled:

- a) The guest is infinitely dilute;
- b) the guest and host differ only by isotopic substitution;
- c) resonance interaction between the guest and host is negligible;
- d) the guest and host have the same dimensions and symmetry;
- e) the effects of isotopic substitution on the gas to ideal mixed crystal shift can be neglected.

Items (c) and (e) can be more easily understood by referring to Figure 2, where the structure of an arbitrary exciton band of ethylene is shown. A is the gas-to-ideal mixed crystal shift,

$$A = D^f + B. \quad (26)$$

B is referred to as the quasiresonance shift and accounts for any resonance interactions between the guest and host in the dilute-mixed crystal. The quasiresonance interaction may be assumed to be negligible if the host and guest bands are well separated. C is the resonance shifting caused by interactions of

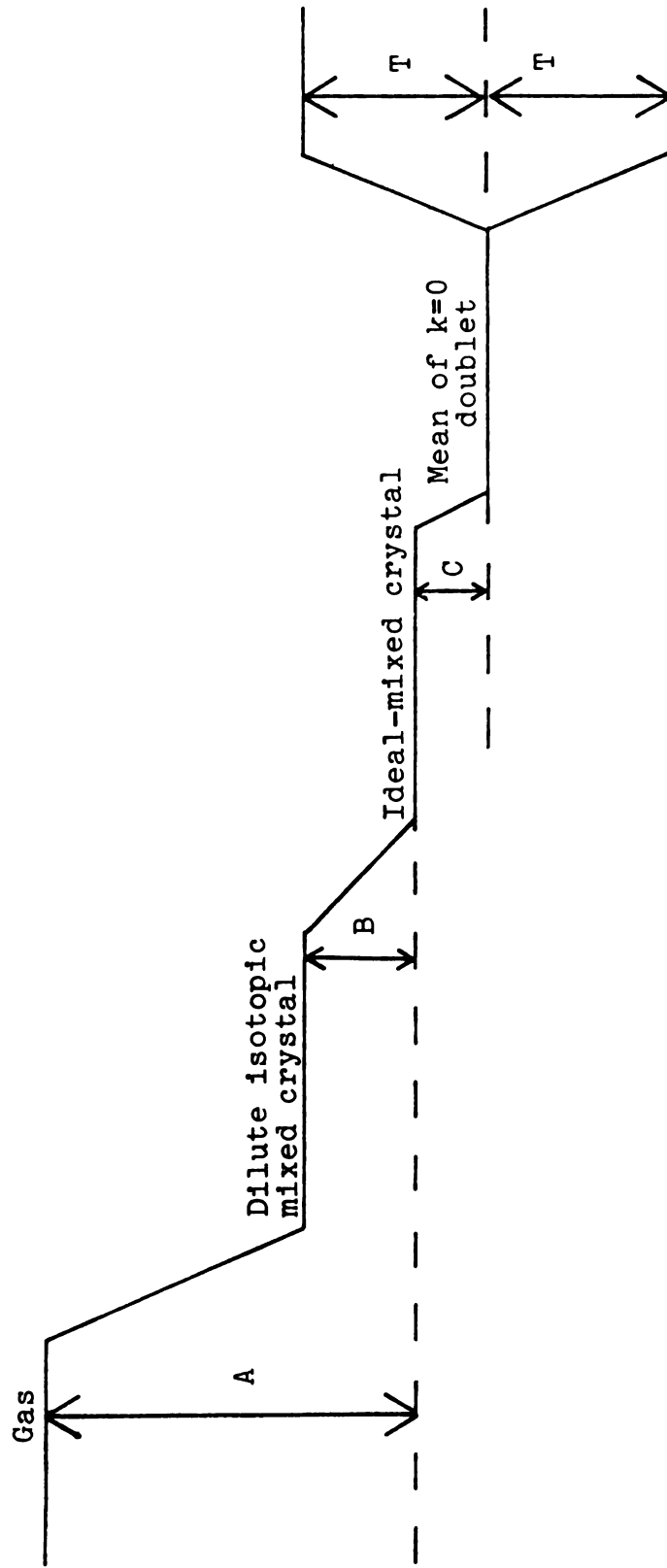


Figure 2. The structure of an arbitrary exciton band of ethylene.

1

2
3
4
5
6

translationally-equivalent molecules, and equals $L_{\alpha\alpha}^f$. For ethylene, this term may be experimentally determined by finding the difference between the mixed-crystal frequency and the mean of the $k = 0$ doublet assuming quasiresonance effects to be negligible. C is usually small for hydrocarbon-molecular crystals but it is not zero. T is one-half the exciton band width and is the same as $L_{\alpha\alpha}^f$. It reflects the resonance contributions directly related to interactions of the translationally-inequivalent molecules in the crystal.

Another type of splitting which may be observed in the spectra of molecular crystals is site-group, or static-field splitting. This is caused by the destruction of molecular degeneracies when the gas phase molecular symmetry is lowered in the crystal. Because this is a static effect it must be accounted for in the D^f term, and if this effect were included in Figure 2 there would be two A's, one for each of the site-group components. Ethylene has no degenerate vibrations; therefore, site-group splitting need not be considered. However, the orientational effect observed for some of the partially-deuterated ethylenes is very similar to site-group splitting. This will be discussed in detail in the next section.

It should be noted that bands involving both site and factor-group effects cannot usually be treated as

a simple superposition of the two independently because once the degeneracy has been removed additional coupling terms not present in the degenerate case must now be considered. This will become quite obvious in the discussion of the spectra of the partially-deuterated ethylenes. There the neat crystal spectra cannot be explained on the basis of a simple superposition of the orientational components and the Davydov components.

D. The Orientational Effect-Crystals of the Partially-Deuterated Ethylenes

Partial deuteration of ethylene destroys the D_{2h} symmetry of the free molecule and this loss of symmetry has a marked effect on the symmetry of the molecular crystal. The molecular structures and point-group symmetries of the partially-deuterated ethylenes are shown in Figure 3. The only partially-deuterated ethylene which retains a center of inversion is trans-ethylene- d_2 ; therefore, mutual exclusion of the infrared and Raman bands can no longer be expected for these compounds except for trans- $C_2H_2D_2$. Furthermore, mutual exclusion for the trans-ethylene- d_2 crystal can only be expected if allowed by the site symmetry of the crystal.

The altered symmetries of the free molecules introduce additional features to the spectra of dilute isotopic

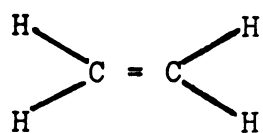
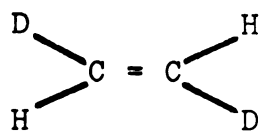
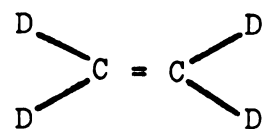
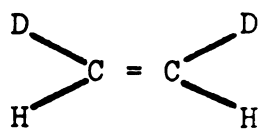
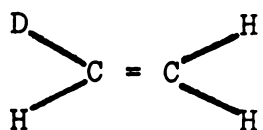
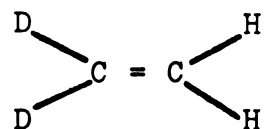
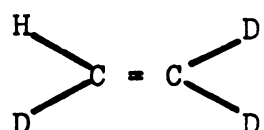
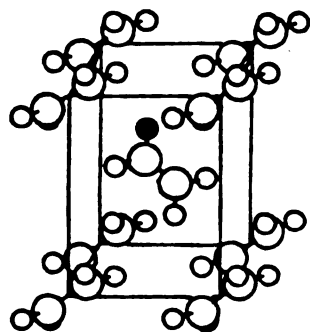
 D_{2h}  C_{2h}  C_{2v}  C_s 

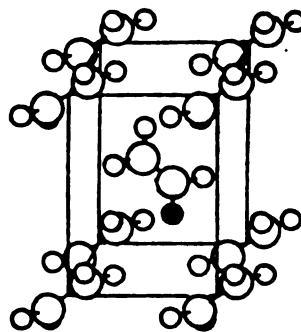
Figure 3. The molecular structure and point-group symmetries of the ethylenes.

mixed crystals of these compounds in comparison to mixed C_2H_4/C_2D_4 crystals. This arises because the guest may sit on a lattice site in different ways with possibly different intermolecular interactions. This is illustrated in Figure 4 for a dilute-mixed crystal of C_2H_3D in C_2H_4 or C_2HD_3 in C_2D_4 . If the nearest neighbor interactions are examined for the C_1 site of the host, it is seen that the interactions in Figures 4a and 4b are identical as are those in Figures 4c and 4d. Therefore, although there exist four translationally-inequivalent orientations in the crystal, for a C_1 site there are only two energetically-inequivalent orientations. Thus doublets are observed for the ethylene- d_1 bands of a dilute-mixed crystal of C_2H_3D in C_2H_4 rather than singlets as found for example for the guest bands of a dilute mixed crystal of C_2D_4 in C_2H_4 .^{13,17,24} This added complexity is referred to as the orientational effect. Bernstein²⁶ reported orientational "splittings" of up to 5 cm^{-1} for dilute mixed crystals of partially-deuterated benzenes in C_6H_6 and C_6D_6 hosts.

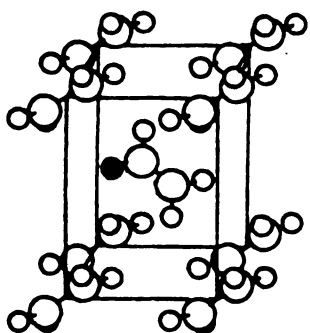
A group-theoretical procedure as described by Kopelman³⁷ may be used to determine the number of translationally-inequivalent orientations and the number of energetically-inequivalent orientations which exist for a given isotope. The number of energetically-inequivalent orientations which exist for the five partially-deuterated ethylenes in a C_1 site are as follows: $C_2H_3D(2)$,



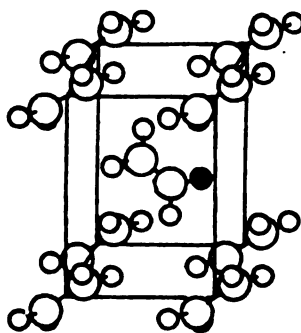
(a)



(b)



(c)



(d)

Figure 4. The orientations of C_2H_3D in C_2H_4 (C_2HD_3 in C_2D_4).

asym-C₂H₂D₂(1), cis-C₂H₂D₂(1), trans-C₂H₂D₂(2), C₂HD₃(2).

It should be noted that the orientational effect is a static effect and is a function of both the site symmetry of the host and the molecular symmetry of the guest. If two orientations are assumed (orientation A and orientation B), two D^f terms must be considered in the exciton formalism,

$$D_A^f = \langle \phi_{n\alpha}^{Af} | H^1 | \phi_{n\alpha}^{Af} \rangle \quad (27)$$

and

$$D_B^f = \langle \phi_{n\alpha}^{Bf} | H^1 | \phi_{n\alpha}^{Bf} \rangle, \quad (28)$$

where the orientation of the molecule is indicated by the superscripts A and B. The orientational splitting is equivalent to the difference between D_A^f and D_B^f .

As mentioned previously, partial deuteration of ethylene destroys the D_{2h} symmetry of the free molecule and this loss of symmetry has a marked effect on the symmetry of the molecular crystal since the partially-deuterated molecules assume translationally-distinct orientations in the crystal. This results in a destruction of the translational as well as the C_1 site symmetry of the crystal lattice. These crystals are disordered; however, it should be noted that if the substituents or the C=C

frame are ignored, the crystal structure is the same as that of C_2H_4 , assuming changes in the lattice parameters are negligible upon deuteration.

Strictly, the theory discussed in the previous sections does not apply to the partially-deuterated ethylene crystals because they lack translational symmetry. Nevertheless, qualitative applicability remains. The usefulness of the pure-crystal theory for the lattice and internal modes of the partially-deuterated ethylenes is discussed in detail in Chapters IV, V and VI.

CHAPTER III

EXPERIMENTAL

The deuterated ethylenes were obtained from Merck, Sharp and Dohme of Canada with stated purities as shown in Table 4. Research grade ethylene (C_2H_4) was obtained from Matheson and had a stated minimum purity of 99.98%. The mass spectrum of each compound was obtained using electron beam energies of 15 eV, 20 eV and 70 eV, but no additional information on impurities was determined.

The samples were cooled using either an Air Products model CS-202 or CSA-202 cryogenic helium refrigerator system. Temperatures were measured with a gold (0.07% iron) versus chromel thermocouple attached to the cold block of the cooler, or with a hydrogen-vapor bulb thermometer for cooler model CSA-202. The temperature of the samples was controlled with either a Cryodial model ML 1400 temperature controller or an Air Products temperature controller with calibrated platinum resistors for temperature sensing. The temperature of the samples was 15-25°K when the spectra were recorded. The higher temperature limit usually applied for the Raman experiments. The higher temperature is believed to be caused by the size of the Raman cell and the fact that the cell and shroud were not nickel plated. The lack of nickel

Table 4. Partially-deuterated ethylenes-Analytical data.

C_2H_3D	G.C. > 99%
	Mass Anal: C_2H_4 < 1.57%
	C_2H_3D ~ 98.43%
	CO_2 < 0.2%
<i>cis</i> - $C_2H_2D_2$	G.C. > 99%
	Mass Anal: C_2H_3D < 3.9%
	$C_2H_2D_2$ ~ 98.83%
	Atom % D = 98.05%
<i>trans</i> - $C_2H_2D_2$	G.C. > 99%
	Mass Anal: C_2H_3D < 1.17%
	$C_2H_2D_2$ ~ 98.83%
	Atom % D = 99.41%
1,1- $C_2H_2D_2$	G.C. > 99%
	Mass Anal: C_2H_4 < 0.72%
	C_2H_3D ~ 4.06%
	$C_2H_2D_2$ ~ 95.22%
C_2HD_3	G.C. > 99%
	Mass Anal: 99.55 Atom % D

plating makes the cold block more susceptible to heating effects caused by surrounding radiation.

The gas-phase samples were sprayed on to the cold-cell substrate for both the infrared and Raman experiments. The vapor-deposition technique was used because it allowed samples of different thicknesses to be studied in the infrared most conveniently. The spray-on technique was used in the Raman to enable a truer comparison of the Raman spectra with the infrared data.

The dilute mixtures of the partially-deuterated ethylenes in ethylene were made by mixing premeasured amounts of gas-phase samples of the guest and host. The amounts of gas-phase samples were measured using bulbs of different predetermined volumes and measuring the pressures of the gases with a mercury manometer. Very small bulbs were used for the partially-deuterated ethylenes, which were 1% of the mixture, to insure that the pressure of the gas exceeded the uncertainty of the manometrical reading. After the mixtures were condensed in a bulb, they were repeatedly frozen and warmed to room temperature to insure adequate mixing.

The amount of mixture made was less than the total amounts of the pure samples available for the pure crystal experiment; therefore the back-pressure during the spray-on deposition was less. This was compensated for by using a needle valve to control the flow of the

samples. The needle valve was opened further for the mixtures to insure a similar-flow rate.

The Raman sample cell which was used has been described previously by Elliott and Leroi.¹³ It is a closed cell which enabled evacuation independent to that of the shroud. The vacuum in the sample cell was at least as good as 1×10^{-5} Torr before the cell was cooled and the sample was deposited. The Raman samples were deposited at low temperature ($\sim 20^\circ\text{K}$) and then annealed at approximately 80°K for an hour or more prior to recooling for spectroscopic observation.

An Air Products cryogenic infrared cell was used for the infrared experiment. Cesium iodide windows served as the substrate and outer windows on the infrared vacuum shroud. Good thermal contact was achieved between the window and cell with indium wire. Indium sheets were used to insure good thermal contact between the infrared and Raman cells and the cold block of the cooler. For the infrared experiments the sample cell was not independent of the crystal and thus the vacuum in the shroud was critical. Therefore, a vacuum at least as good as 1×10^{-5} Torr was achieved before cooling the cell and the shroud was continuously pumped on throughout the experiment. The cesium iodide substrate was maintained at approximately 65°K during deposition of the infrared samples, and then cooled to low temperature. No

significant difference in sample quality was detected if the sample remained at 65°K for some time before cooling. Additional sample was then added when desired at low temperature, at a rate just fast enough to prevent high scattering. The deposition rate was monitored manometrically and was usually about 2 mm Hg/min. Approximately 0.75 liters of the pure samples at STP were sprayed-on to the CsI window which was round with a diameter of approximately 2 mm. The total volume of the mixtures deposited was approximately .25 liters.

A Perkin-Elmer model 225 infrared grating spectrophotometer ($4000\text{ cm}^{-1} - 200\text{ cm}^{-1}$) with 1 cm^{-1} resolution above 450 cm^{-1} and $1 - 2\text{ cm}^{-1}$ resolution below 450 cm^{-1} was used to measure the mid-infrared spectra. The Raman spectrophotometer consisted of a Jarrell-Ash model 25-100 double Czerny-Turner monochromator with a thermoelectrically cooled RCA C31034 photomultiplier tube. Both the 5145 \AA and 4880 \AA lines of a Spectra Physic model 164 argon ion laser were used as exciting lines for all Raman experiments in order to distinguish laser-fluorescence lines. Baird-Atomic spike filters were also employed to help eliminate laser-plasma lines. In some cases the lattice spectra were also observed using the 4765 \AA line of the argon-ion laser as the exciting line to eliminate interference from laser-fluorescence lines. The resolution in the Raman spectra was 1 cm^{-1} or better

for the fundamentals and lattice modes, and the spectrometer calibration was checked using a neon lamp.

Most of the reported infrared frequencies are believed to have an accuracy of $\pm 1 \text{ cm}^{-1}$. However, for very broad bands in both the infrared and Raman the accuracy may only be $\pm 4 \text{ cm}^{-1}$. The accuracy of the Raman fundamentals is believed to be $\pm 1 \text{ cm}^{-1}$ as is that of the lattice modes except in cases where the bands are broad or poorly resolved. In these cases the accuracy is believed to be $\pm 2 \text{ cm}^{-1}$. The Raman overtones and combinations reported in Appendix A are believed to be accurate within $\pm 3 \text{ cm}^{-1}$.

An attempt was made to measure the far-infrared spectrum of the ethylenes using a Digilab model FTS-16 fourier transform far-infrared spectrometer. Crystalline quartz was used as the substrate and both polyethylene and Mylar (thickness $200 \mu\text{m}$) were used as outer windows for the infrared vacuum shroud.

Instrumental limitations caused by the cryogenic cell, detector sensitivity and computer software and hardware capacities limited the success of these experiments in that only very noisy spectra with low signal-to-noise ratio were obtained. However, the 73 cm^{-1} and 110 cm^{-1} translations¹⁹ of ethylene were observed, and the observed spectra suggested the existence of another mode at approximately 35 cm^{-1} . This most certainly could be the as yet unobserved translation of the ethylene crystal

(see Chapter IV). Attempts to confirm this observation using a different beam splitter and different outer windows were unsuccessful. Due to the instrumental limitations, an attempt to observe the translations of all the ethylene crystals was abandoned.

CHAPTER IV

THE LATTICE VIBRATIONS OF THE PARTIALLY-DEUTERATED ETHYLENES

A. Phonons in Disordered Solids

As was discussed in Chapter II, the crystals of the partially-deuterated ethylenes are translationally disordered, and therefore lack both translational and site symmetry. Since the crystals are no longer periodic, one might expect the \underline{k} selection rules to be invalid, and the mutual exclusion of the lattice phonon modes to be destroyed due to the lack of C_1 site symmetry.

The study of phonons in disordered solids is certainly not a new interest of physicists and chemists. The first papers on the subject were published by Lifshitz in 1943.³⁸ However, most of the past work has concentrated on atomic crystals, where only translational lattice vibrations occur. Molecules are the building blocks of a molecular crystal and therefore introduce rotational degrees of freedom which do not have to be considered in the atomic case. Much of the work on atomic crystals has been reviewed by Elliot, Krumhansl and Leath³⁹ and by Baker and Sievers.⁴⁰

Recently, phonons of heavily-doped isotopic mixed

molecular crystals have been investigated. It is believed that the study of these simpler disordered systems will aid in the understanding of more complicated systems. The mixed crystals which have been studied include naphthalene-h₈: naphthalene-d₈,⁴¹ durene-h₁₄: durene-d₁₄⁴² and benzene-h₆: benzene-d₆.⁴³ It has been observed that the phonon states of isotopic-mixed crystals are amalgamated;⁴⁴ that is, if x phonon bands are observed for the pure crystal then x bands will be observed for the crystal doped with its isotopic constituent of the same molecular symmetry.

If the perturbation caused by the guest molecules is small (vide infra), the so-called virtual crystal limit^{39,45} applies, and the mixed crystal is a substitutional disordered system. In a substitutionally-disordered system the intermolecular force constant of the mixed crystals are the same as those of the pure crystal.

In the virtual crystal limit the phonon energies of the mixed isotopic crystals can be expressed as follows,^{43,46,47}

$$\epsilon = \epsilon_A / (1 - C_B \Delta^f)^{1/2}, \quad (29)$$

where ϵ_A is the frequency of the pure host and C_B is the concentration of the guest. Δ^f is the perturbation strength of the band and is defined as $(\eta_A^f - \eta_B^f) / \eta_A^f$,

where f designates the degree of freedom (that is, R_x , R_y , R_z , T_x , T_y , T_z) and η is the mass for translations or the moment of inertia for librations. If Δ^f is very small, Equation (1) can be rewritten as

$$\epsilon = \epsilon_A \left(1 + \frac{1}{2} C_B \Delta^f \right), \quad (30)$$

which predicts a linear dependence of the frequencies on the guest concentration.

In a substitutionally-disordered solid k is a good quantum number, the phonons are delocalized, and the normal coordinates described in the mass - or moment-of-inertia-weighted coordinate system remain unchanged in going from the pure host crystal to the pure guest crystal. This leads to no change in the spectroscopic activity of the modes; thus if the pure crystal has centrosymmetric site symmetry, mutual exclusion would be retained for the isotopically-mixed crystals. No significant changes in the phonon band widths are predicted in the virtual crystal limit; however, the relative intensities of the phonon modes may be altered relative to the pure crystal if Δ^f is different for each of the different degrees of freedom. For example, if the crystal has inversion symmetry, the translations are usually infrared active and the librations are usually Raman active. For the mixed crystal the relative intensities of the translations

would remain unchanged because Δ^f is the same for each translation. The total Raman intensity would remain unchanged, but the relative intensities of the librations are expected to be altered, since Δ^f is usually different for each rotation except for spherical and planar symmetric tops.

The crystals of the partially-deuterated ethylenes are comparable to isotopic-mixed crystals. The nearest neighbor atoms in both cases can be either hydrogens or deuteriums, so the intermolecular interactions should be quite similar. The changes in energy of the phonons of the isotopic-mixed crystals are mass-dependent, so an analogy can be drawn between the percent deuteration of a partially-deuterated ethylene and the concentration of the guest in a $C_2D_4:C_2H_4$ mixed crystal. For example, the "effective mass" of the ethylene- d_1 crystal would be the same as that of a mixed crystal of 25% C_2D_4/C_2H_4 .

Since in the virtual crystal limit the force constants and "effective" symmetry, that is, not the strict mathematical symmetry but the spectroscopically observed symmetry, of the crystal remain unchanged, the phonon frequencies of the partially-deuterated crystals in this limit can be calculated assuming they are pure crystals. Therefore the semi-classical method of calculating the phonon frequencies (TBON) discussed in Chapter II would still apply. The crystal symmetry and potential function

remain the same for each ethylene; only the masses of the molecules are different. It is also assumed that the contributions to the normal coordinates from each degree of freedom; R_x , R_y and R_z do not change much upon deuteration. This can be easily checked because program TBON also determines the eigenvectors.

B. The Potential Function of Ethylene

Elliott and Leroi¹³ tested several intermolecular potential functions for ethylene in order to determine which potential gave the best fit to the observed lattice frequencies. Since then, slightly better lattice parameters have been obtained by neutron diffraction^{22,23} and single crystal x-ray²¹ experiments, and some new potential functions, which were not previously tested on ethylene, have appeared in the literature.^{32,48-52} The best potential functions of Elliott and Leroi, as well as several new potential functions, have been used in the calculation of the lattice frequencies of ethylene. Table 5 lists the parameters of the potentials tested.

Potential functions I, III and V were obtained by Williams^{49,50} by a least squares fit of observed and calculated crystal data of aromatic, both aromatic and aliphatic, and aliphatic hydrocarbons, respectively. These correspond to the potential functions labeled VI,

Table 5. Nonbonded potential parameters, where $V_{ij} = B \exp(-Cr) - Ar^{-6} + Er^{-1}$.

Set	H-H			H-C			C-C			Ref.			
	A	B	C	A	B	C	A	B	C		E		
I	36.0	4000.0	3.74	0	139.0	9410.0	3.67	0	535.0	74460.0	3.60	0	49
II	44.14	3429.8	3.787	0	150.03	9772.8	3.669	0	443.17	65821.3	3.611	0	32
III	27.3	2650.0	3.74	0	125.0	8770.0	3.67	0	568.0	83630.0	3.60	0	50
IV	26.5	2260.3	3.738	0	127.62	8809.9	3.669	0	566.69	78658.8	3.610	0	32
V	32.3	2630.0	3.74	0	128.0	11000.0	3.67	0	505.0	61900.0	3.60	0	50
VI	24.4	2170.2	3.74	0	111.7	8508.6	3.67	0	511.5	71701.7	3.60	0	52
VII	40.2	2868.1	3.74	0.032	134.4	14316.5	3.67	-0.032	449.3	71462.7	3.60	0.032	48
VIII	57	42000	4.86	0	154	42000	4.12	0	358	42000	3.58	0	51

V and VII by Elliott and Leroi. Potential functions II and IV have been obtained by Taddei, et al.³² by a least squares refinement of potential functions I and III to obtain the best agreement between the calculated and observed lattice frequencies of benzene. VI and VII have been obtained by least squares refinement between the observed and calculated crystal structures of both saturated and aromatic hydrocarbons,^{52,48} where VII has an added electrostatic contribution. Potential function VIII was obtained by Kitaigorodsky⁵¹ by fitting the crystal structures of various aromatic crystals.

Each interaction potential was used to calculate the lattice frequencies of ethylene and the results compared to the observed values. The calculated and observed frequencies are tabulated in Table 6. The best agreements with the observed librational frequencies are obtained with potential functions I, III and V. The agreement for the translations is best with potential VII; however, an imaginary librational frequency is calculated with this potential, so it must be eliminated. The next best agreements with the observed translational frequencies are obtained with potentials I, III and V. To further examine which is the best interaction potential, the three best potentials for C_2H_4 were used to calculate the lattice frequencies of C_2D_4 . The calculated and observed frequencies of C_2D_4 are tabulated in Table 7. Again, the

Table 6. The observed and calculated lattice frequencies (cm^{-1}) of solid ethylene.

Observed Librations ^a	Potential Set							
	I	II	III	IV	V	VI	VII	VIII
73	68	54	60	55	64	57	78	40
90	83	68	73	68	75	69	85	55
97	94	75	79	72	82	74	94	64
114	107	86	93	86	95	87	Imag.	68
167	163	127	132	120	133	120	102	109
177	175	139	142	129	143	129	129	128
Translations ^b								
35 ^c	48	45	46	44	48	44	61	43
73	61	52	55	52	56	52	67	53
110	86	73	79	73	82	75	93	68

^aFrom Reference 13.

^bFrom Reference 19.

^cSee Chapter III and text.

Table 7. The observed and calculated lattice frequencies (cm^{-1}) of solid ethylene- d_4 .

Observed Librations ^a	Potential Set		
	I	III	V
60	57	49	53
75	71	63	64
78	77	65	68
95	92	80	81
123	115	93	95
135	124	101	102
Translations ^b			
---	45	43	45
69.5	57	52	53
104	80	74	77

^aFrom Reference 13.

^bFrom Reference 19.

best agreement between the observed and calculated frequencies is obtained with potential I. Therefore potential I, which was obtained by a least squares refinement to the crystal data of aromatic hydrocarbons, and is also the potential adopted by Elliott and Leroi, is the best potential function of the set for the calculation of the ethylene crystal lattice frequencies.

With this potential the lowest translational frequency is calculated to be 48 cm^{-1} . As mentioned in Chapter III, it is believed that a mode at 35 cm^{-1} was observed during the attempt to obtain the far-infrared spectrum of C_2H_4 . This calculation shows that the third translation should be lower in frequency than the other two; supporting the possibility that the 35 cm^{-1} observation may be the "unobserved" translation of ethylene. However, it is of interest to point out that the other observed lattice frequencies of ethylene are higher than the calculated frequencies. The reverse is true for the 35 cm^{-1} mode.

The exciton splitting ($k = 0$ components) of the ethylene internal modes were also calculated using program TBON. However, all calculated-splittings were less than 1 cm^{-1} , therefore little meaning could be assigned to them. This certainly indicates that potential I is not the "correct" interaction potential of ethylene in that it only does a "good" job of calculating the librational

frequencies, a poor job of calculating the translations, and does not calculate the exciton splittings.

C. The Librations of the Partially-Deuterated Ethylenes

The Raman spectra in the lattice region of the partially-deuterated ethylenes are shown in Figures 5 and 6. At least five bands were observed for each molecule and a shoulder was resolved on the high-frequency side of the highest frequency bands of C_2H_3D , $1,1-C_2H_2D_2$ and C_2HD_3 (see Figure 7). It is believed that a sixth band is present also for $cis-C_2H_2D_2$ and $trans-C_2H_2D_2$, which was unresolvable because of poorer sample quality. The relative intensities of the bands are similar to those of ethylene and ethylene- d_4 ,¹³ although minor differences do exist.

Only two of the three expected infrared-active translations of ethylene have been observed.¹⁹ The energies of these phonons are 73 cm^{-1} and 110 cm^{-1} for C_2H_4 and 69.5 cm^{-1} and 104 cm^{-1} for C_2D_4 . The third optically-active translational mode has been calculated to be at lower frequency (see Table 6 and preceding section). Therefore, if any translations are to be observed in the Raman phonon spectra of the partially-deuterated ethylenes where they are not rigorously excluded, they are expected to fall between 110 cm^{-1} and 104 cm^{-1} or below 73 cm^{-1} .

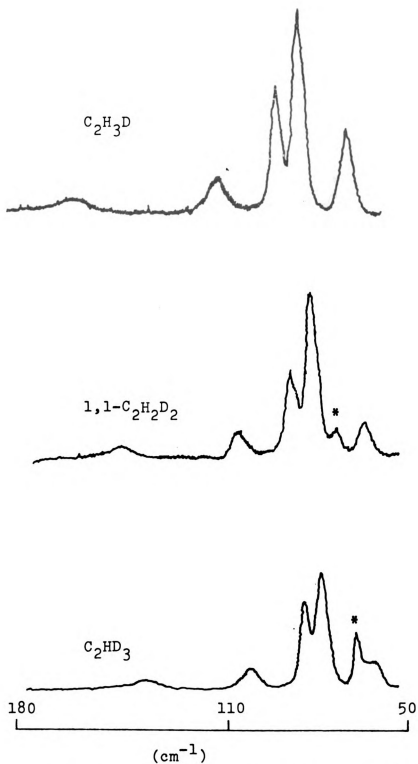


Figure 5. The Raman lattice region of $\text{C}_2\text{H}_3\text{D}$, $1,1\text{-C}_2\text{H}_2\text{D}_2$ and C_2HD_3 . The peaks marked with an asterisk are laser-fluorescence lines.

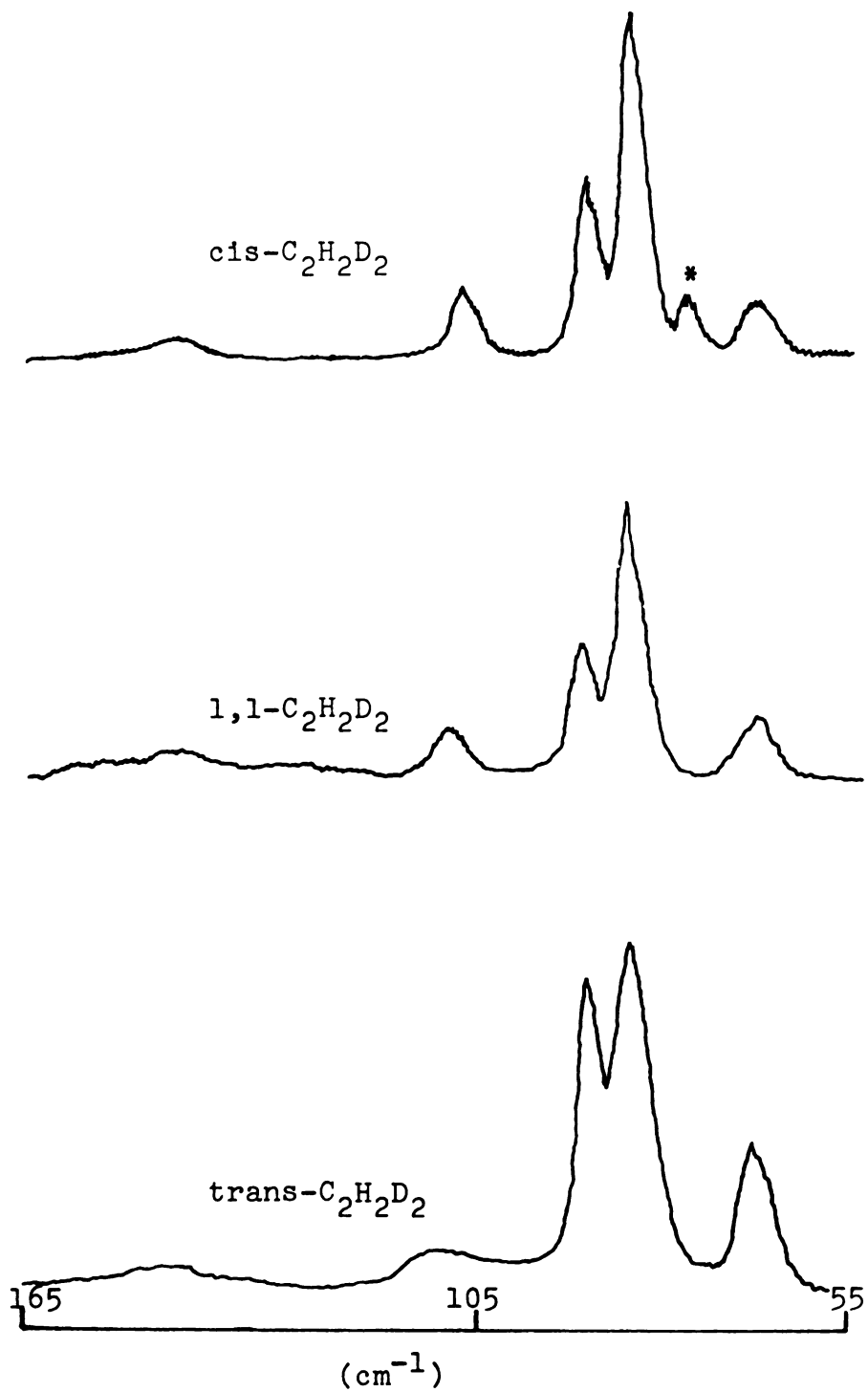


Figure 6. The Raman lattice region of *cis*- $\text{C}_2\text{H}_2\text{D}_2$, 1,1- $\text{C}_2\text{H}_2\text{D}_2$ and *trans*- $\text{C}_2\text{H}_2\text{D}_2$. The peak marked with an asterisk is a laser-fluorescence line.

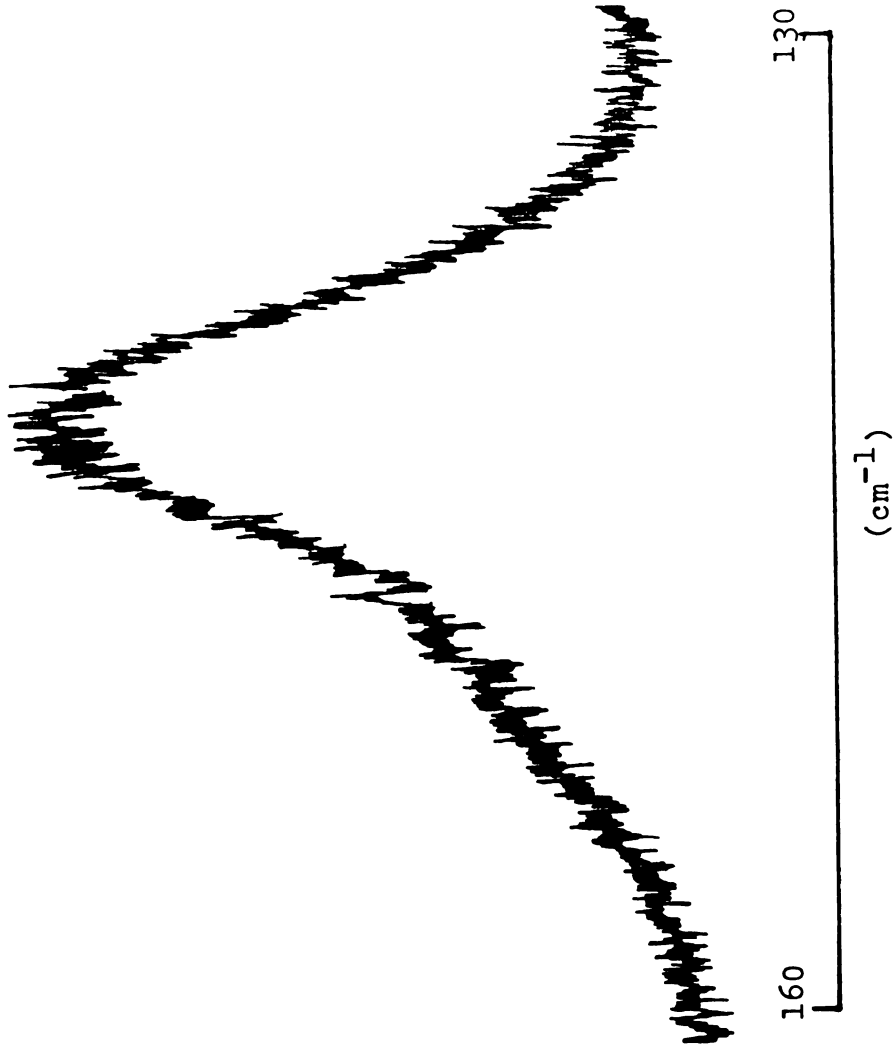


Figure 7. The highest frequency lattice modes of 1,1- $\text{C}_2\text{H}_2\text{D}_2$.

Unfortunately these regions overlap the lattice librational frequency range, so the observed bands cannot be assigned as librations or translations simply on the basis of their positions.

The frequencies of the lattice modes of the partially-deuterated ethylenes were calculated using interaction potential function I. It was assumed that deuteration causes only a change in the mass of the molecules, and that the symmetry of the lattice remains unchanged. The calculated and observed librational frequencies are given in Table 8. The agreement between the calculated and observed values is quite satisfactory - as good as that for ethylene and ethylene-d₄. The slight differences in the calculated C₂H₂D₂ frequencies is caused by the placement of the deuteriums on the C=C frame. The bond-length changes caused by deuteration as listed in Table 2 were accounted for in the calculation; so depending on whether the nearest neighbor was a hydrogen or deuterium, the interatomic distance varied. This effect resulted in a varying of the calculated frequencies by less than a wavenumber.

Note that the frequencies were calculated assuming centrosymmetric site symmetry for each ethylene crystal; therefore mixing of the translational and rotational degrees of freedom was strictly forbidden. The crystal normal coordinates obtained from TBON for the librations

Table 8. The calculated and observed librational frequencies of the ethylenes.

C_2H_4		C_2H_3D		$cis-C_2H_2D_2$		$trans-C_2H_2D_2$		$1,1-C_2H_2D_2$		C_2HD_3		C_2D_4	
Calc.	Obs. ^a	Calc.	Obs.	Calc.	Obs.	Calc.	Obs.	Calc.	Obs.	Calc.	Obs.	Calc.	Obs. ^a
68	73	65	69	62	68	62	66	61	67	59	64	57	60
83	90	79	87	76	83	76	82	76	83	74	79	71	75
94	97	89	93	85	90	85	88	84	90	81	84	77	78
107	114	102	112	98	107	98	109	98	107	95	102	92	95
163	167	145	155	133	145	133	145	133	143	123	134	115	123
175	177	157	164	143	---	144	---	143	151	133	142	124	135

^aFrom Reference 13.

of the crystalline ethylenes are given in Table 9. None of the librational modes can be described as a pure rotation about a single principal axis, but the relative contributions of each rotation to each normal coordinate remain essentially unchanged in going from C_2H_4 to C_2D_4 .

The calculated and observed librational frequencies are plotted against the number of deuterium atoms on the molecule in Figures 8 and 9, respectively. A virtually linear dependence between the frequencies and number of deuteriums is predicted for the four lowest frequency vibrations in Figure 8; therefore the frequency dependence on the percentage deuteration should be described by Equation (30) for these bands. A deviation from linearity is predicted for the two highest frequency bands; thus Equation (29) should describe the curves for these.

The perturbation strengths, Δ^f 's, of the calculated frequencies are given in Table 10 along with the experimentally observed Δ^f 's and those calculated from the moments-of-inertia of ethylene and ethylene- d_4 . The Δ^f 's of the calculated frequencies were determined by calculating the perturbation strength for each point with Equation (29) and then finding the average Δ^f for the band. The experimental perturbation strengths were found by determining the slopes of the lines shown in Figure 9 for the five lowest frequency bands and using Equation (30) to determine Δ^f . Δ^f of the highest frequency band

Table 9. The crystal normal coordinates of the librations of the isotopic ethylene crystals.

Crystal	Species	$\nu_{\text{calc.}}$	R_x	R_y	R_z
C_2H_4	A_g	83	-0.06	-0.22	0.97
		94	0.17	0.96	0.22
		175	0.98	-0.18	0.02
	B_g	68	-0.05	-0.96	0.27
		107	0.00	-0.27	-0.96
		163	-1.00	0.05	-0.02
C_2H_3D	A_g	79	-0.06	-0.24	0.97
		89	-0.19	-0.95	-0.25
		157	0.98	-0.20	0.02
	B_g	65	0.06	0.96	-0.26
		102	0.00	0.26	0.96
		145	-1.00	0.06	-0.01
cis- $C_2H_2D_2$	A_g	76	0.08	0.27	-0.96
		85	-0.20	-0.94	-0.28
		143	-0.98	0.21	-0.02
	B_g	62	0.06	0.96	-0.26
		98	0.00	0.26	0.97
		133	1.00	-0.06	0.02
trans- $C_2H_2D_2$	A_g	76	-0.07	-0.26	0.96
		85	-0.20	-0.94	-0.27
		144	0.98	-0.21	0.02
	B_g	62	0.06	0.96	-0.26
		98	0.00	0.26	0.97
		133	1.00	-0.06	0.01
1,1- $C_2H_2D_2$	A_g	76	0.08	0.29	-0.95
		84	-0.19	-0.93	-0.30
		143	0.98	-0.21	0.02
	B_g	61	0.06	0.97	-0.25
		98	0.01	-0.25	-0.97
		133	1.00	-0.06	0.02

Table 9. Continued.

Crystal	Species	$\nu_{\text{calc.}}$	R_x	R_y	R_z
C_2HD_3	A_g	74	0.09	0.31	-0.95
		81	0.21	0.92	0.32
		133	0.97	-0.23	0.02
	B_g	59	-0.07	-0.97	0.25
		95	0.00	-0.25	-0.97
		123	-1.00	0.06	-0.02
C_2D_4	A_g	71	-0.10	-0.33	0.94
		77	0.22	0.91	0.34
		124	0.97	-0.24	0.02
	B_g	57	-0.07	-0.97	0.25
		92	-0.01	0.25	0.97
		115	1.00	-0.06	0.02

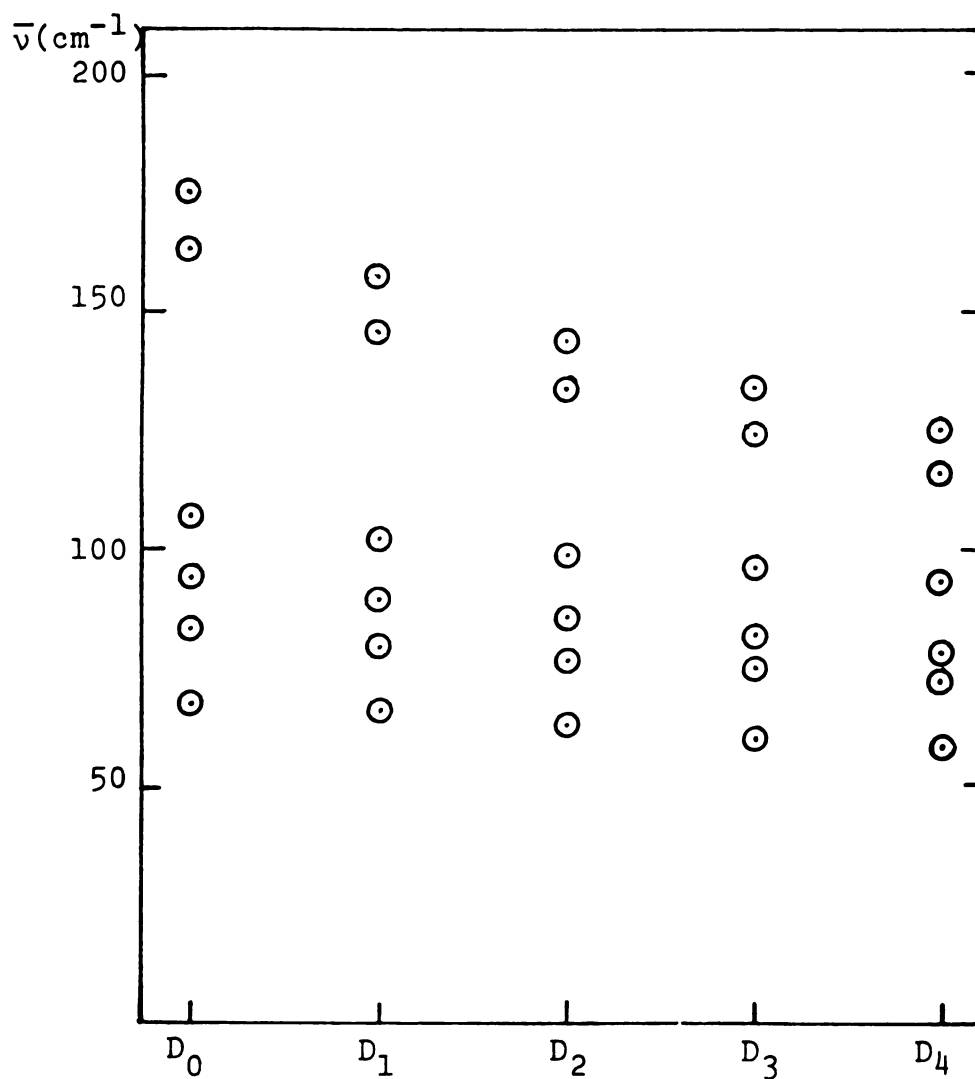


Figure 8. The calculated librational frequencies versus the number of deuteriums.

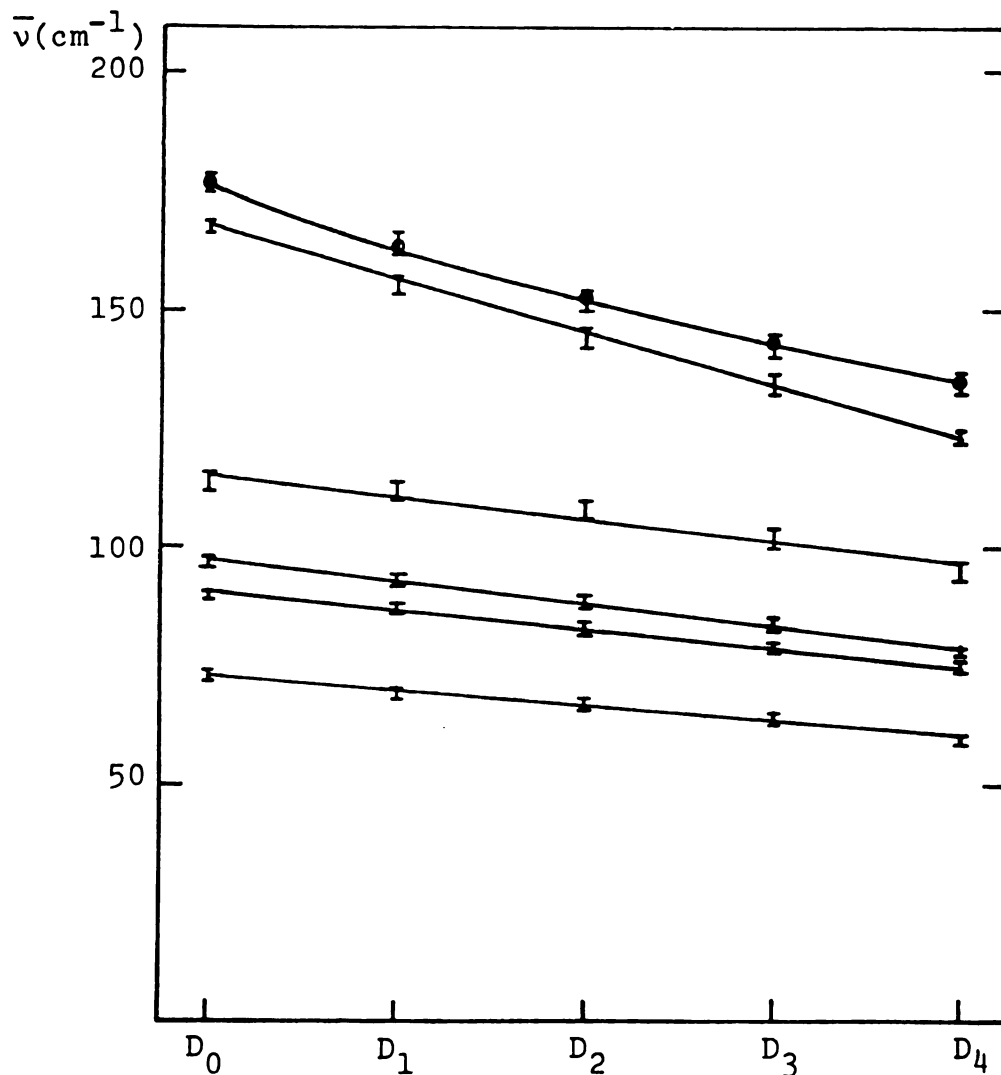


Figure 9. The observed librational frequencies versus the number of deuteriums. The D_2 frequencies are the mean of the $\text{cis-C}_2\text{H}_2\text{D}_2$, $1,1\text{-C}_2\text{H}_2\text{D}_2$ and $\text{trans-C}_2\text{H}_2\text{D}_2$ values.

Table 10. Perturbation strengths of the ethylene librations.

$\Delta^{R_x} = -1.00$

$\Delta^{R_y} = -0.47$

$\Delta^{R_z} = -0.36$

Librations (C_2H_4) cm^{-1}	Δ^f (exp) ^a	Δ^f (cal) ^b
73	-0.36	-0.41
90	-0.36	-0.38
97	-0.37	-0.47
114	-0.33	-0.37
167	-0.53	-1.02
177	-0.72	-0.97

^aFrom Figure 9.^bFrom Figure 8.

was determined by finding the value for each point with Equation (29) and then taking the average of these determinations. The curve shown in Figure 9 for this band was calculated using Equation (29) with $\Delta^f = -0.72$. In order to draw a straight line through the points of the 114 cm^{-1} (C_2H_4), it was necessary to increase the uncertainty of the 114 cm^{-1} band of C_2H_4 and the 95 cm^{-1} band of C_2D_4 to $\pm 2 \text{ cm}^{-1}$ even though the reported uncertainty was $\pm 1 \text{ cm}^{-1}$.¹³

The experimentally determined perturbation strengths are consistent with the general rotational contributions given in Table 9. The four lowest frequency librations are primarily motions about the y and z principal rotational axes of the molecule, and the highest frequency bands have larger perturbation strengths consistent with the larger strength predicted for rotations about the x axis. The observed Δ^f 's indicate that the librations of the ethylene crystals are amalgamated and can be treated in the virtual crystal limit. This suggests that they are substitutionally-disordered solids. Moreover, this implies that the effective lattice symmetry of the partially-deuterated ethylene crystals is the same as that of the C_2H_4 and C_2D_4 lattice, and that the intermolecular force constants are unchanged.

No significant changes in the relative intensities of the librations are observed for the partially-deuterated ethylenes although this is permitted by the virtual

crystal theory, since for ethylene $\Delta^{Rx} \neq \Delta^{Ry} \neq \Delta^{Rz}$. The band widths of the bands are a bit larger than those of C_2H_4 and C_2D_4 , but this may be attributed to poorer sample quality and to the multiple orientations of the partially-deuterated ethylenes. Thus, the bandwidths are also consistent with the virtual crystal theory.

D. Conclusions

The following conclusions have been drawn in this chapter:

(a) The interaction potential adopted by Elliott and Leroi¹³ (Potential I) is still the best available potential function for ethylene. The potential is "soft", in that the calculated lattice frequencies of the ethylenes are consistently less than the observed frequencies.

(b) The third optically-active translation of the C_2H_4 crystal may have been observed at 35 cm^{-1} .

(c) The librations of the ethylenes are amalgamated and can be described in the virtual crystal limit. This implies that:

(1) The effective lattice symmetry of the partially-deuterated ethylene crystals is the same as the lattice symmetry of the C_2H_4 and C_2D_4 crystal. Therefore, k is still a good quantum number and the effective site symmetry is C_1 .

(2) The intermolecular force constants and the lattice normal coordinates remain unchanged in going from the C_2H_4 to the C_2D_4 crystal.

(3) The bands observed in the Raman phonon region are the librations - no interference from the translations was observed consistent with a C_1 site.

(d) The observed Δ^f 's predict a mixing of the rotations about the principal axes as does the frequency calculation.

CHAPTER V

PROBING THE SITE SYMMETRY OF THE PARTIALLY-DEUTERATED ETHYLENES VIA THE ORIENTATIONAL EFFECT

A. Theory

In the previous chapter it was concluded that the crystals of the partially-deuterated ethylenes can be treated in the virtual-crystal limit. This implies that the symmetry of the C_2H_4 lattice is retained for these lattices. The retention of mutual exclusion for the lattice vibrations of the partially-deuterated ethylenes is said to be caused by an "effective" C_1 site symmetry. That is, although strictly the molecules are in sites of no symmetry, the molecules are said to be "nearsighted" and cannot distinguish between hydrogens and deuteriums on the neighboring molecules. The intermolecular forces are very similar to those of the molecule in a C_1 site.

A knowledge of the "effective" site symmetry is necessary for the interpretation of the spectra of the internal modes of the partially-deuterated ethylenes because the orientational effect may complicate these modes, and the number of energetically inequivalent orientations depends on the site symmetry. However the orientational effect may also be used to probe the "effective" site symmetry

of the partially-deuterated crystals.

The number of orientational components observed for the guest modes of a dilute isotopic mixed crystal depends on the point-group symmetry of the free guest molecule and the site group of the host. A group-theoretical procedure as discussed by Kopelman³⁷ can be used to determine the number of orientational components expected for the partially-deuterated ethylenes in sites of C_1 , C_1 or any other symmetry. The number of energetically inequivalent orientational components determined for a C_1 or C_1 site is listed in Table 11.

The number of orientational components observed for one of the partially-deuterated ethylenes as a dilute guest in another one of the partially-deuterated ethylenes gives an indication of the "effective" site symmetry of the host. For example, if the guest modes in the dilute mixed crystal spectrum of ethylene- d_1 in ethylene- d_3 are observed the number of orientational components would indicate the following:

- (1) 2 components \rightarrow an "effective" C_1 site symmetry.
- (2) 4 components \rightarrow C_1 site symmetry.
- (3) More than 4 components \rightarrow site symmetry is not a useful concept for the disordered host.

All of the partially-deuterated ethylenes except the trans- $C_2H_2D_2$ can be used as probes of the site symmetries

Table 11. The number of orientational components for the partially-deuterated ethylenes in a C_1 or C_1 site.

Molecule	Site Symmetry	
	C_1	C_1
C_2H_3D	4	2
1,1- $C_2H_2D_2$	2	1
cis- $C_2H_2D_2$	2	1
trans- $C_2H_2D_2$	2	2
C_2HD_3	4	2

of the other partially-deuterated ethylenes. The center of inversion symmetry of the trans-C₂H₂D₂ makes it impossible to distinguish between a C₁ or C₁ site.

B. Experimental

The utility of probing the "effective" site symmetries of the partially-deuterated ethylenes using another partially-deuterated ethylene as the guest, may be investigated by observing the spectra of dilute-mixed crystals of the partially-deuterated ethylenes in C₂H₄ host which has a site which is known to have C₁ symmetry. If the magnitude of the orientational splitting is too small, the number of components predicted in Table 11 may not be resolvable and the technique could be useless. Therefore, the guest modes of dilute-mixed crystals of the partially-deuterated ethylenes in C₂H₄ host were observed in order to determine if the magnitude of the orientational splitting is large enough to be of value and to confirm if the group-theoretical predictions are indeed correct.

Tables 12-16 list the observed guest frequencies of the dilute-mixed crystals of the partially-deuterated ethylenes in C₂H₄ host. A C-H(D) stretching vibration ($\nu_1, \nu_5, \nu_9, \nu_{11}$), an in-plane bending vibration ($\nu_3, \nu_6, \nu_{10}, \nu_{12}$) and an out-of-plane bending mode (ν_4, ν_7, ν_8)

Table 12. Observed frequencies of C_2H_3D fundamentals in
 1% C_2H_3D/C_2H_4 .

Infrared (cm^{-1})	Raman (cm^{-1})	Assignment
3010.0		ν_1
1597.0		ν_2
1285.2	1285.4	
1283.0	1282.8	ν_3
1010.9		
1002.9		ν_4
	3047.8	
	3043.2	ν_5
812.5		
809.2		ν_7
730.8		
729.6		ν_{10}
2262.4		
2259.8		ν_{11}
1396.2	1395.0	ν_{12}

Table 13. Observed frequencies of $\text{cis-C}_2\text{H}_2\text{D}_2$ fundamentals in 1% $\text{cis-C}_2\text{H}_2\text{D}_2/\text{C}_2\text{H}_4$.

Infrared (cm^{-1})	Raman (cm^{-1})	Assignment
2286.0	2284.2	ν_1
	1563.7	ν_2
	1212.7	ν_3
3038.2	3036.1	ν_5
853.4		ν_7
3044.8	3043.2	ν_9
661.3		ν_{10}
2241.8		ν_{11}
1335.0		ν_{12}

Table 14. Observed frequencies of trans-C₂H₂D₂ fundamentals
in 1% trans-C₂H₂D₂/C₂H₄.

Infrared (cm ⁻¹)	Raman (cm ⁻¹)	Assignment
	2270.9	ν ₁
	2268.7	
	1565.4	ν ₂
	1563.7	
	1282.3	ν ₃
	1279.9	
1001.8		ν ₄
990.8		
	3030.6	ν ₅
	3025.9	
731.5		ν ₇
724.1		
	870.2	ν ₈
	865.7	
3051.5		ν ₉
3047.0		
672.8		ν ₁₀
670.6		
2266.6		ν ₁₁
1295.3		ν ₁₂
1291.8		

Table 15. Observed frequencies of 1,1-C₂H₂D₂ fundamentals
in 1% 1,1-C₂H₂D₂/C₂H₄.

Infrared (cm ⁻¹)	Raman (cm ⁻¹)	Assignment
2999.8		ν_1
1578.8	1579.6	ν_2
	1034.7	ν_3
2322.8	2322.8	ν_5
754.8		ν_7
	3077.5	ν_9
683.4		ν_{10}
2217.0	2216.6	ν_{11}
1379.1	1380.3	ν_{12}

Table 16. Observed frequencies of C_2HD_3 fundamentals in
 1% C_2HD_3/C_2H_4 .

Infrared (cm^{-1})	Raman (cm^{-1})	Assignment
2270.0	2270.1 2266.6	ν_1
	1546.3 1544.0	ν_2
	1041.9	ν_3
769.1 766.9	767.6	ν_4
2320.0	2320.2	ν_5
	995.4	ν_6
735.0 723.8		ν_7
920.9		ν_8
3034.0 3030.2	3033.6 3030.1	ν_9
627.5		ν_{10}
2209.6	2209.1	ν_{11}
1285.2 1282.9	1287.0 1284.2	ν_{12}

of each partially-deuterated ethylene are shown in Figures 10 through 16. Additional modes of 1% C_2H_3D/C_2H_4 are shown for later comparison with the spectra of C_2H_3D in the other partially-deuterated ethylenes.

Singlets are expected for the guest modes of cis- $C_2H_2D_2/C_2H_4$ and 1,1- $C_2H_2D_2/C_2H_4$ crystals, and are indeed observed. (See Tables 13 and 15 and Figures 12 and 15). Doublets are predicted for the guest fundamentals of C_2H_3D/C_2H_4 , trans- $C_2H_2D_2/C_2H_4$ and C_2HD_3/C_2H_4 . Many of the observed modes show doublets consistent with this prediction. In the cases where singlets are observed it can be assumed that the orientational splitting is too small to allow the components to be resolved or the resolution is hampered by the sample quality. In any event, the orientational components were resolved in many cases so the determination of the site symmetries of the partially-deuterated by way of the orientational effect should be suitable. The observed orientational splittings varied from unresolvable to 11.0 cm^{-1} .

In most cases it was not necessary to separately make up the dilute mixtures because the impurities present in the neat samples (see Table 4) served quite adequately as dilute guests. This was not necessarily an advantage since it made it impossible to compare the spectrum of the pure host with that of the dilute-mixed crystal. The frequency region of less than approximately

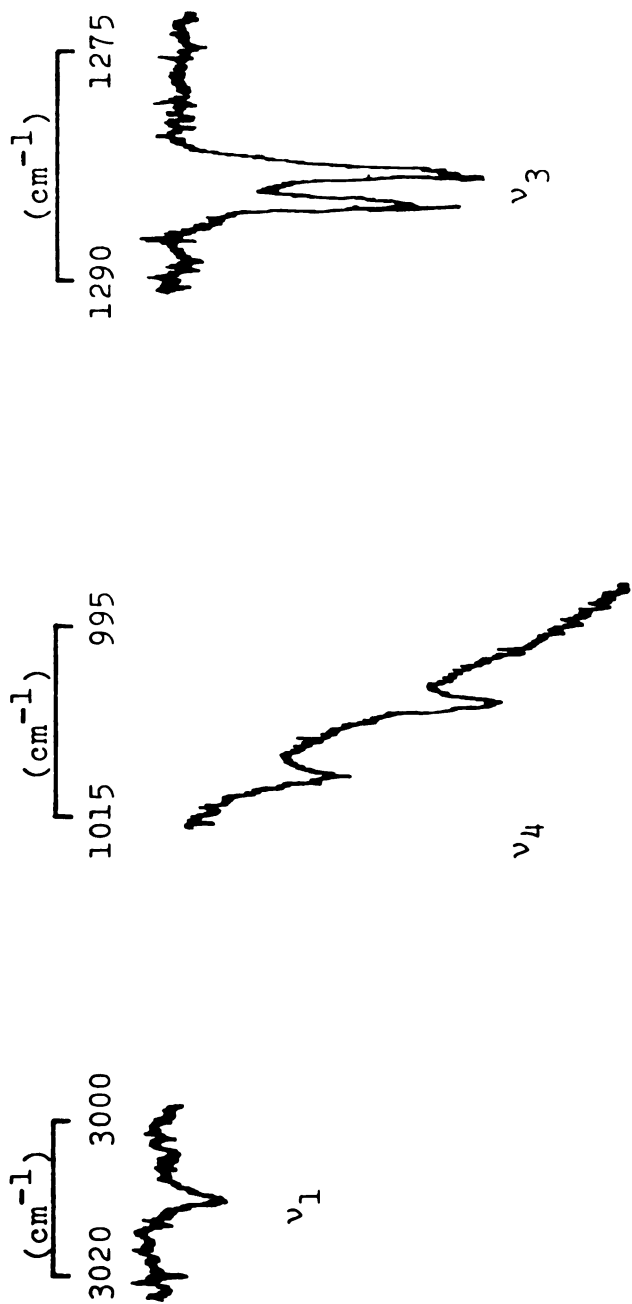


Figure 10. Part of the infrared spectrum of 1% C_2H_3D/C_2H_4 ; ν_1 , ν_4 and ν_3 of C_2H_3D .

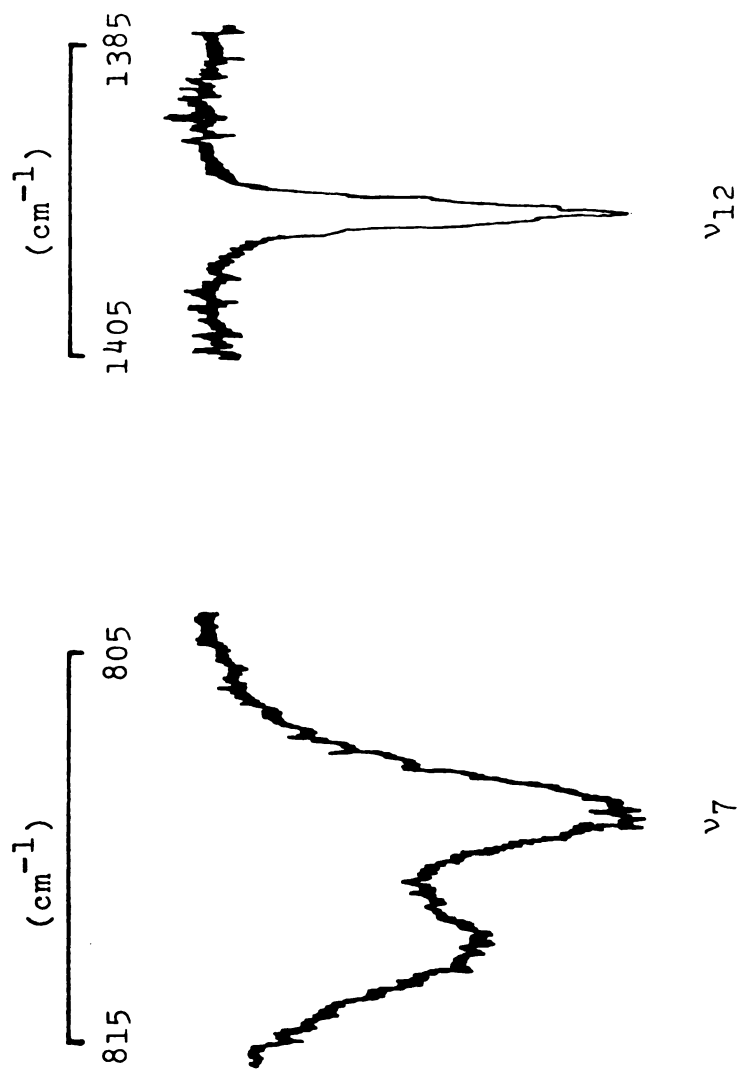


Figure 11. Part of the infrared spectrum of 1% $\text{C}_2\text{H}_3\text{D}/\text{C}_2\text{H}_4$; ν_7 and ν_{12} of $\text{C}_2\text{H}_3\text{D}$.

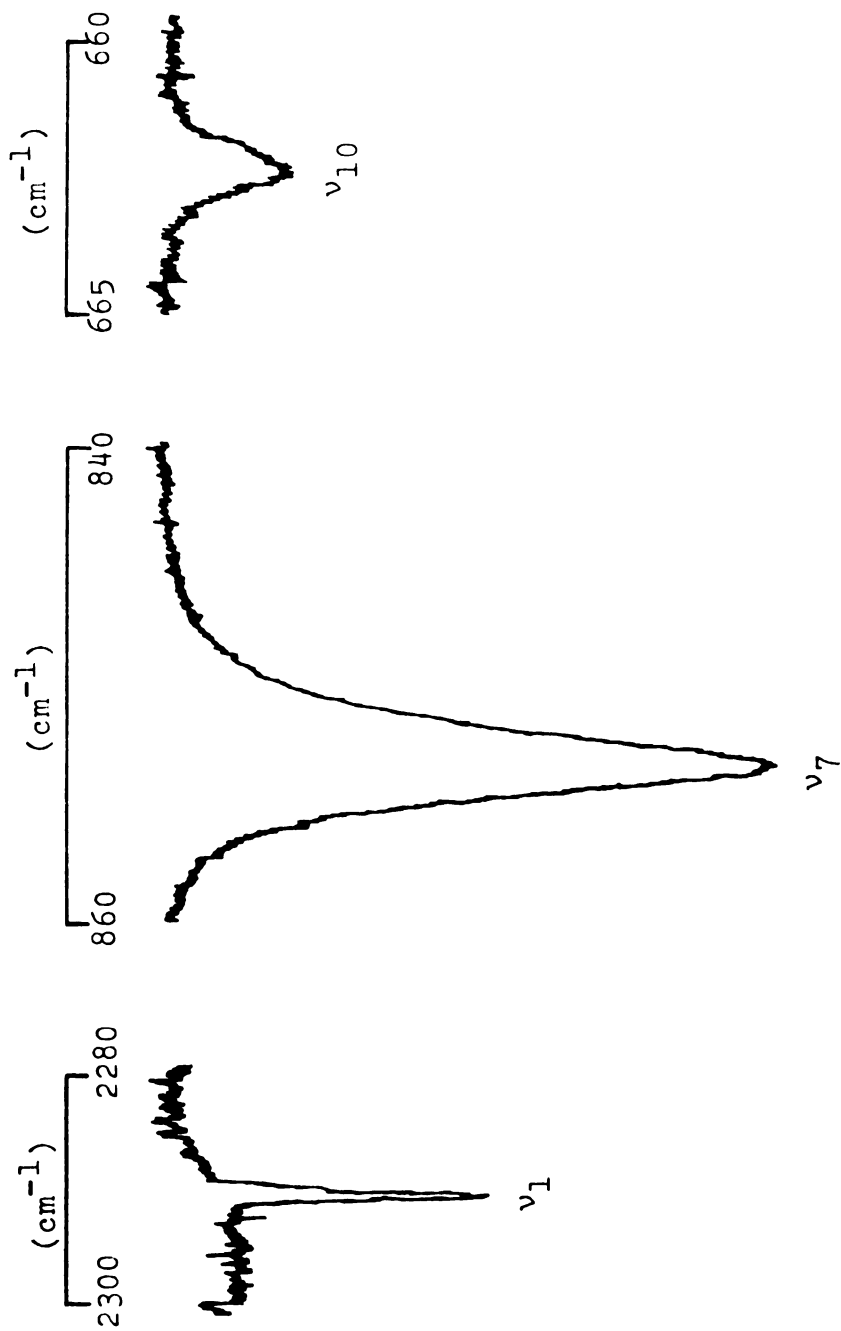


Figure 12. Part of the infrared spectrum of 1% cis- $\text{C}_2\text{H}_2\text{D}_2/\text{C}_2\text{H}_4$; ν_1 , ν_7 and ν_{10} of cis- $\text{C}_2\text{H}_2\text{D}_2$.

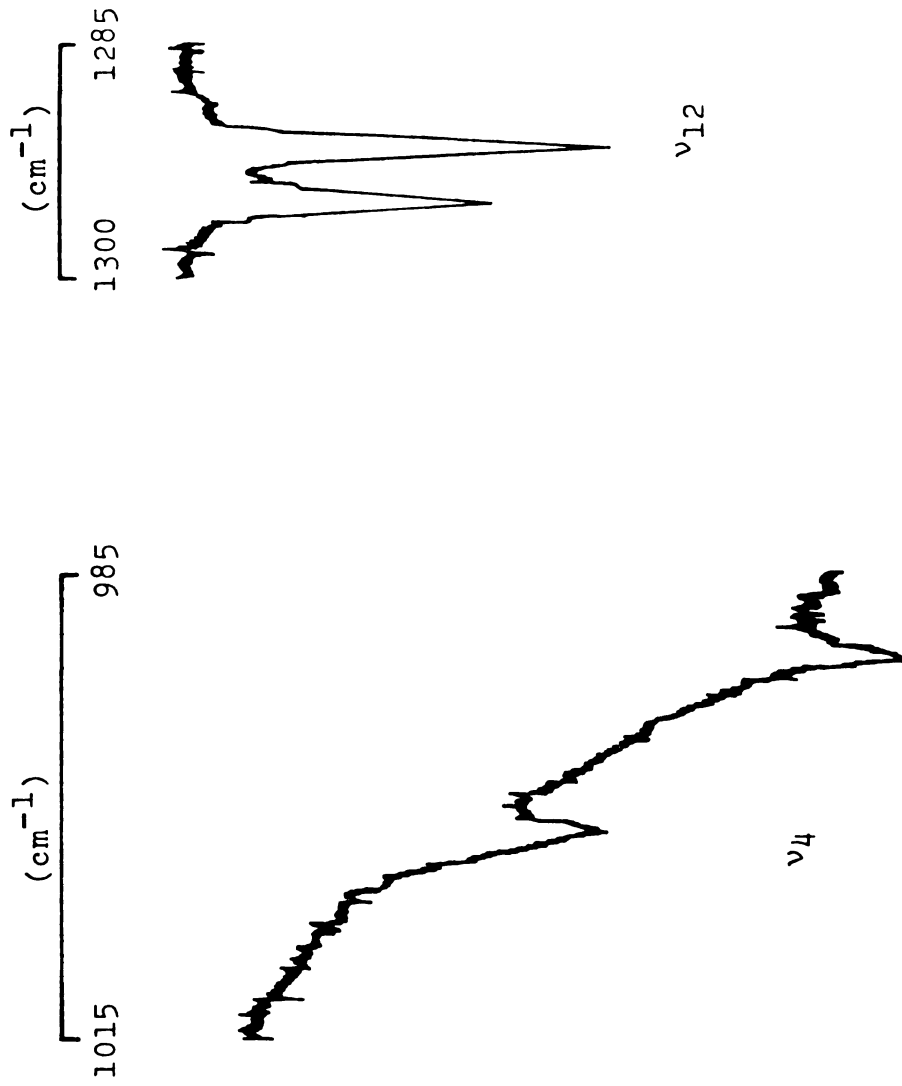


Figure 13. Part of the infrared spectrum of 1% trans- $\text{C}_2\text{H}_2\text{D}_2/\text{C}_2\text{H}_4$; ν_4 and ν_{12} of trans- $\text{C}_2\text{H}_2\text{D}_2$.

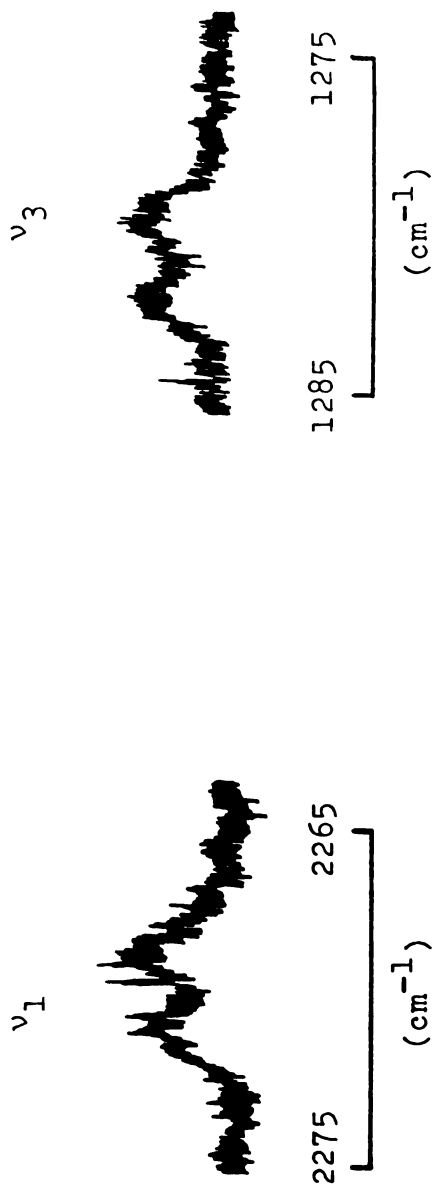


Figure 14. Part of the Raman spectrum of 1% trans-C₂H₂D₂/C₂H₄; ν_1 and ν_3 of trans-C₂H₂D₂.

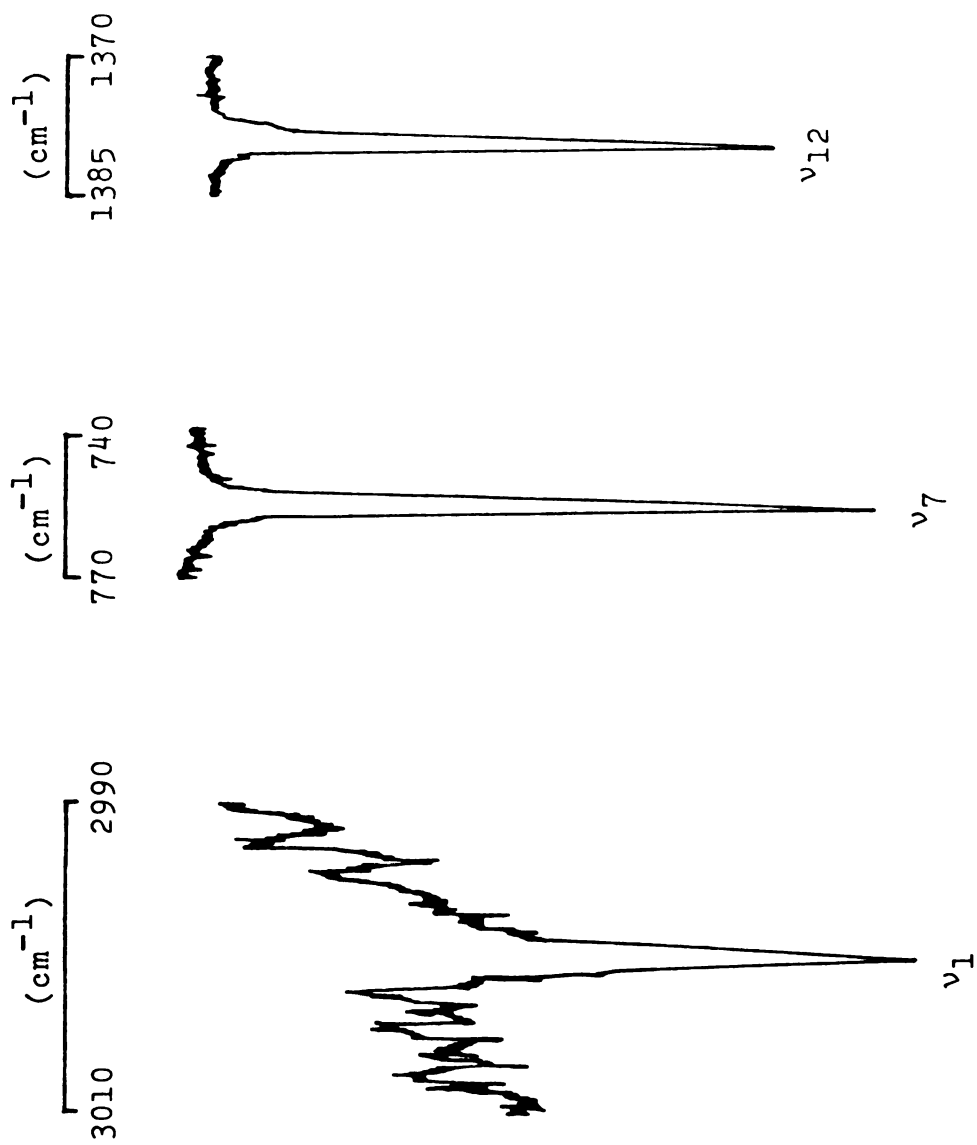


Figure 15. Part of the infrared spectrum of 1% 1,1,1-C₂H₂D₂/C₂H₄; ν₁, ν₇ and ν₁₂ of 1,1,1-C₂H₂D₂.

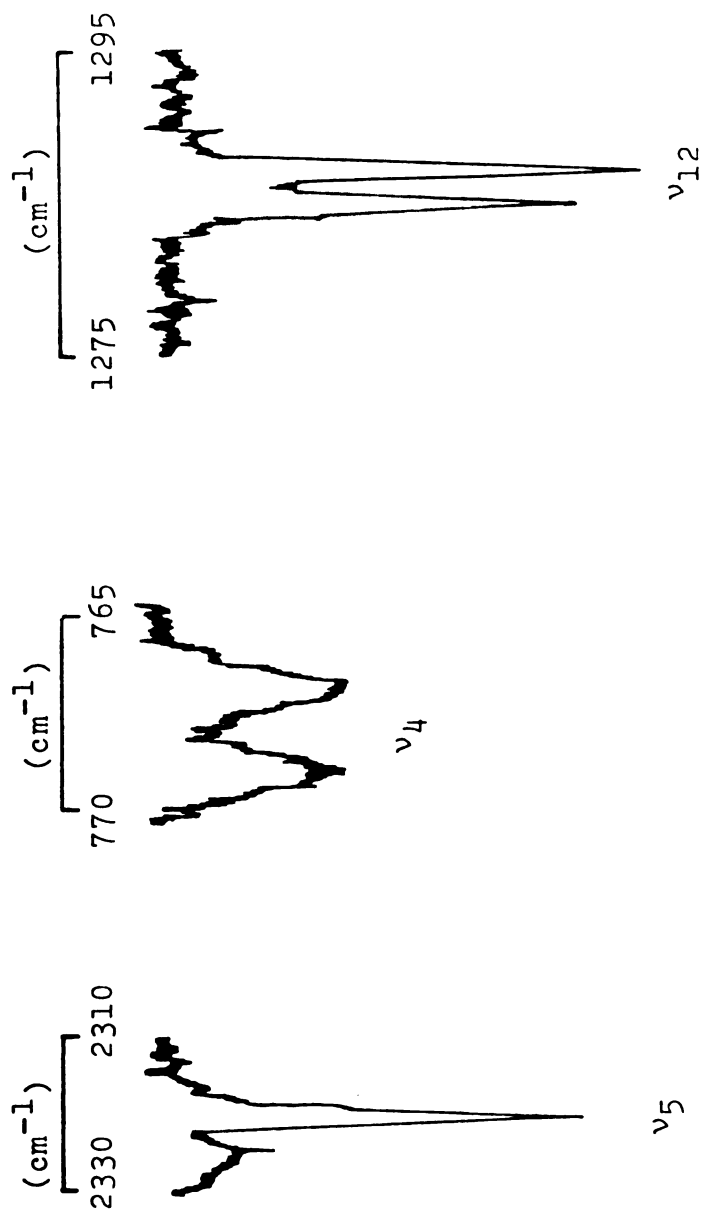


Figure 16. Part of the infrared spectrum of 1% C₂HD₃/C₂H₄; ν₅, ν₄ and ν₁₂ of C₂HD₃.

1500 cm^{-1} was considered the best place to observe the guest modes of the dilute-mixed crystal for this reason. The lack of overtones and combinations in this region facilitated the assignment of the guest modes. The guest bands are also less likely to be perturbed (quasiresonance) in this spectral region due to the lower density of host bands. The guest modes were most easily observed in the infrared, where thick samples could be studied. The uncertainty of the reported frequencies is expected to be higher for the Raman because wider slits were necessary to observe the guest modes.

$\text{C}_2\text{H}_3\text{D}$ impurity was present in all of the neat samples except C_2HD_3 , so $\text{C}_2\text{H}_3\text{D}$ was used as the probe species. The C_2HD_3 site symmetry was probed by the addition of 1% ethylene- d_1 impurity, and checked by observing the modes of the 1,1- $\text{C}_2\text{H}_2\text{D}_2$ impurity which was present in the neat sample. The site symmetry of the $\text{C}_2\text{H}_3\text{D}$ crystal was probed by adding 1% ethylene- d_3 impurity.

Some of the guest modes of these dilute mixed crystals are displayed in Figures 17-24. The displayed modes were selected where possible to enable comparison with the modes in C_2H_4 . The frequencies of all the guest modes are tabulated in Tables 17-22, and in Appendix A if the guest was an impurity in the neat sample. In the crystals where the ethylene- d_1 is the probe, the guest modes are either doublets or singlets, and the ethylene- d_3

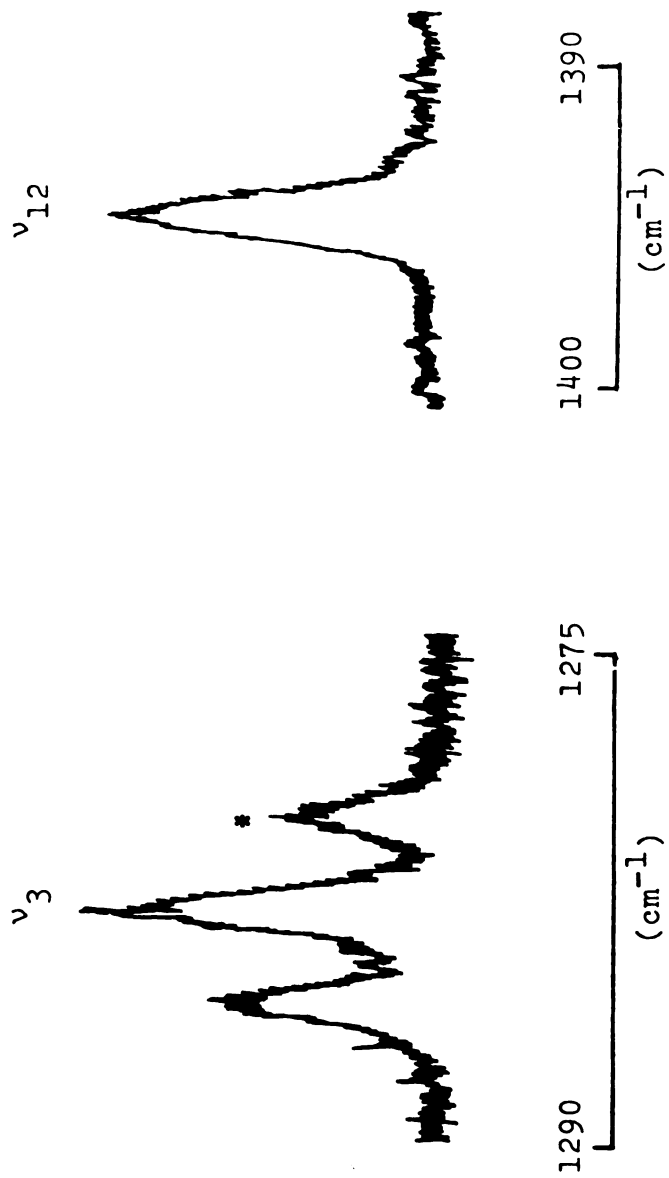


Figure 17. Part of the Raman spectrum of 4% $\text{C}_2\text{H}_3\text{D}/\text{cis}-\text{C}_2\text{H}_2\text{D}_2$; ν_3 and ν_{12} of $\text{C}_2\text{H}_3\text{D}$. The peak marked with an asterisk is assigned as ν_3 of $\text{trans}-\text{C}_2\text{H}_2\text{D}_2$.

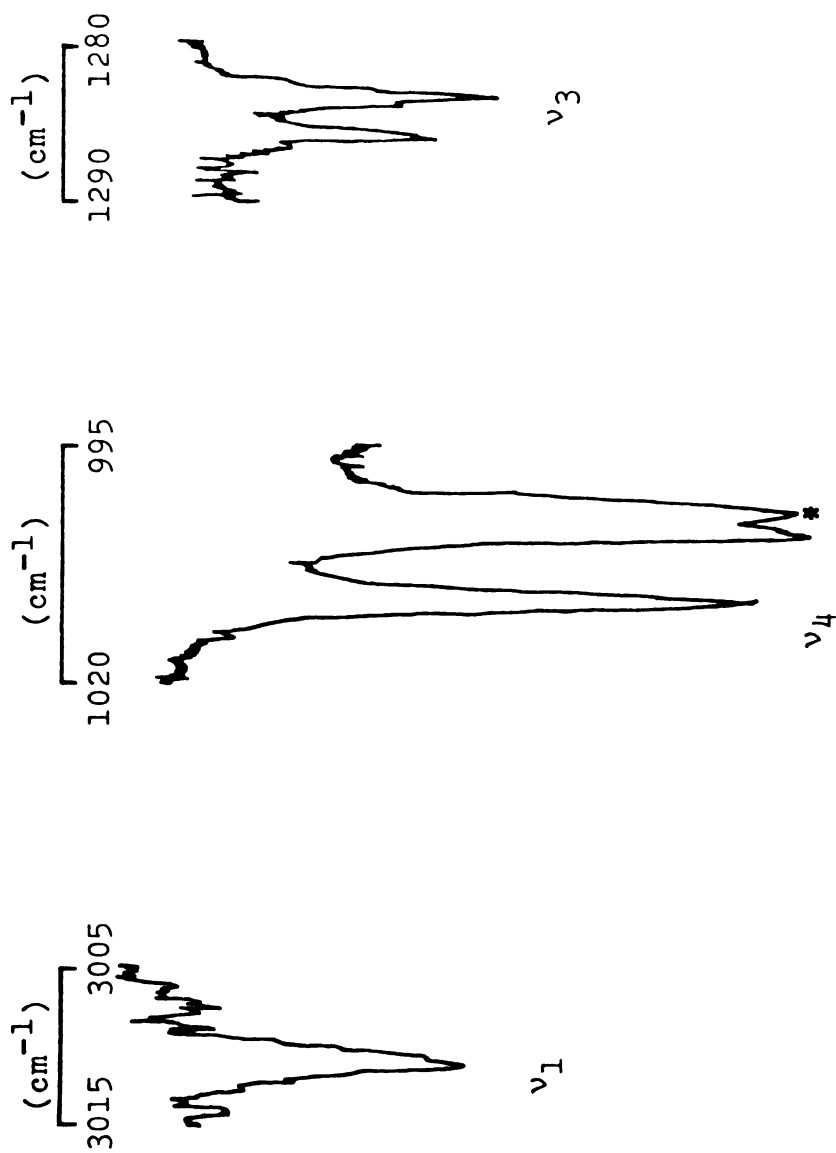


Figure 18. Part of the infrared spectrum of 4% $\text{C}_2\text{H}_3\text{D}/\text{cis-C}_2\text{H}_2\text{D}_2$; ν_1 , ν_4 and ν_3 of $\text{C}_2\text{H}_3\text{D}$. The peak marked with an asterisk is assigned as ν_4 $\text{trans-C}_2\text{H}_2\text{D}_2$.

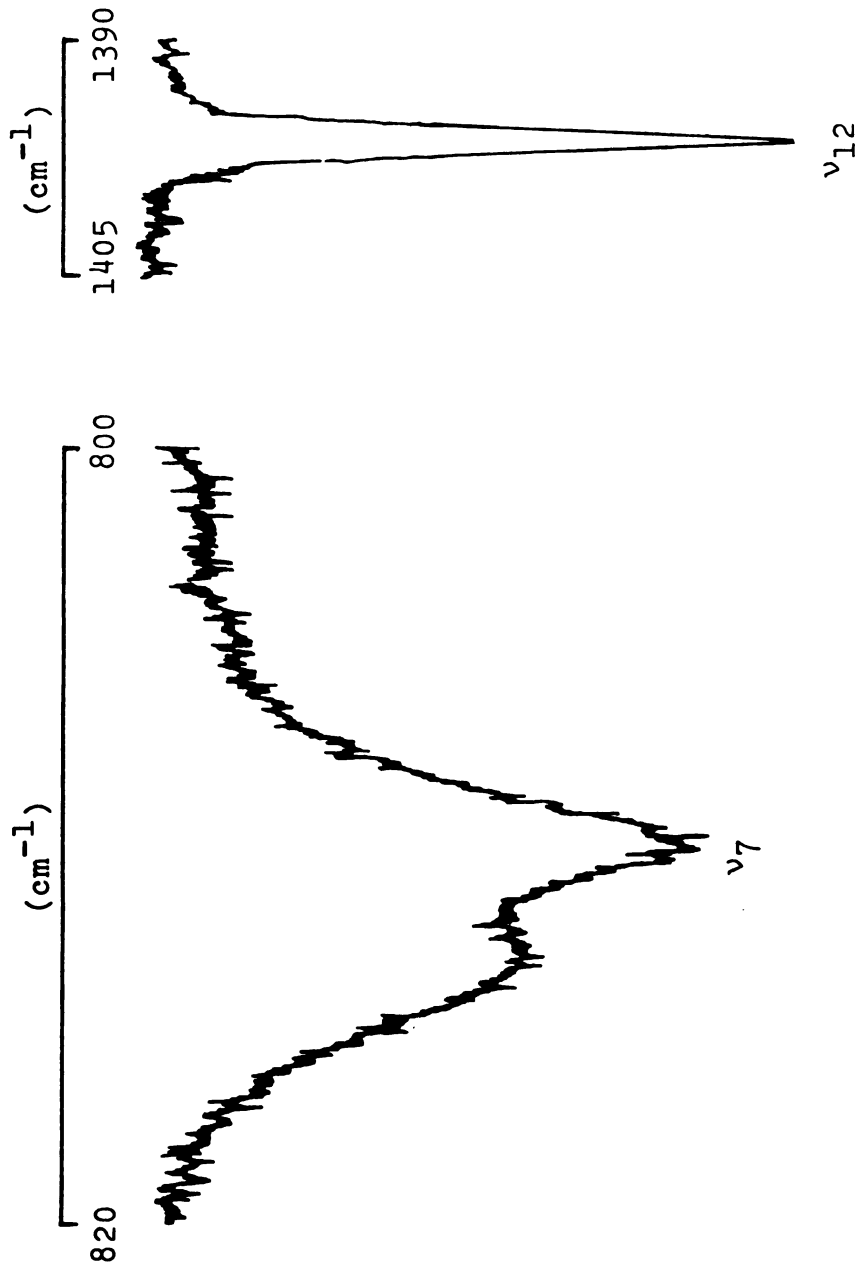


Figure 19. Part of the infrared spectrum of 1% $\text{C}_2\text{H}_3\text{D}/\text{trans}-\text{C}_2\text{H}_2\text{D}$; ν_7 and ν_{12} of $\text{C}_2\text{H}_3\text{D}$.

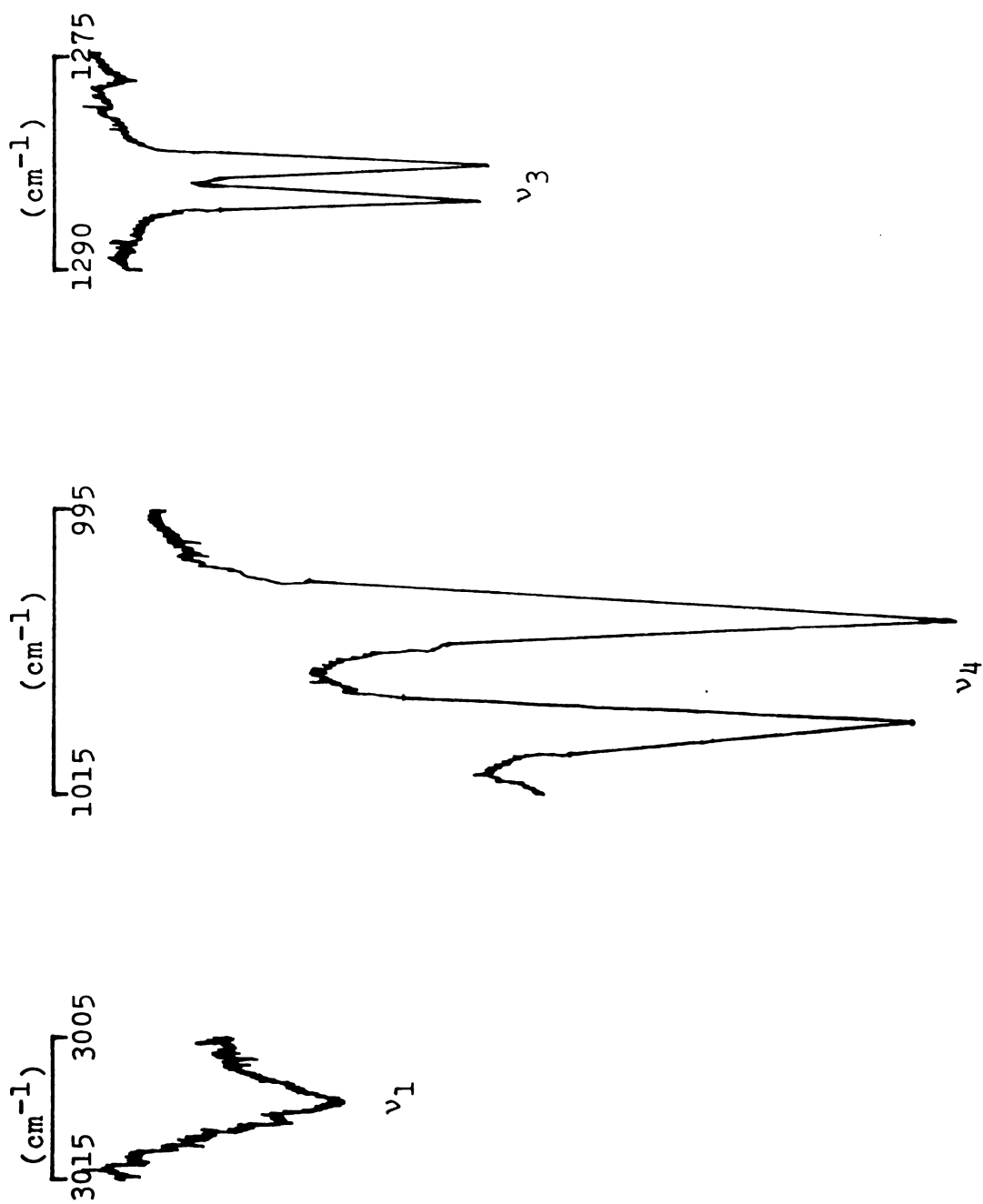


Figure 20. Part of the infrared spectrum of 4% $\text{C}_2\text{H}_3\text{D}/1,1\text{-C}_2\text{H}_2\text{D}_2$: ν_1 , ν_4 and ν_3 of $\text{C}_2\text{H}_3\text{D}$.

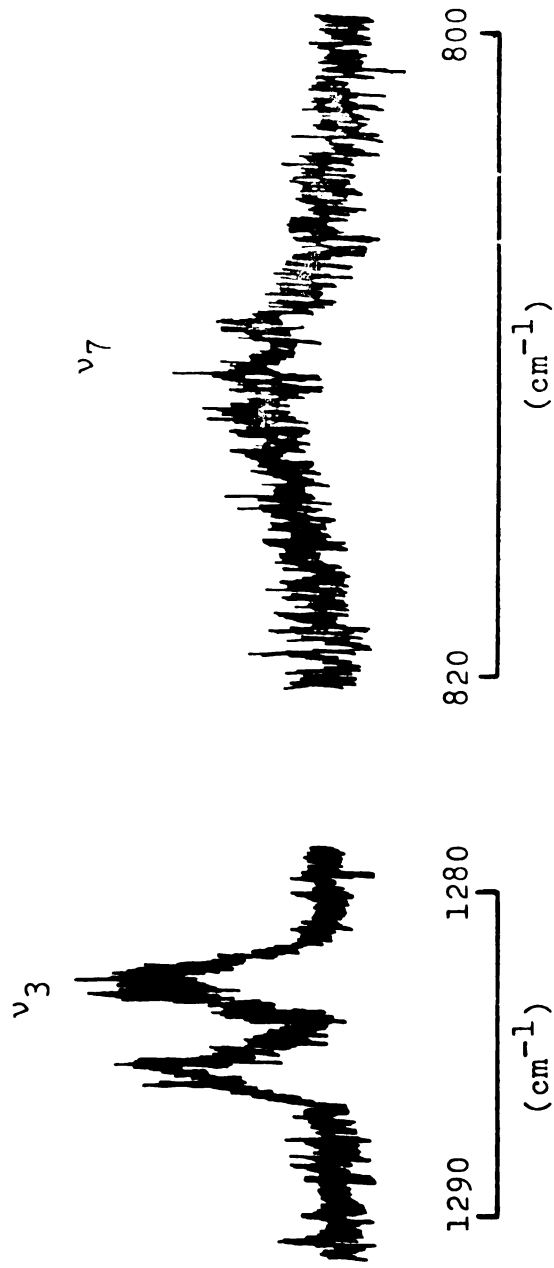


Figure 21. Part of the Raman spectrum of 4% $\text{C}_2\text{H}_3\text{D}/1,1\text{-C}_2\text{H}_2\text{D}_2$; ν_3 and ν_7 of $\text{C}_2\text{H}_3\text{D}$.

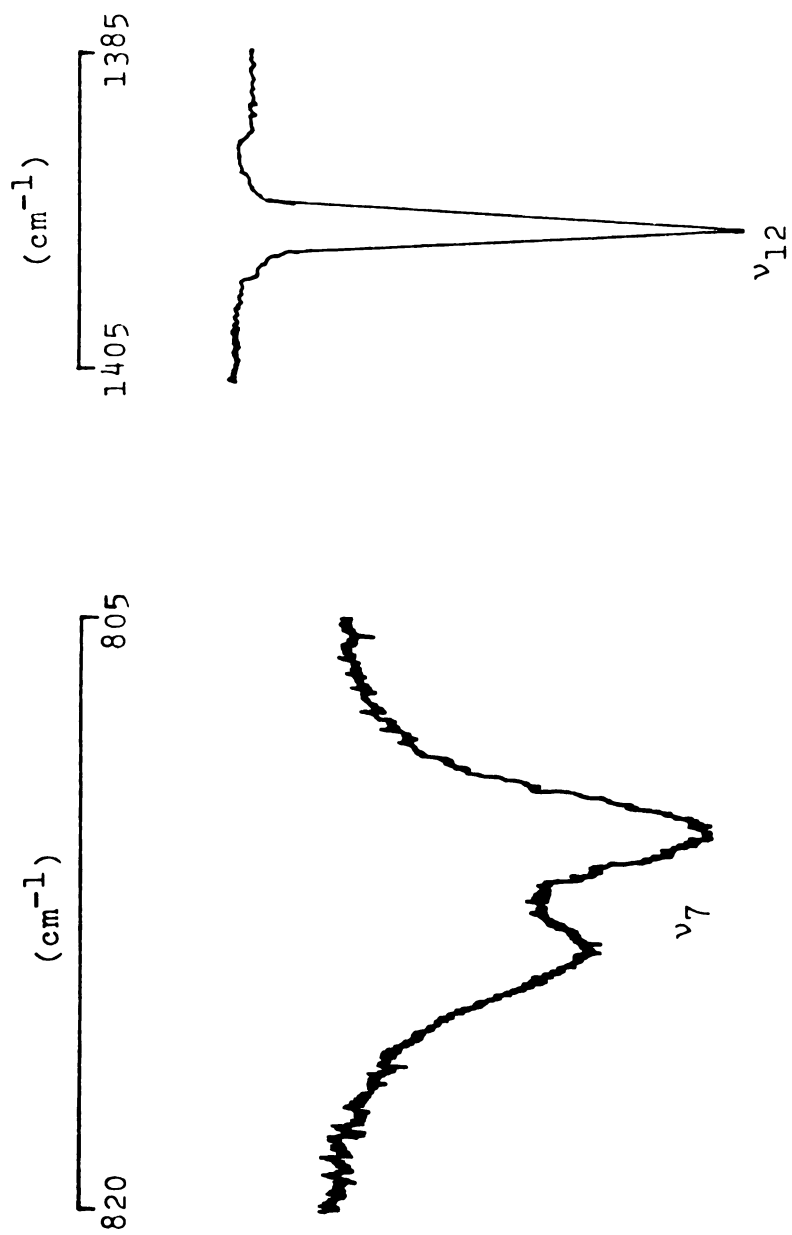


Figure 22. Part of the infrared spectrum of 1% $\text{C}_2\text{H}_3\text{D}/\text{C}_2\text{HD}_3$; ν_7 and ν_{12} of $\text{C}_2\text{H}_3\text{D}$.

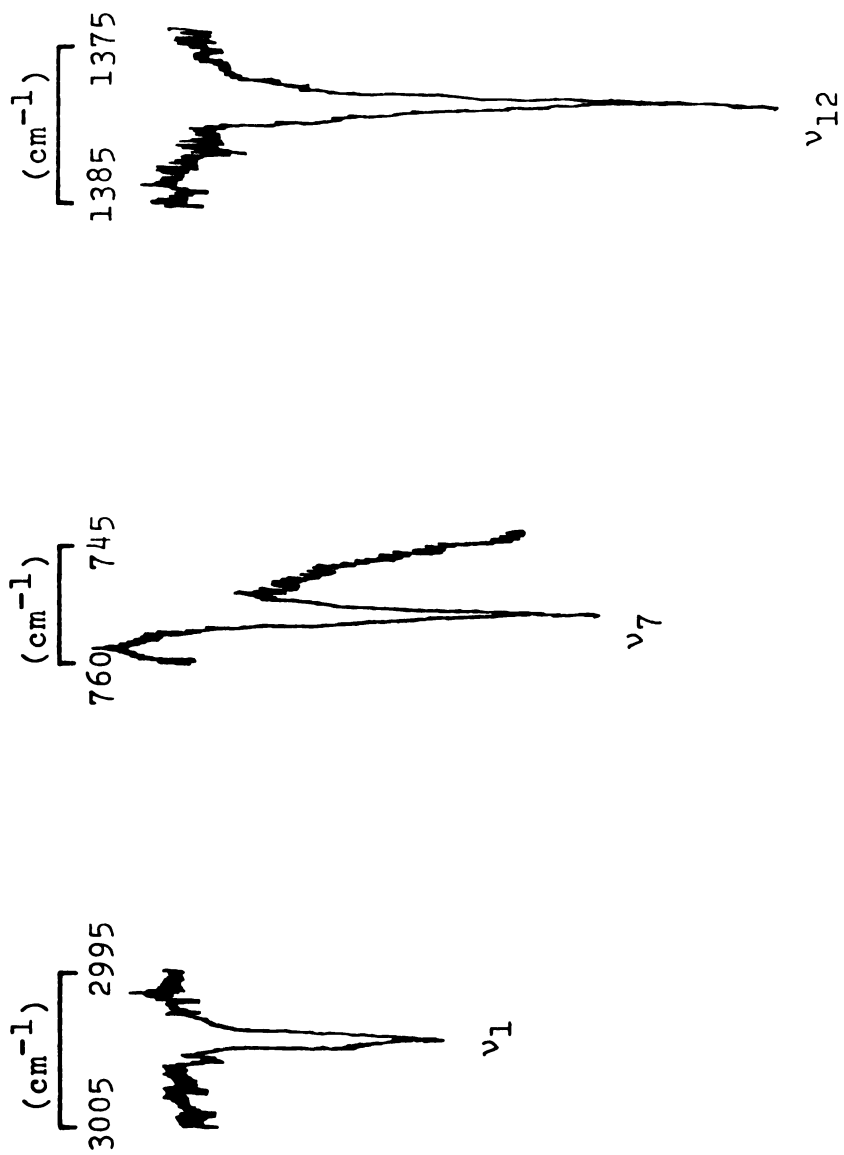


Figure 23. Part of the infrared spectrum of 1,1-C₂H₂D₂/C₂HD₃; ν_1 , ν_7 and ν_{12} of 1,1-C₂H₂D₂.

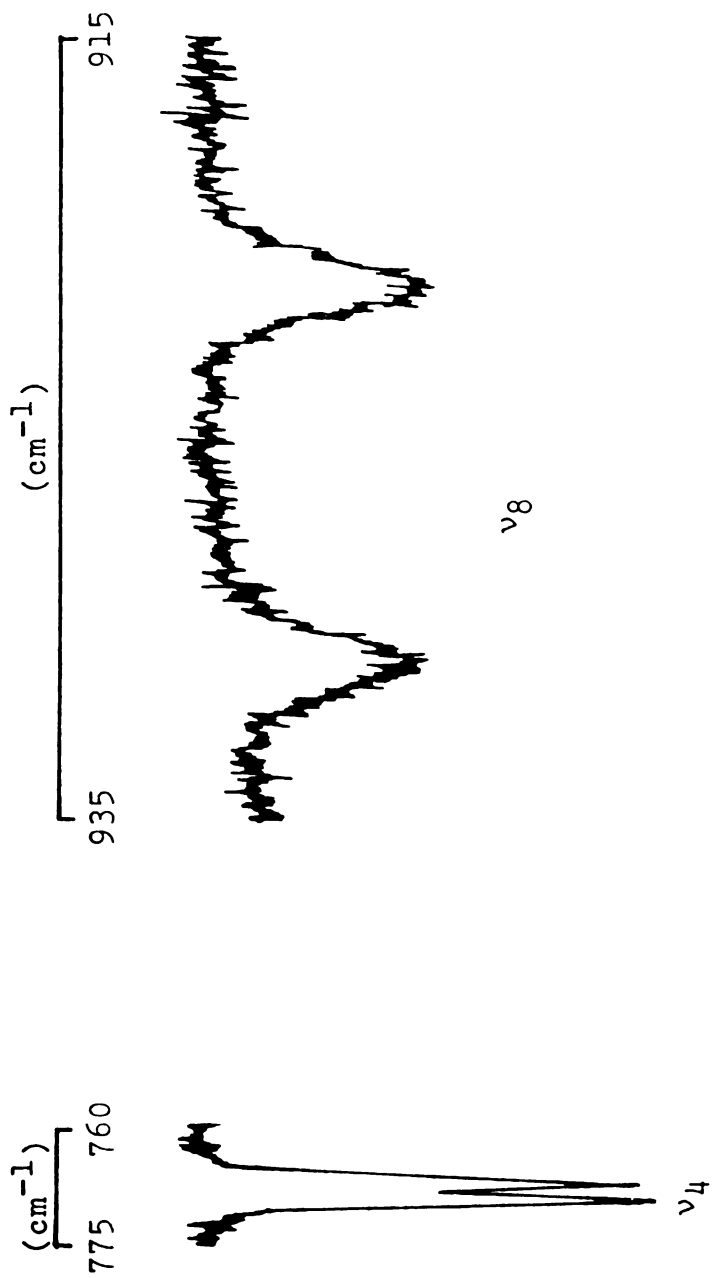


Figure 24. Part of the infrared spectrum of 1% $\text{C}_2\text{HD}_3/\text{C}_2\text{H}_3\text{D}$; ν_4 and ν_8 of C_2HD_3 .

Table 17. Observed frequencies of C_2H_3D fundamentals in
4% $C_2H_3D/cis-C_2H_2D_2$.

Infrared (cm^{-1})	Raman (cm^{-1})	Assignment
3011.2	3010.5	ν_1
1597.8	1595.4	ν_2
1286.1	1285.7	ν_3
1283.4	1282.8	
1011.1		ν_4
1003.9		
	3047.5	ν_5
	1124.0	ν_6
812.8	810.2	ν_7
809.6		
	2261.8	ν_{11}
	2259.3	
1396.8	1394.7	ν_{12}

Table 18. Observed frequencies of C_2H_3D fundamentals in
1% $C_2H_3D/trans-C_2H_2D_2$.

Infrared (cm^{-1})	Raman (cm^{-1})	Assignment
1597.1	1598.7	ν_2
813.2		ν_7
810.1		
1396.8		ν_{12}

Table 19. Observed frequencies of C_2H_3D fundamentals in
 4% $C_2H_3D/1,1-C_2H_2D_2$.

Infrared (cm^{-1})	Raman (cm^{-1})	Assignment
3009.8	3011.5	ν_1
1596.9	1596.8	ν_2
1285.0	1285.5	ν_3
1282.8	1283.1	
1010.2		ν_4
1002.9		
3048.0	3048.5	ν_5
3044.8	3044.8	
813.2	810.4	ν_7
810.0		
730.9		ν_{10}
729.5		
2262.1		ν_{11}
2260.2		
1396.8	1396.6	ν_{12}

Table 20. Observed frequencies of C_2H_3D fundamentals in
1% C_2H_3D/C_2HD_3 .

Infrared (cm^{-1})	Assignment
1012.0	ν_4
813.4	
810.3	ν_7
1396.0	ν_{12}

Table 21. Observed frequencies of 1,1-C₂H₂D₂ fundamentals
in 1,1-C₂H₂D₂/C₂HD₃.

Infrared (cm ⁻¹)	Raman (cm ⁻¹)	Assignment
2999.7		ν_1
1578.4		ν_2
754.4		ν_7
2216.6	2217.5	ν_{11}
1378.6	1381.3	ν_{12}

Table 22. Observed frequencies of C_2HD_3 fundamentals in 1% C_2HD_3/C_2H_3D .

Infrared (cm^{-1})	Assignment
1039.8	ν_3
769.8	
767.8	ν_4
2320.9	ν_5
736.6	
723.6	ν_7
931.0	
921.4	ν_8
3031.3	ν_9
2209.5	ν_{11}

modes of ethylene-d₃/ethylene-d₁ are also either doublets or singlets. For the ethylene-1,1-d₂/C₂HD₃ only singlets were observed. In no case was a multiplet higher than that allowed by a C₁ site observed.

In the ν_4 region of C₂H₃D in the 4% C₂H₃D/cis-C₂H₂D₂ infrared spectrum a triplet is observed as shown in Figure 18. The 1001.8 cm⁻¹ peak has been assigned as an orientational component of ν_4 of trans-C₂H₂D₂. The other ν_4 component of the trans-C₂H₂D₂ is believed to be hidden by ν_4 of cis-C₂H₂D₂. Unfortunately this could not be compared with the Raman spectrum in this region because even for neat C₂H₃D ν_4 was not observed in the Raman (see next chapter). However, ν_4 of the trans-C₂H₂D₂ is not expected to be Raman active, and the 1001.8 component was not observed either. (Many trans-C₂H₂D₂ impurity modes were observed in the spectrum of neat cis-C₂H₂D₂.)

Another triplet was observed in the ν_3 of C₂H₃D region in the C₂H₂D/cis-C₂H₂D₂ Raman spectrum (see Figure 17). The low frequency component (1280.0 cm⁻¹) is assigned as an orientational component of ν_3 of trans-C₂H₂D₂. The middle component is comprised of the low frequency orientational component of ν_3 of C₂H₃D and the high frequency component of ν_3 of the trans-C₂H₂D₂ (note its greater intensity). These assignments are consistent with the spectra of C₂H₃D/C₂H₄ and trans-C₂H₂D₂/C₂H₄. A doublet is observed in this region in the infrared.

This is consistent with the observed activity of the trans-C₂H₂D₂ modes.

The dilute-mixed crystal spectra clearly indicate an "effective" centrosymmetric site symmetry. The near-sightedness of the ethylenes can be further investigated by comparing the spectrum of the probe molecule in the partially-deuterated host with the spectrum of the probe in the C₂H₄ lattice, which has sites which are known to have C₁ symmetry.

The difference in the orientational splittings of ν_7 (C₂HD₃) in C₂H₃D and C₂H₄ hosts is thought to be caused by the presence of ν_{10} of C₂H₃D between the orientational components of ν_7 (C₂HD₃) in the C₂HD₃/C₂H₃D crystal. Resonance interactions between the C₂HD₃ molecules and the C₂H₃D molecules is believed to cause the difference in orientational splittings of 1.6 cm⁻¹. This is the only case where the difference in splittings from one host to another exceeds the experimental uncertainty.

The following bands have shown a different number of orientational components in different hosts.

ν_8 (C₂HD₃) - Shows two components in the C₂H₃D host, at 931.0 cm⁻¹ and 921.4 cm⁻¹, but shows only one component, at 920.9 cm⁻¹ in the C₂H₄ host. It is believed that the high frequency component in C₂H₄ host is hidden by the low frequency Davydov component of ν_7 (C₂H₄) at 941.0 cm⁻¹.

- ν_9 (C_2HD_3) - Shows two components in C_2H_4 at 3034.0 cm^{-1} and 3030.2 cm^{-1} but only one component at 3031.3 cm^{-1} is observed in C_2H_3D host. Undoubtedly the peak at 3034.0 cm^{-1} in the C_2H_3D neat crystal spectrum (see Appendix A) hides the 3034.0 cm^{-1} component.
- ν_5 (C_2H_3D) - Shows two components in C_2H_4 at 3047.8 cm^{-1} and 3043.2 cm^{-1} but only one component at 3047.5 cm^{-1} is observed in the *cis*- $C_2H_2D_2$ host. The 3043.2 cm^{-1} peak is obviously hidden in the *cis*- $C_2H_2D_2$ host by ν_9 (*cis*- $C_2H_2D_2$) at 3043.2 cm^{-1} .

A comparison of the spectra of the mixed-partially deuterated ethylenes with those of the partially-deuterated ethylenes in C_2H_4 reveals the number and frequency of the orientational components are the same in most cases. This clearly indicates that the ethylenes are "nearsighted", that is the intermolecular interactions are very similar in all the ethylenes.

C. Conclusions

The following conclusions can be drawn from the observations of the guest modes of the dilute-mixed crystals of the partially-deuterated ethylenes in C_2H_4 host and

in each other.

The "effective" site symmetry of the partially-deuterated ethylene crystals is C_1 . Therefore the ethylene molecules are nearsighted in that they cannot distinguish between hydrogens and deuteriums on neighboring molecules in the crystal. The intermolecular interactions are myopic; deuteration causes little change in the intermolecular force field of the ethylene crystals.

CHAPTER VI

THE INTERNAL MODES OF THE PARTIALLY-DEUTERATED ETHYLENES

A. Introduction

It has been shown in the last two chapters that the crystals of the partially-deuterated ethylenes have an "effective" C_1 site symmetry. This leads to the existence of only one energetically-distinguishable orientation of the molecules in the cis- $C_2H_2D_2$ and 1,1- $C_2H_2D_2$ crystals, and two energetically-inequivalent orientations in the C_2H_3D , trans- $C_2H_2D_2$ and C_2HD_3 crystals (see Table 11). This chapter is therefore divided into six sections. Section B concerns the assignments of the internal modes of the cis- $C_2H_2D_2$ and 1,1- $C_2H_2D_2$ crystals; C describes the coherent potential approximation calculation used to compute the band splittings of the C_2H_3D , trans- $C_2H_2D_2$ and C_2HD_3 crystals; D deals with the observed fundamental vibrations of these crystals; and in Section E a comparison of all the internal mode data is discussed.

A comment on the assignments of the observed frequencies is in order. The free molecules of the partially-deuterated ethylenes are of lower symmetry than the D_{2h} symmetry of ethylene. Therefore, fundamentals, overtones and combinations which were inactive for the C_2H_4 and C_2D_4

crystals may now become active, and Fermi resonance,⁵³ which is observed only to a small extent in the ethylene crystal,²⁴ may become more prevalent in the crystals of the partially-deuterated ethylenes due to the lower symmetry of the molecules. The neat samples also contained some impurities as discussed in Chapter III, and natural abundance C-13 impurity was present in all the samples. Thus the spectra of the neat partially-deuterated samples exhibit many bands and assignment of these is at best tedious. The spectra are most complicated in the higher frequency regions ($>1500\text{ cm}^{-1}$) where the overtones and combinations appear, and therefore Fermi resonances become more likely. Bands due to C-13 substituted molecules, present in 2.2% natural abundance, may also complicate the C-12 bands through intermolecular Fermi resonance.^{13,26} The calculated C-13 harmonic shifts from the free molecule C-12 frequencies of the partially-deuterated ethylenes are given in Table 23. The shifts were calculated by Duncan^{24,54} using standard normal coordinate analysis procedures.⁵⁵

The assignments given in this chapter were based on gas phase frequencies, relative intensities, calculated C-13 shifts and observed dilute mixed crystal frequencies (see Chapter 5). Also, mutual exclusion was not observed except for trans-ethylene-d₂, so a comparison of infrared and Raman data aided in the assignments. Only bands

Table 23. Calculated harmonic C-13 shifts (cm^{-1}) from the C-12 frequencies.

$\text{C}_2\text{H}_3\text{D}^{\text{a}}$	$\text{H}_2^{12}\text{C}=\text{}^{13}\text{CHD}$	$\text{H}_2^{13}\text{C}=\text{}^{12}\text{CHD}$
ν_1	0.3	5.9
ν_2	18.3	26.1
ν_3	3.2	6.9
ν_4	1.8	0.0
ν_5	9.5	0.6
ν_6	5.2	8.6
ν_7	8.0	0.2
ν_8	0.8	9.2
ν_9	0.3	12.8
ν_{10}	1.9	0.2
ν_{11}	15.1	0.4
ν_{12}	10.7	0.2
$1,1\text{-C}_2\text{H}_2\text{D}_2^{\text{b}}$	$\text{H}_2^{13}\text{C}=\text{}^{12}\text{CD}_2$	$\text{H}_2^{12}\text{C}=\text{}^{13}\text{CD}_2$
ν_1	5.8	0.1
ν_2	25.7	13.3
ν_3	3.7	0.4
ν_4	0	0
ν_5	0.0	16.7
ν_6	9.9	6.9
ν_7	0.3	10.7
ν_8	8.8	0.7
ν_9	11.6	0.1
ν_{10}	0.1	2.3
ν_{11}	0.9	12.1
ν_{12}	1.4	12.4

Table 23. Continued.

$C_2HD_3^a$	$HD^{12}C=^{13}CD_2$	$HD^{13}C=^{12}CD_2$
ν_1	3.8	14.0
ν_2	20.2	25.9
ν_3	3.6	6.4
ν_4	8.2	2.6
ν_5	17.8	0.4
ν_6	4.9	5.6
ν_7	3.0	2.1
ν_8	0.5	5.8
ν_9	0.1	10.0
ν_{10}	1.1	0.2
ν_{11}	9.7	1.4
ν_{12}	6.8	1.4

$cis-C_2H_2D_2^a$	$cis-HD^{12}C=^{13}CHD$	$trans-C_2H_2D_2^a$	$trans-HD^{12}C=^{13}CHD$
ν_1	8.2	ν_1	6.9
ν_2	23.9	ν_2	23.5
ν_3	2.3	ν_3	7.5
ν_4	2.8	ν_4	1.0
ν_5	5.7	ν_5	10.0
ν_6	8.6	ν_6	6.7
ν_7	2.9	ν_7	2.2
ν_8	4.8	ν_8	7.3
ν_9	4.3	ν_9	0.1
ν_{10}	0.5	ν_{10}	0.9
ν_{11}	7.2	ν_{11}	8.6
ν_{12}	4.1	ν_{12}	1.1

^aFrom Reference 54.^bFrom Reference 24.

assigned as fundamentals are presented in the wavenumber tables in this chapter; however, all the frequencies observed for the neat crystals, and their relative intensities are listed in Appendix A.

B. The Internal Modes of cis-C₂H₂D₂ and 1,1-C₂H₂D₂

An analogy can be drawn between the internal modes of the cis-C₂H₂D₂, 1,1-C₂H₂D₂, C₂H₄ and C₂D₄ crystals because the internal mode spectrum is not complicated by the orientational effect. However, it must be noted that cis-ethylene-d₂ and ethylene-1,1-d₂ are still disordered because of the existence of the translationally-inequivalent orientations. Therefore adherence to the \underline{k} selection rules may be questionable.

Unfortunately there have been only a few studies of the internal modes of disordered molecular crystals.⁵⁶⁻⁵⁹ Most of these have dealt with isotopic mixed crystals whose modes are in the separate-band limit⁴⁴ (see next section), and the goal has been to resolve disputes over the splittings in the pure crystal spectrum. Little effort has been concentrated on the internal modes in the amalgamation limit⁴⁴ (see next section). However, studies of the phonons of isotopic mixed molecular crystals have revealed the usefulness of \underline{k} in the amalgamation limit (see Chapter IV).

The amalgamation limit is achieved when the energy difference between the host and guest vibration is much less than the bandwidth of the pure-crystal mode. Formally one can say that the energy difference between the orientational components of the $\text{cis-C}_2\text{H}_2\text{D}_2$ and $1,1\text{-C}_2\text{H}_2\text{D}_2$ crystals is zero. That is, for each vibration all orientations have only one energy, and thus the energy difference is zero. Zero is certainly less than the bandwidth of the vibration, and thus the internal vibrations of these crystals are in the amalgamation limit.

Excitons are more localized than phonons, and thus the phonons of a crystal probe the periodicity of the lattice over a larger range than do the vibrational excitons. Therefore, if \underline{k} is a "good quantum number" for the phonons of a disordered solid in the amalgamation limit it is certainly expected to be a "good quantum number" for the vibrational excitons of the disordered solid in this limit. If \underline{k} selection rules still apply to these disordered solids, then the bands should show two Davydov components as do the bands of ethylene and ethylene- d_4 . A breakdown of \underline{k} selection rules would lead to broad, structureless bands.

The observed fundamental vibrational frequencies of $\text{cis-C}_2\text{H}_2\text{D}_2$ and $1,1\text{-C}_2\text{H}_2\text{D}_2$ are listed in Tables 24 and 25. Two Davydov components were resolved for eight of the twelve $\text{cis-C}_2\text{H}_2\text{D}_2$ fundamentals and nine of the twelve

Table 24. Internal fundamental frequencies (cm^{-1}) of cis- $\text{C}_2\text{H}_2\text{D}_2$.^a

Mode	Infrared	Raman	In C_2H_4 ^b	Gas ^c
ν_1	2286.2 vs (1.9) 2278.0 vw	2287.1 vs (1.1) 2278.9 ^e w	2285.1	2299
ν_2	1564.0 m,asy (3.9)	1563.7 vw 1560.3 vs 1541.6 ^e w	1563.7	1571
ν_3	1218.0 w,bd 1205.1 w,sp	1219.6 vs 1202.0 vs	1212.7	1218
ν_4	991.5 m,asy (4.8)	989.0 sh 985.3 s 982.2 s		
ν_5	3038.0 vs (3.2) 3032.4 ^e w	3037.3 s,sh 3035.9 s 3032.3 ^e w	3037.2	3054
ν_6	1034.0 m,asy (4.5) 1026.5 ^e w	1036.7 m 1033.0 m		1044
ν_7	849.4 vs 842.8 vs	850.8 vw (8.0)	853.4	842
ν_8	766.6 m (5.6)	761.8 m (7.0)		763
ν_9	3044.6 vs (3.0)	(3047.5) ^d 3043.2 vs (1.3)	3044.0	3059
ν_{10}	663.1 m 660.7 ^e w 658.4 s	661.3 s 658.8 sh	661.3	662

Table 24. Continued.

Mode	Infrared	Raman	In C ₂ H ₄ ^b	Gas ^c
ν_{11}	2242.1 s,asy (4.9)	2241.7 s,asy (2.2)	2241.8	2254
ν_{12}	1338.6 vs 1335.0 vs 1331.9 ^e w,sh		1335.0	1342

Key to Table:

- (a) ν = very, s = strong, m = moderate, w = weak, sh = shoulder, bd = broad, sh = sharp, asy = asymmetric; the full width at half height is given in parenthesis for the unresolved Davydov doublets.
- (b) Mean of observed infrared and Raman frequencies.
- (c) See Reference 24.
- (d) See text.
- (e) These frequencies attributed to C-13 substituted molecules.

Table 25. Internal fundamental frequencies (cm^{-1}) of
 $1,1\text{-C}_2\text{H}_2\text{D}_2$.*

Mode	Infrared	Raman	In C_2H_4 ^b	Gas ^c
ν_1	2998.9 s (3.2) 2993.2 ^g w	3000.6 sh 2999.3 vs 2993.1 ^g w	2999.8	3017
ν_2	1577.9 m (5.2) 1564.1 ^f w 1552.5 ^g w	1575.9 vs (.8) 1564.0 ^f m 1552.4 ^g m	1579.2	1585
ν_3	1024.9 s,bd (17.0)	1029.1 vs 1017.5 vs	1034.7	1031
ν_4	905.4 vs 901.6 vs			887
ν_5	2322.9 s (3.7) 2304.0 ^f w	2322.6 vs (1.6) 2305.7 ^f w	2322.8	2335
ν_6	1139.0 vw (7.0)	1142.4 w 1138.2 w		1142.4
ν_7	753.5 vs 749.1 vs 742.8 ^f s	752.8 s,asy (3.9)	754.8	750.5
ν_8	946.0 vs,asy(13.0)	955.3 sh 951.5 ^f sh 947.7 s		942.4
ν_9	3080.2 s 3078.4 s 3066.4 ^g w	3078.3 vs (2.3) 3067.8 ^g vw	3077.5	3094

Table 25. Continued.

Mode	Infrared	Raman	In C ₂ H ₄ ^b	Gas ^c
ν ₁₀	685.1 m	683.4 vw (9.4)	683.4	687.4
	682.6 ^g w			
	680.1 s			
ν ₁₁	2216.9 s (2.4)	2217.4 vs (1.0)	2216.6	2230
	2204.8 ^f w	2205.5 ^f w		
ν ₁₂	1379.8 vs (8.8)	1382.6 s	1380.3	1384
		1375.8 vs		
	1369.6 ^f s	1371.0 ^f m		

*Footnotes as in Table 24 except for f and g.

^fThese frequencies attributed to H₂¹²C = ¹³CD₂.

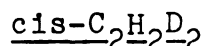
^gThese frequencies attributed to H₂¹³C = ¹²CD₂.

1,1-C₂H₂D₂ fundamentals. Only ν_4 of ethylene-1,1-d₂ and ν_{12} of cis-ethylene-d₂ were not observed in both the infrared and Raman spectra, although different relative intensities of the bands and of the components of the bands were observed in some cases in the infrared and Raman spectra. In general, the full width at half height of the peaks was larger in the infrared spectrum than in the Raman spectrum. This is attributed to a difference in sample quality and the fact that a larger portion of the solid is sampled by the infrared radiation, which thus detects imperfections in the sample that the Raman experiment does not detect. The full widths at half height of the infrared Davydov components were normally 3-5 cm⁻¹ and those in the Raman approximately 1-2 cm⁻¹. In the infrared, the stronger the component the broader it tended to be, whereas in the Raman the very strong components tended to have instrumentally-narrow bandwidths.

C-13 isotopic shifts were observed for six of the twelve cis-C₂H₂D₂ fundamentals and nine of the twelve 1,1-C₂H₂D₂ fundamentals. Both C-13 shifts of 1,1-C₂H₂D₂ were observed only for the ν_2 mode. The C-13 isotope with the largest shift was generally the one which was observed. The full widths at half height of the C-13 components were usually approximately 1 cm⁻¹ in the Raman and 2 cm⁻¹ in the infrared.

Selected bands of cis-C₂H₂D₂ and 1,1-C₂H₂D₂ are

shown in Figures 25-28. These bands exemplified the general features of the groups of bands discussed below.



ν_1 and ν_{11} show strong singlets in both the infrared and Raman spectra; however ν_{11} is asymmetric, suggesting the existence of two components. The ^{13}C component of ν_{11} was not observed even though the shift is calculated to be 7.2 cm^{-1} .

ν_2 shows one very strong and one very weak component in the Raman spectrum. In the infrared an asymmetric band of moderate intensity is observed. The band in the infrared is wide enough to encompass the two Raman components.

ν_3 , ν_5 , ν_6 , ν_7 and ν_{12} show two Davydov components of similar relative intensity in either the infrared or Raman spectrum (see Figure 25). Seldom could the two components be resolved in both spectra; however, the bands were resolved in the infrared if they are active for ethylene in the infrared (ν_7 , ν_{12}) and the same result was observed for the ethylene Raman active bands. (ν_3 , ν_5 , ν_6).

ν_4 and ν_{10} show triplets in the Raman and infrared spectra, respectively, where the lowest frequency peak is the most intense. Unfortunately, ν_4 was not observed in the matrix-isolated sample. The calculated C-13 shift for ν_4 is 2.8 cm^{-1} . If the peaks at 989.0 cm^{-1} and

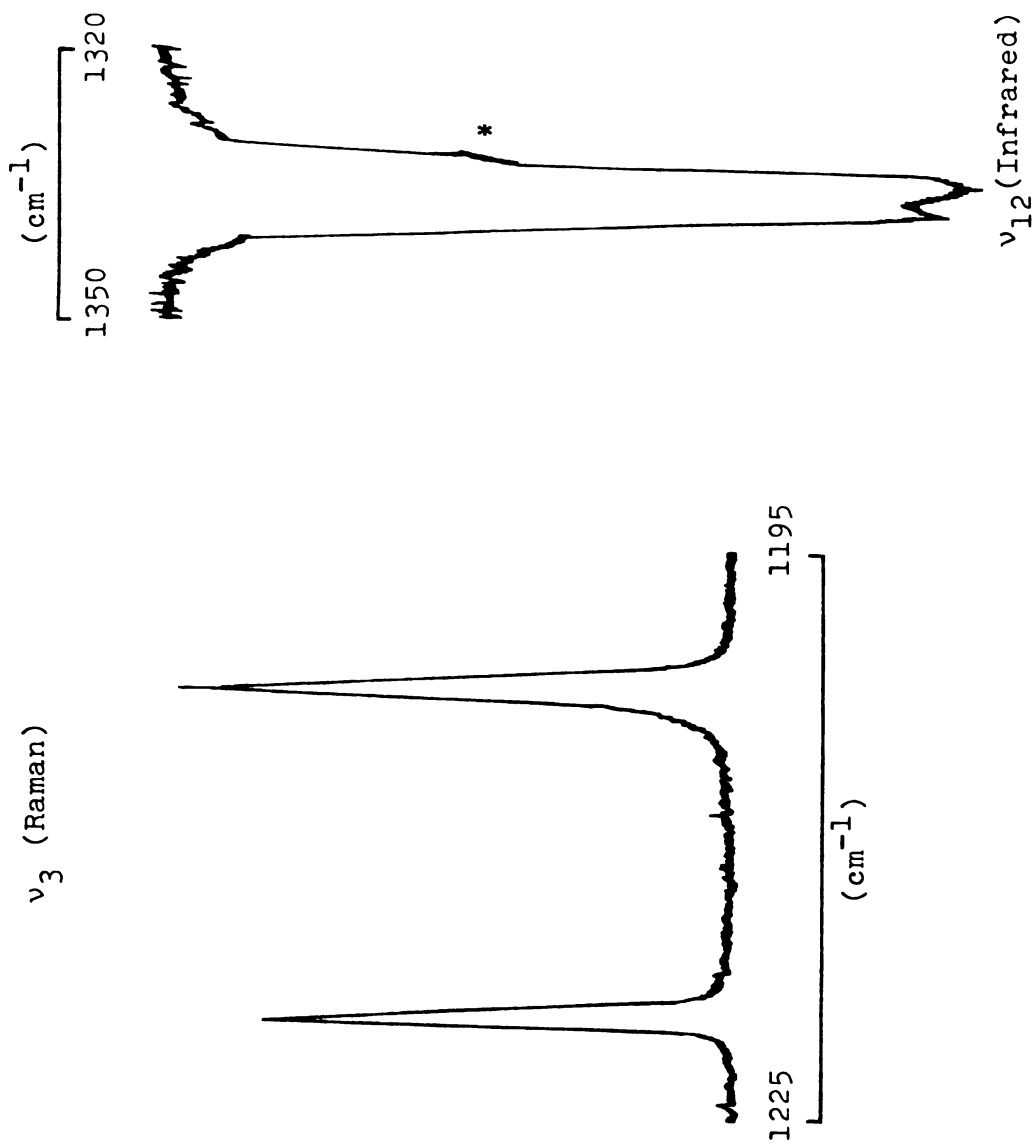


Figure 25. Internal modes of $\text{cis-C}_2\text{H}_2\text{D}_2$; ν_3 and ν_{12} . The peak marked with an asterisk is attributed to C-13 substituted molecules.

Figure 26. Internal modes of $\text{cis-C}_2\text{H}_2\text{D}_2$; ν_{10} and ν_9 . The peak marked with an asterisk is attributed to C-13 substituted molecules.

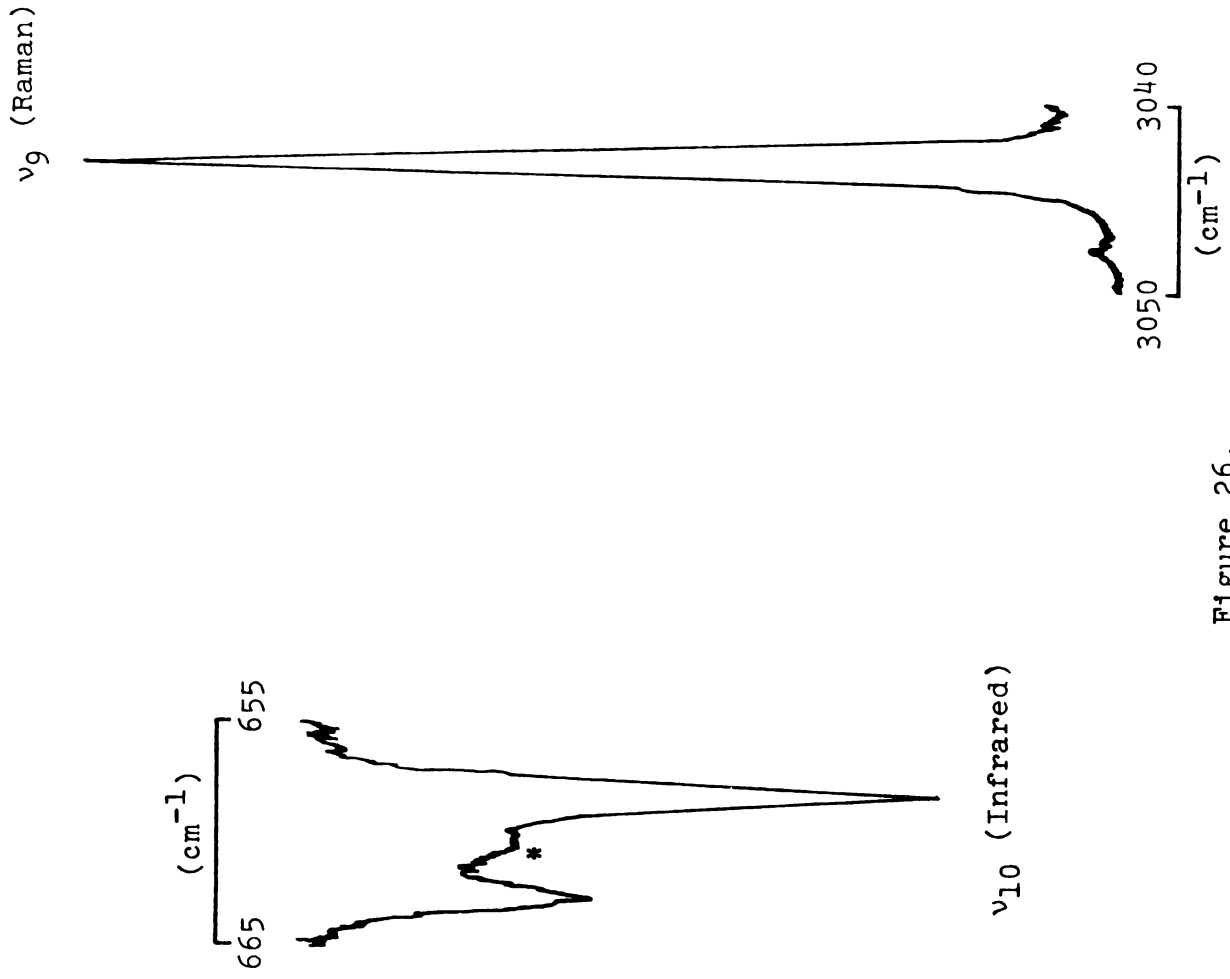


Figure 26.

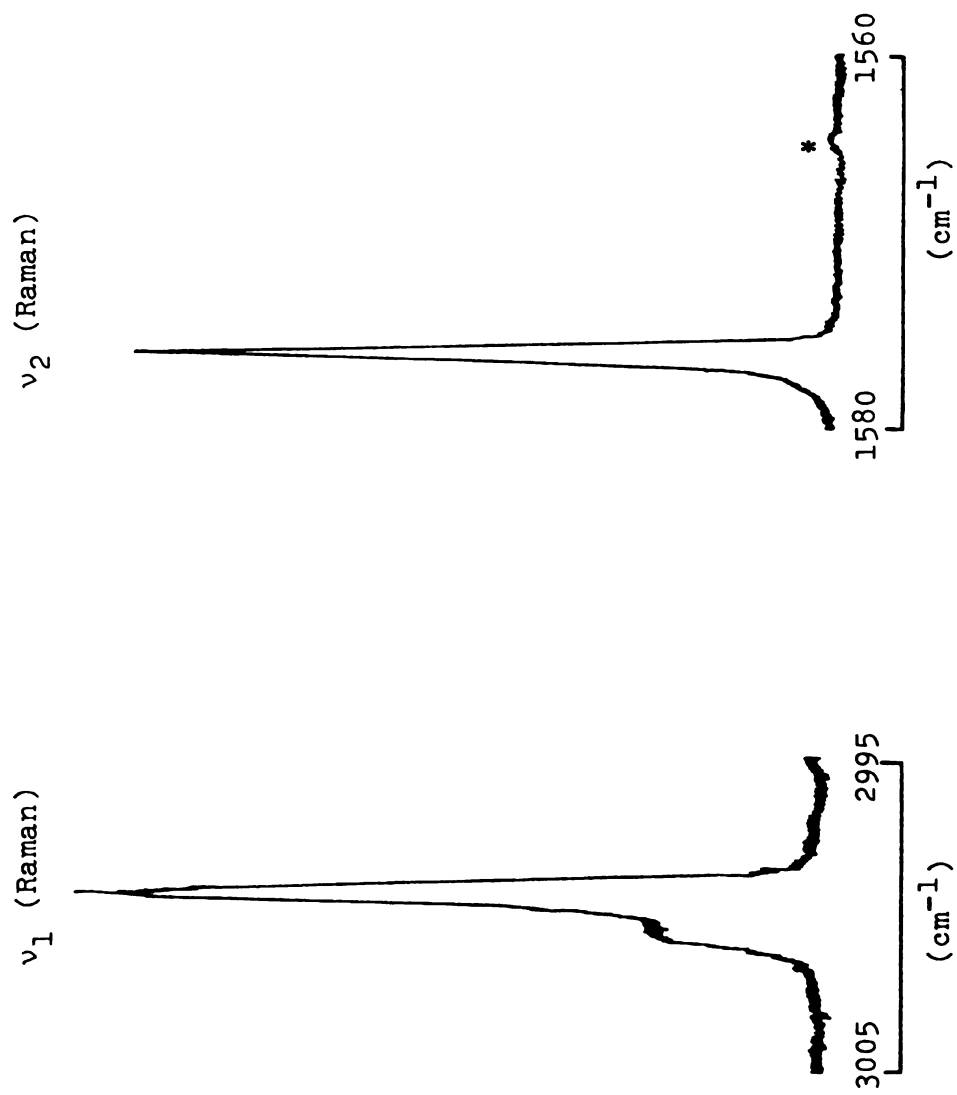


Figure 27. Internal modes of 1,1- $\text{C}_2\text{H}_2\text{D}_2$; ν_1 and ν_2 . The peak marked with an asterisk is attributed to $\text{H}_2^{12}\text{C} = \text{C}^{13}\text{CD}_2$.

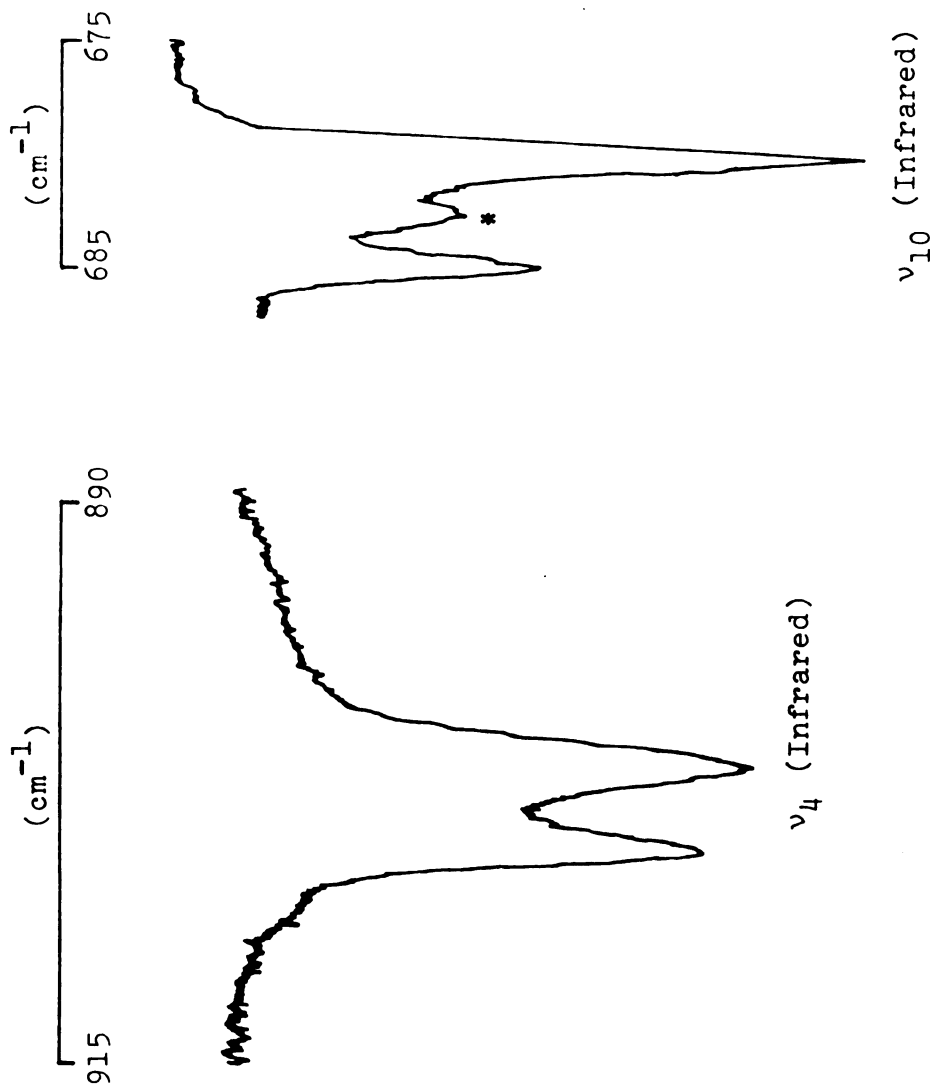


Figure 28. Internal modes of $1,1\text{-C}_2\text{H}_2\text{D}_2$; ν_4 and ν_{10} . The peak marked with an asterisk is attributed to $\text{H}_2^{13}\text{C} = 1^2\text{CD}_2$.

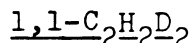
985.3 cm^{-1} are assigned as the Davydov components, then the 982.2 cm^{-1} peak has a shift of 5.0 cm^{-1} from the mean of the Davydov components - which is much larger than the calculated C-13 shift. The larger shift can be explained on the basis of a large gas to crystal field shift or as being due to an intermolecular Fermi resonance between the C-12 and C-13 molecules. The intensity of the 982.2 cm^{-1} peak would support the intermolecular Fermi resonance argument.

The ν_{10} triplet (Figure 26) is assigned on the basis of the dilute mixed crystal data. ν_{10} in C_2H_4 shows a peak at 661.3 cm^{-1} and the calculated C-13 shift is 0.5 cm^{-1} ; therefore the peak at 660.7 cm^{-1} in the pure crystal is attributed to C-13. The intensity of this peak is weak, consistent with the expected C-13 intensities.

ν_8 shows a single, relatively broad band in both the infrared and Raman spectra at 766.6 cm^{-1} and 761.8 cm^{-1} , respectively. The difference between the observed infrared and Raman frequencies is larger than the experimental uncertainty, suggesting that each may be a different Davydov component.

ν_9 shows a very strong component in the infrared spectrum (Figure 26). In the Raman spectrum a very strong component at 3043.2 cm^{-1} is observed and there is a very weak component at 3047.5 cm^{-1} . It is possible that the very weak feature is a Davydov component of ν_9 , or an

orientational component of ν_5 of the C_2H_3D impurity which was present in the sample.



ν_1 , ν_5 and ν_{11} are similar to ν_1 and ν_{11} of $cis-C_2H_2D_2$. They all show strong single components in the infrared and Raman spectra. However, a shoulder was observed in the Raman spectrum of ν_1 (Figure 27). This has been assigned as one of the Davydov components.

ν_2 is the only vibration for which both of the C-13 shifts were observed. A strong narrow band was observed for ν_2 in the Raman spectrum (Figure 27), and a relatively broad, moderately intense peak was observed in the infrared spectrum. The C-13 band shown in Figure 27 corresponds to $H_2^{12}C = ^{13}CD_2$. The $H_2^{13}C = ^{12}CD_2$ band is observed at about 10 cm^{-1} lower energy with almost equivalent intensity.

ν_3 , ν_4 , ν_7 , ν_9 and ν_{12} show two relatively strong Davydov components in either the infrared or the Raman spectrum. The two components were resolved in only one of the two types of experiments. Again, these were resolved in either the infrared or Raman spectrum depending on the activity of the modes for the C_2H_4 crystal except for ν_{12} . ν_4 is shown in Figure 28.

ν_6 is very weak in both the infrared and Raman spectra. The infrared band is quite broad, but the two Davydov components are resolved in the Raman spectrum.

ν_8 and ν_{10} both exhibit interesting triplets in the Raman and infrared spectra, respectively (see Figure 28). Unfortunately, neither mode was observed in the matrix isolation experiments. If the 955.3 cm^{-1} and 947.7 cm^{-1} bands of ν_8 are assigned as the two Davydov components, the experimentally measured shift of the 951.5 cm^{-1} component from the mean of the Davydov components is zero. This would correspond to the calculated shift of 0.7 cm^{-1} for $\text{H}_2^{12}\text{C} = ^{13}\text{CD}_2$, assuming the gas to crystal field shift is small. Precisely the same argument holds for the 682.6 cm^{-1} peak of ν_{10} ; however, in this case the weak central feature corresponds to $\text{H}_2^{13}\text{C} = ^{12}\text{CD}_2$.

C. Excitons of Binary Mixed Molecular Crystals - The Coherent Potential Approximation

The molecules in the crystals of $\text{C}_2\text{H}_3\text{D}$, $\text{trans-C}_2\text{H}_2\text{D}_2$, and C_2HD_3 can assume two energetically-inequivalent orientations in a C_1 lattice site. Thus, these solids can be considered to be binary mixed crystals with 50% of the molecules having orientation "A" at energy ϵ_A , and 50% of the molecules having orientation "B" at energy ϵ_B . Figure 29 shows the evolution of the mixed-crystal band. This diagram is similar to Figure 2; however, the B and C contributions to the gas-to-crystal shift have been

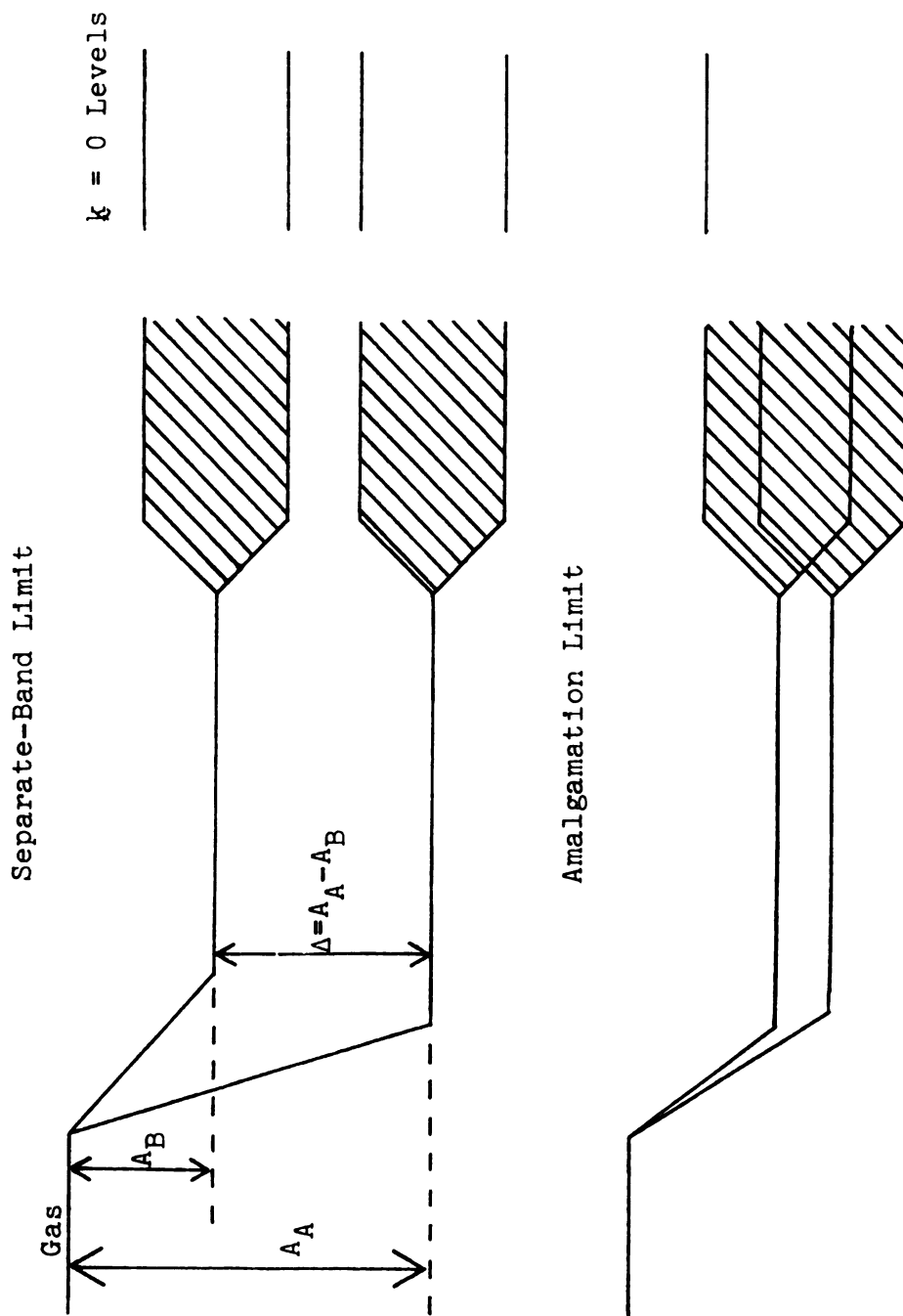


Figure 29. Mixed crystal exciton band structure.

ignored here for simplicity. The two possible limits which may exist for the bands of the mixed crystal are shown in Figure 29. In the separate band limit,^{40,44} the orientational splitting Δ (or the trap-depth in mixed crystal terminology), is larger than the bandwidth of the "pure" A or B crystal. In this situation there is little mixing of the \underline{k} -states of the two components, and if two Davydov components are observed for each "pure" crystal, four $\underline{k} = 0$ components are expected for the mixed crystal. In the amalgamation limit,^{40,44} the trap-depth is less than the bandwidth of either pure crystal and the \underline{k} states of each component mix. In this limit only two optically active components would be observed. Obviously, there exist intermediate situations where mixing of \underline{k} states occur but the mixing is not as complete as that of the amalgamation limit. In the intermediate cases four components may still be observed but the middle two components become less allowed as the trap-depth decreases in that these components lose their $\underline{k} = 0$ character as the \underline{k} state mixing increases. Thus, the intensity of these components diminish rapidly.

Most of the spectroscopic studies of mixed-molecular crystals have concentrated on electronic excitations.⁶⁰⁻⁶³ Various theoretical approaches have been utilized to explain the observed phenomena. These include the virtual crystal approximation,³⁹ the average T-matrix

approximations,^{39,64} and the coherent-potential approximation.^{39,65,66} Each of these approximations has met with limited success in describing the electronic excitations of mixed crystals. The virtual crystal approximation has been found to be useful for small perturbations (trap-depths).⁶⁷ The average T-matrix approximation is more general, but strictly applies to only small impurity concentrations.⁶⁷ The coherent-potential approximation is the most general and has been most successfully used for describing the limiting behavior of the mixed crystal,⁶⁷ that is amalgamation and separate-band limits.

The electronic-exciton model is precisely the same as the vibrational-exciton model, except that the electronic wavefunctions are antisymmetrized. Therefore, the mixed crystal theories of electronic excitons should apply to the vibrational problems, as has been shown for the phonons of isotopically mixed molecular crystals.^{46,47}

In the crystals of the partially-deuterated ethylenes, two parameters important in mixed-crystal theory are varying from band to band. They are the trap-depth (orientational splitting) and the bandwidth. It is therefore possible for the bands to be in the amalgamation limit, the separate band limit, or somewhere in between. This eliminates the virtual crystal approximation for this general application since the perturbation

strengths can vary from weak to strong.

Two energetically-inequivalent orientations exist in crystals of C_2H_3D , C_2HD_3 and $trans-C_2H_2D_2$, and if the molecules are assumed to be randomly distributed, the concentration of each component (orientation) is 50%. The 50% concentration of the components eliminates the usefulness of the average T-matrix approximation for the partially-deuterated ethylenes. Thus the coherent potential approximation (CPA) is the most useful for application to the vibrational states of the partially-deuterated ethylenes.

Hoshen and Jortner have applied the coherent potential approximation to the electronic states of substitutionally disordered molecular crystals.^{62,63} The details of their application are discussed in Appendix B, where the symbols used in the following discussion are derived. The application of the CPA to the vibrational bands of the partially-deuterated ethylenes is quite direct; however, a comment on the following two assumptions of the CPA is in order.

Assumption (A) - The environmental shift terms, D^f for the two components are equal and concentration independent.

Assumption (B) - The two components differ by only their gas-phase excitation energies and are characterized by the same wavefunctions.

Assumptions (A) and (B) as stated do not apply to the crystals of the partially-deuterated ethylenes. For example, for the ethylene-d₁ crystal the gas phase excitation energies of both "components" are the same. That is, both components are ethylene-d₁. The environmental shift, D^f , for each component (a C₂H₃D molecule in each of the two energetically-inequivalent orientations) differs. However, the total effect, that is $(\epsilon^f + D^f)$, on the band structure is the same whether the energy difference arises in the gas-phase energies or in the environmental shifts (see Figure 29), so the general band structure is the same in both the general electronic case of Hoshen and Jortner or in the cases of the partially-deuterated ethylenes.

Assumption (B) also states that both components are characterized by the same wavefunction. This is certainly not generally true for the vibrational wavefunctions of isotopes; however, in the case of the partially-deuterated ethylenes, where the energy difference is arising from crystal-field effects, it is expected to be a good assumption. The general application of the CPA to vibrational states of isotopic mixed crystals thus remains questionable.

The self energy $\sigma(z)$ expresses the deviations of the binary-mixed crystal from the virtual crystal and is given by: (See Appendix B)

$$\sigma(z) = (\Delta C_B - \sigma(z)) f^0(z - \bar{\epsilon} - \sigma(z)) (\Delta C_A + \sigma(z)), \quad (31)$$

where C_A is the concentration of component A at energy ϵ_A and C_B is the concentration of component B at energy ϵ_B . Δ is the difference in energy of component A and component B (the orientational splitting), and $\bar{\epsilon}$ is the mean single molecule excitation energy,

$$\bar{\epsilon} = C_A \epsilon_A + C_B \epsilon_B \quad (32)$$

$f^0(z)$ is a complex function related to the density of states of the pure crystal. The spectral density,⁴⁵ which can be considered to express the \underline{k} components of the density of states and thus is intimately related to the optical properties of the crystal, is then expressed as for $\underline{k} = 0$:

$$S(0, j, E) = \pi^{-1} \frac{\text{Im}\sigma(E - i0^+)}{[E - \bar{\epsilon} - t_j - \text{Re}\sigma(E - i0^+)]^2 + [\text{Im}\sigma(E - i0^+)]^2} \quad (33)$$

where t_j is the energy of the j^{th} Davydov component of the pure crystal. $E - i0^+$ indicates that the density of states is nonvanishing in the energy range where the self energy is complex.

A plot of $S(0, j, E)$ versus E shows the calculated optical absorption for the binary-mixed crystal. The calculated optical absorption depends on the concentration of the components, the energy difference of the

states of the two components, the pure crystal density of states, and the locations of the pure crystal Davydov components.

For the crystals of C_2H_3D , $trans-C_2H_2D_2$ and C_2HD_3 the concentrations of each component is assumed to be 50% and the Δ 's are the observed orientational splittings which, due to the "nearsightedness" of the ethylenes, can be determined in any ethylene host. The experimentally determined orientational splittings of the ethylenes in a C_2H_4 host crystal are given in Table 26. The numerical frequencies of the modes are given in Chapter V, Tables 12-14.

The pure crystal density of states of the ethylenes are unknown and the locations of the pure crystal Davydov components are unmeasurable since a crystal with only one orientation of the molecules does not exist.

A one-dimensional pure crystal density of states was assumed for the partially-deuterated ethylenes. It has the form:⁶³

$$\rho^0(E) = \pi^{-1}(T^2 - E^2)^{-1/2}, \quad (34)$$

where T is one-half the exciton bandwidth of the vibration. This model density of states is not necessarily a good assumption for the ethylene crystals because the ethylene molecules are planar and therefore the

Table 26. Orientational splittings (cm^{-1}) of $\text{C}_2\text{H}_3\text{D}$, trans- $\text{C}_2\text{H}_2\text{D}_2$ and C_2HD_3 .^a

	$\text{C}_2\text{H}_3\text{D}$	trans- $\text{C}_2\text{H}_2\text{D}_2$	C_2HD_3
ν_1	0	2.2	3.5
ν_2	0	1.7	2.3
ν_3	2.4	2.4	0
ν_4	8.0	11.0	2.2 ^c
ν_5	4.6	4.7	0
ν_6	---	---	0
ν_7	3.3	7.4	11.2
ν_8	---	4.5	9.6 ^{b,c}
ν_9	---	4.5	3.7
ν_{10}	1.2	2.2	0
ν_{11}	2.6	0	0
ν_{12}	0	3.5	2.6

^aDetermined in C_2H_4 unless otherwise stated, 0 indicates unresolved, --- indicates unobserved.

^bFrom 1% $\text{C}_2\text{HD}_3/\text{C}_2\text{H}_3\text{D}$

^cIt is likely that these assignments should be interchanged (vide infra).

intermolecular interactions are expected to be at least two dimensional. However, semi-quantitative information concerning the band-structure dependence on the trap-depth of the "mixed" crystal can certainly be obtained, and this can be compared with the observed band structure to determine whether the CPA mixed crystal model can be applied to the internal modes of the C_2H_3D , trans- $C_2H_2D_2$ and C_2HD_3 crystals. Therefore, the application of the coherent potential approximation to the crystals of the partially-deuterated ethylenes is not a test of the CPA, although the author is unaware of any previous applications to vibrational excitons. Rather it is assumed that the CPA model works, and the result of the calculations are used to assist in the assignment of the observed exciton components.

The positions of the pure crystal exciton components are unknown and attempts to calculate these positions using program TBON with a variety of intermolecular potential functions have been unsuccessful. Therefore, the bandwidths of the pure crystal is used as a variable in the calculation of the mixed crystal exciton structure. The bandwidths were determined by obtaining the best fit between the observed and calculated exciton components.

The CPA calculations were done using program MIX which was obtained from Woodruff and Kopelman⁶⁸ and revised for this application. The program is listed

in Appendix C.

D. The Internal Modes of C_2H_3D , trans- $C_2H_2D_2$, and C_2HD_3

The frequencies of the observed internal fundamentals for crystalline C_2H_3D , trans- $C_2H_2D_2$ and C_2HD_3 are listed in Tables 27-29; selected bands are illustrated in Figures 30-37. The bands of each crystal have been grouped together according to their orientational splittings in the following discussion. This classification is entirely arbitrary since the structure of each band in a group of bands with equivalent orientational splittings may vary depending on the bandwidth of the pure crystal vibration.

C_2H_3D

ν_1 , ν_2 , and ν_{12} show singlets in the C_2H_4 matrix so the orientational splitting is assumed to be very small and the bands are expected to be in the amalgamation limit. The observed neat crystal bands consist of a singlet for ν_2 and partially resolved doublets for ν_1 and ν_{12} (see Figure 30). This is consistent with amalgamation limit behavior. The bandwidths can be assumed to be the energy difference between the observed Davydov components for ν_1 and ν_{12} , and the full width at half height for ν_2 .

As depicted in Figure 30, ν_{10} shows a doublet in the infrared spectrum of the neat crystal. The observed

Table 27. Internal fundamental frequencies (cm^{-1}) of $\text{C}_2\text{H}_3\text{D}$.*

Mode	Infrared	Raman	In C_2H_4 ^b	Gas ^c
ν_1	3011.1 s (3.3)	3010.8 sh 3009.8 vs 3004.9 ^f vw	3010.0	3002
ν_2	1597.2 s (5.5) 1580.1 ^g w 1572.9 ^h w	1595.3 s (.7) 1579.1 ^g w 1571.0 ^h w	1597.0	1607
ν_3	1285.0 m (12.6)	1292.1 s 1277.7 s	1285.3 1282.9	1290
ν_4	1017.6 w 1012.8 w 1006.2 m 1002.2 m	1002.6 vw (8.0)	1010.9 1002.9	1000
ν_5	3048.0 s 3045.1 s 3037.5 ^g vw	3047.2 vs (1.2) 3043.9 vs (1.6) 3037.3 ^g vw	3047.8 3043.2	3061
ν_6	1123.6 w 1090.8 bd,sh	1120.8 m (13.4)		1129
ν_7	809.6 bd 805.8 asy	809.4 m (11.4)	812.5 809.2	808
ν_8	950.2 s,sh 945.2 s,asy 941.6 ^g w,sh	957.3 sh 953.2 sh 949.0 s		943

Table 27. Continued.

Mode	Infrared	Raman	In C ₂ H ₄ ^b	Gas ^c
ν ₉	3080.1 vs	3080.4 sh		3096.4
	3079.8 sh	3079.6 vs		
	3069.1 ^f w	3069.0 ^f m		
ν ₁₀	729.9 bd asy	729.1 w (6.8)	730.8	730
	726.6 m		729.6	
ν ₁₁	2262.6 s	2262.6 s	2262.4	2276
	2260.2 sh	2259.8 s	2259.8	
ν ₁₂	1395.8 bd (7.9)	1395.3 sh	1395.6	1402
		1392.3 s		
	1385.5 ^g w	1385.4 ^g vw		

*Footnotes as in Table 24 except for f and g.

^fThese frequencies attributed to H₂¹³C=¹²CHD.

^gThese frequencies attributed to H₂¹²C=¹³CHD.

Table 28. Internal fundamental frequencies (cm^{-1}) of trans- $\text{C}_2\text{H}_2\text{D}_2$.*

Mode	Infrared	Raman	In C_2H_4 ^b	Gas ^c
ν_1		2271.6 s (3.4) 2268.9 s (3,5)	2270.9 2268.7	2284
ν_2		1563.8 vw,sh 1562.0 s (2.2) 1541.3 ^e w	1565.4 1563.7	1571
ν_3		1289.5 m 1282.3 w 1275.7 s 1273.5 ^e w	1282.3 1279.9	1286
ν_4	1006.5 sh 1004.1 s 991.0 s 985.4 s		1001.8 990.8	988
ν_5		3030.2 s (2.3) 3026.9 m 3025.2 m 3020.7 ^e w	3030.6 3025.9	3045
ν_6		1005.0 m 996.0 m 993.1 s		1004
ν_7	732.9 s 725.6 s 721.1 s		731.5 724.1	725.2

Table 28. Continued.

Mode	Infrared	Raman	In C ₂ H ₄ ^b	Gas ^c
ν_8		873.8 s	870.2	864
		869.7 w	865.7	
		864.6 m		
		859.9 ^e vw		
ν_9	3052.1 s (4.0)		3051.5	3065
	3048.0 s		3047.0	
	3042.9 w			
ν_{10}	671.6 s		672.8	673
	667.8 s		670.6	
ν_{11}	2265.9 s		2266.6	2273
	2263.6 sh			
ν_{12}	1298.0 s		1295.3	1299
	1296.0 s		1291.8	
	1292.4 s			
	1290.6 s			

*Footnotes as in Table 24.

Table 29. Internal fundamental frequencies (cm^{-1}) of C_2HD_3 .*

Mode	Infrared	Raman	In C_2H_4 ^b	Gas ^c
ν_1	2269.2 s	2269.6 s (1.4)	2270.1	2283
	2266.3 s	2266.3 s (1.8)	2266.6	
	2255.5 ^f vw	2255.3 ^f w		
ν_2	1545.3 vw	1546.1 s	1546.3	1547
	1542.6 w	1542.8 s	1544.0	
ν_3		1046.6 s	1041.9	1045
		1041.4 s		
	1039.2 vs (7.1)	1039.8 s		
	1032.8 ^f w			
ν_4	767.6 vs (6.4)	769.5 sh	769.1	764
		765.9 s	766.9	
ν_5	2320.2 s (9.4)	2319.2 s (3.0)	2320.1	2336
	2304.0 ^g w	2303.1 ^g w		
ν_6	1002.8 w	1002.4 m	995.4	999
	993.2 w,asy	996.5 w		
	989.5 w,sp	991.5 s		
ν_7	735.3 s		735.0	725
	724.8 s		723.8	
	720.8 s			
ν_8	932.0 vs	933.3 m (4.8)	931.0 ^h	919
	921.2 vs	923.4 sh	921.4 ^h	
		921.4 s		
	916.1 ^f w,sh			

Table 29. Continued.

Mode	Infrared	Raman	In C ₂ H ₄ ^b	Gas ^c
ν ₉	3035.8 s	3036.6 s (1.8)	3033.8	3049
	3032.1 s	3032.7 s (1.7)	3030.1	
ν ₁₀	628.8 w	627.5	627.5	~610
	626.8 w			
	624.6 s			
ν ₁₁	2210.1 vs (2.0)	2211.4 s (1.5)	2209.3	2222
	2199.0 ^g w	2201.4 ^g w		
ν ₁₂	1286.0 vs	1287.1 s	1286.2	1290
	1283.0 vs	1284.3 s	1283.7	

*Footnotes as in Table 24 except f, g and h.

^fThese frequencies attributed to HD¹³C=¹²CD₂.

^gThese frequencies attributed to HD¹²C=¹³CD₂.

^hObserved in C₂H₃D matrix.

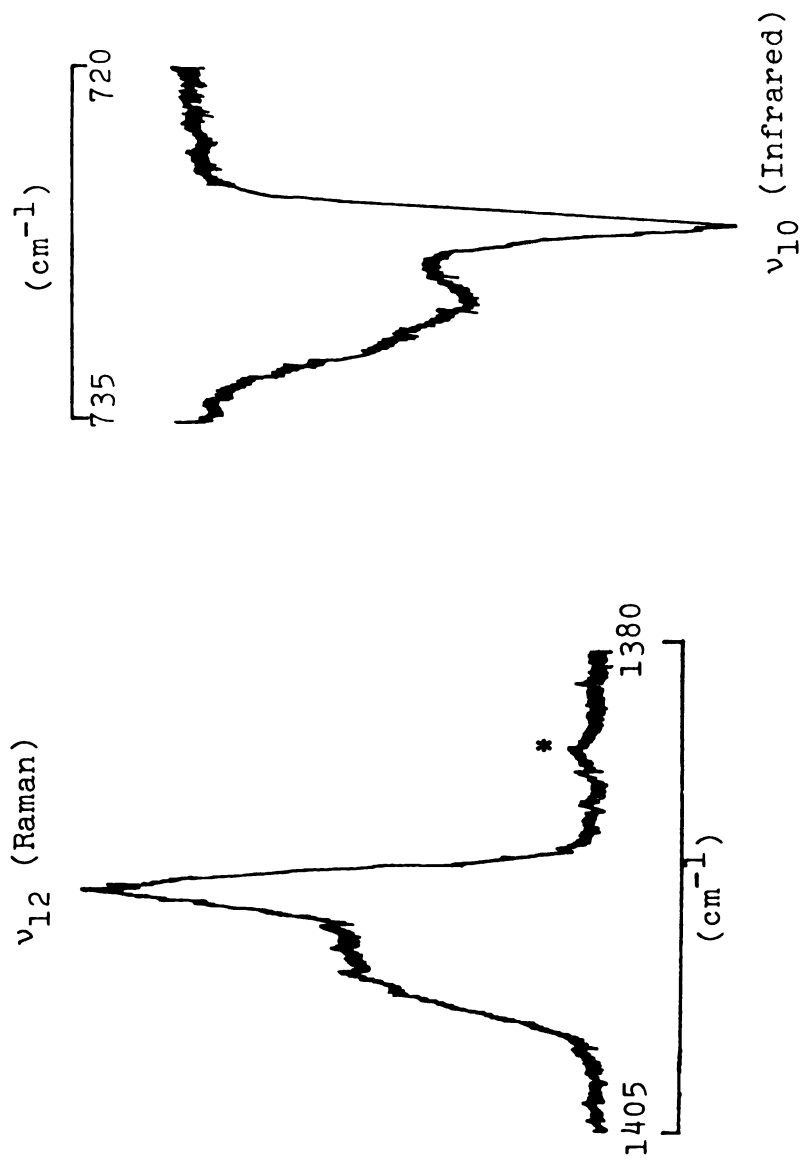


Figure 30. Internal modes of $\text{C}_2\text{H}_3\text{D}$; ν_{12} and ν_{10} . The peak marked with an asterisk is attributed to $\text{H}_2^{12}\text{C}=\text{C}^{13}\text{H}\text{D}$.

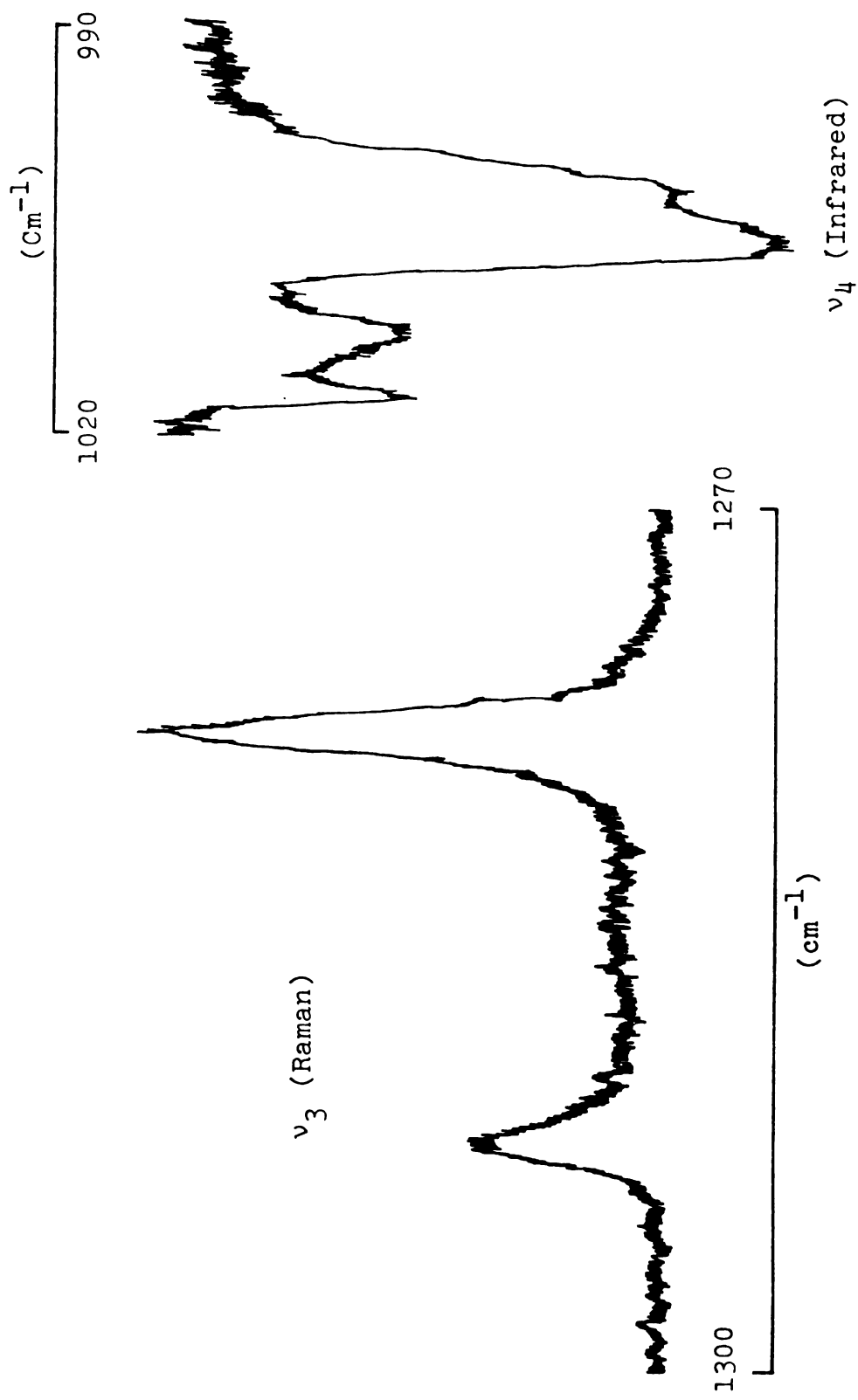


Figure 31. Internal modes of C_2H_3D ; ν_3 and ν_4 .

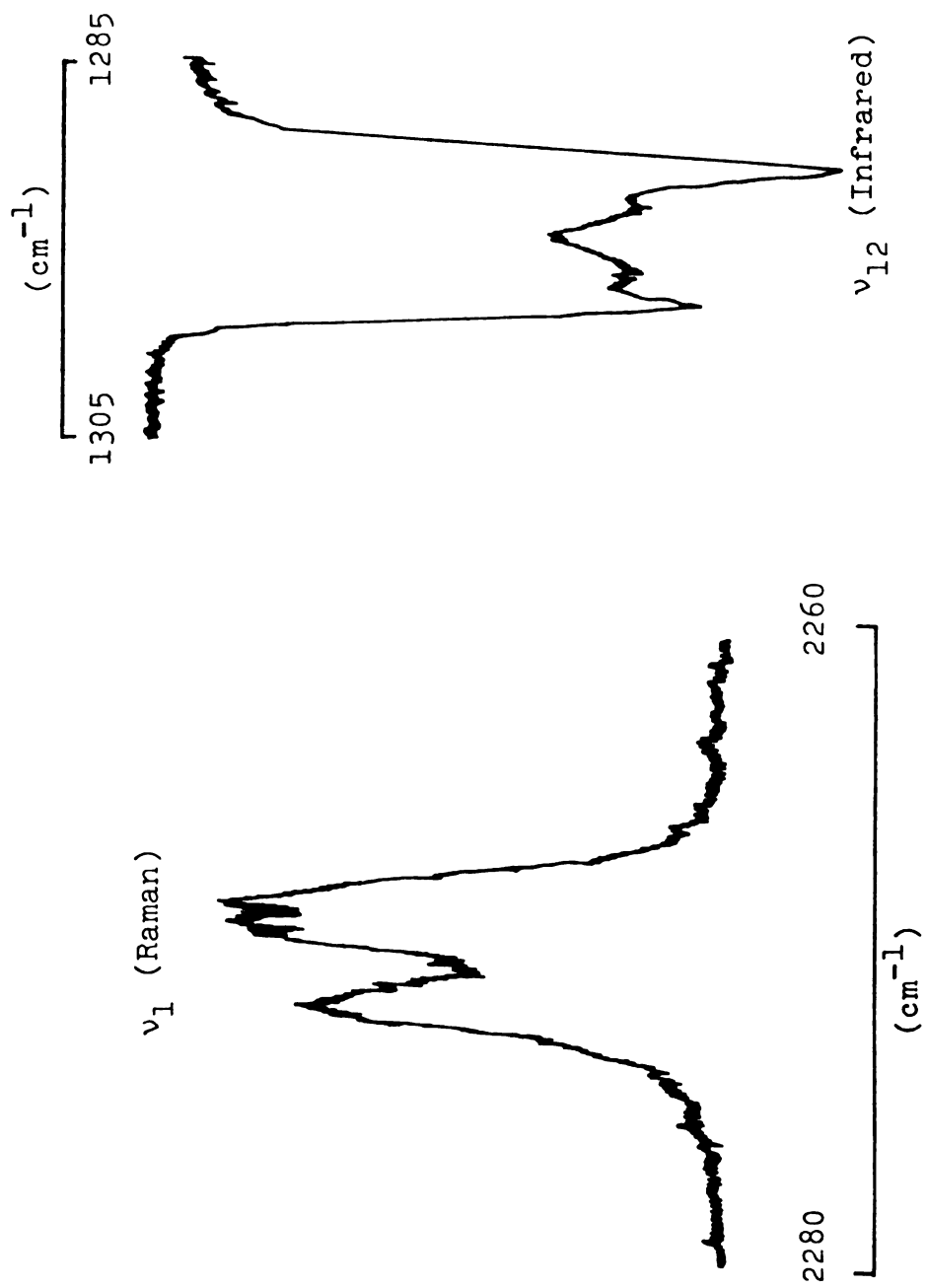


Figure 32. Internal modes of trans-C₂H₂D₂; ν_1 and ν_{12} .

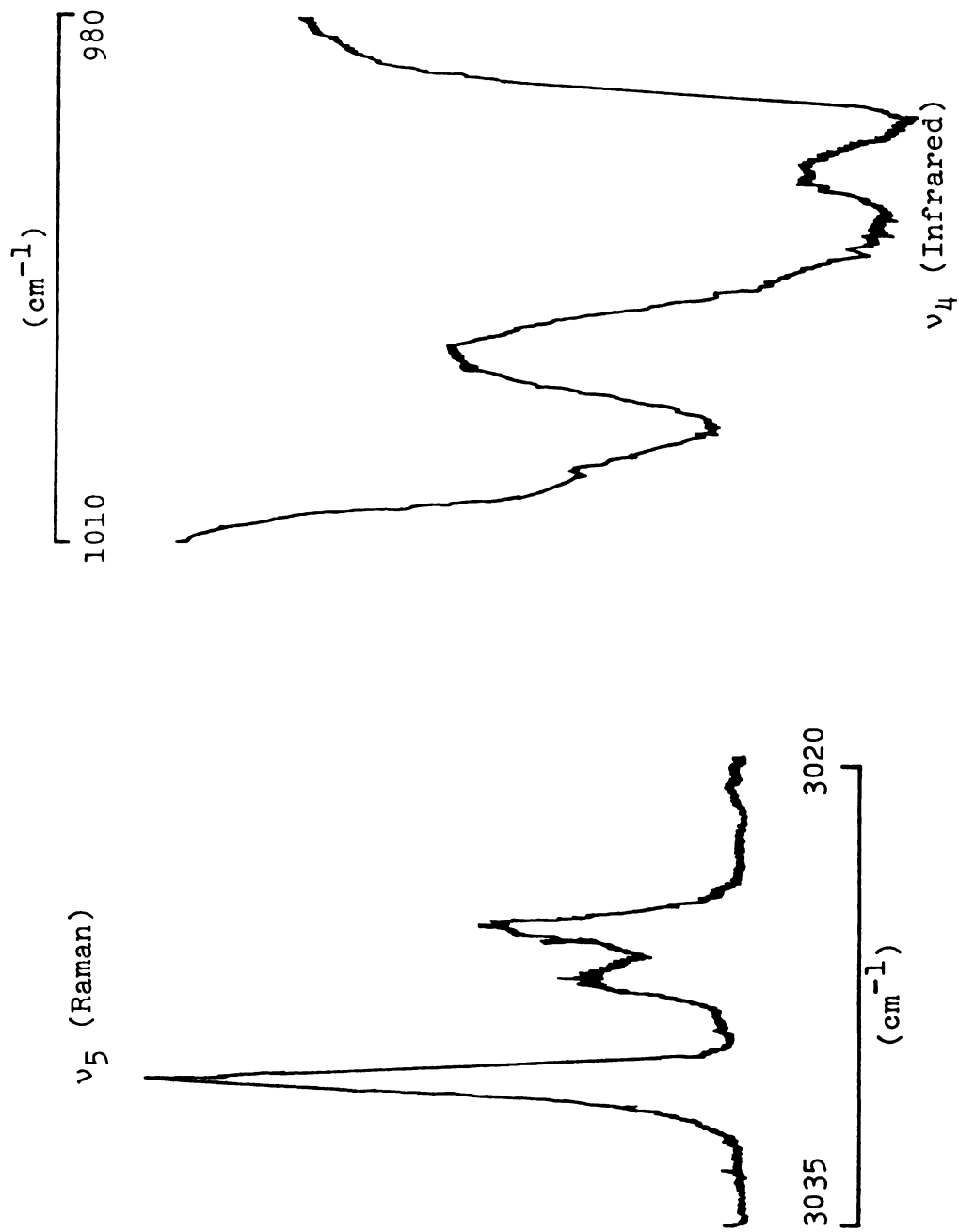
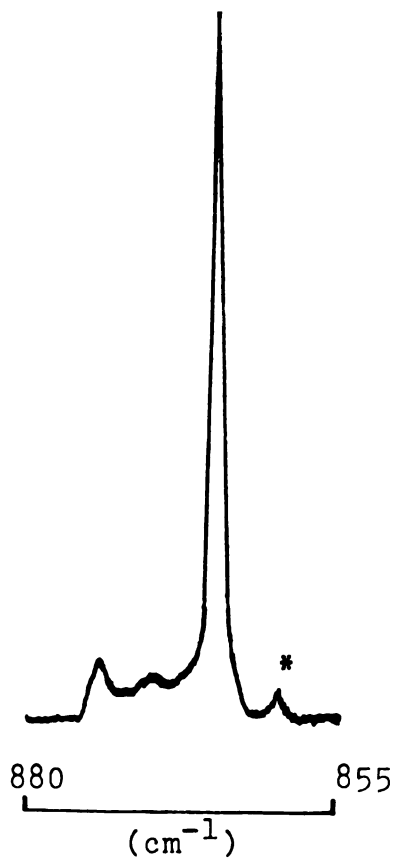


Figure 33. Internal modes of trans-C₂H₂D₂; ν_5 and ν_4 .



Calculated Spectrum

Observed Orientational
Splitting

Figure 34. ν_8 , trans-C₂H₂D₂, calculated and observed Raman band. The peak marked with an asterisk is attributed to C-13 substituted molecules.

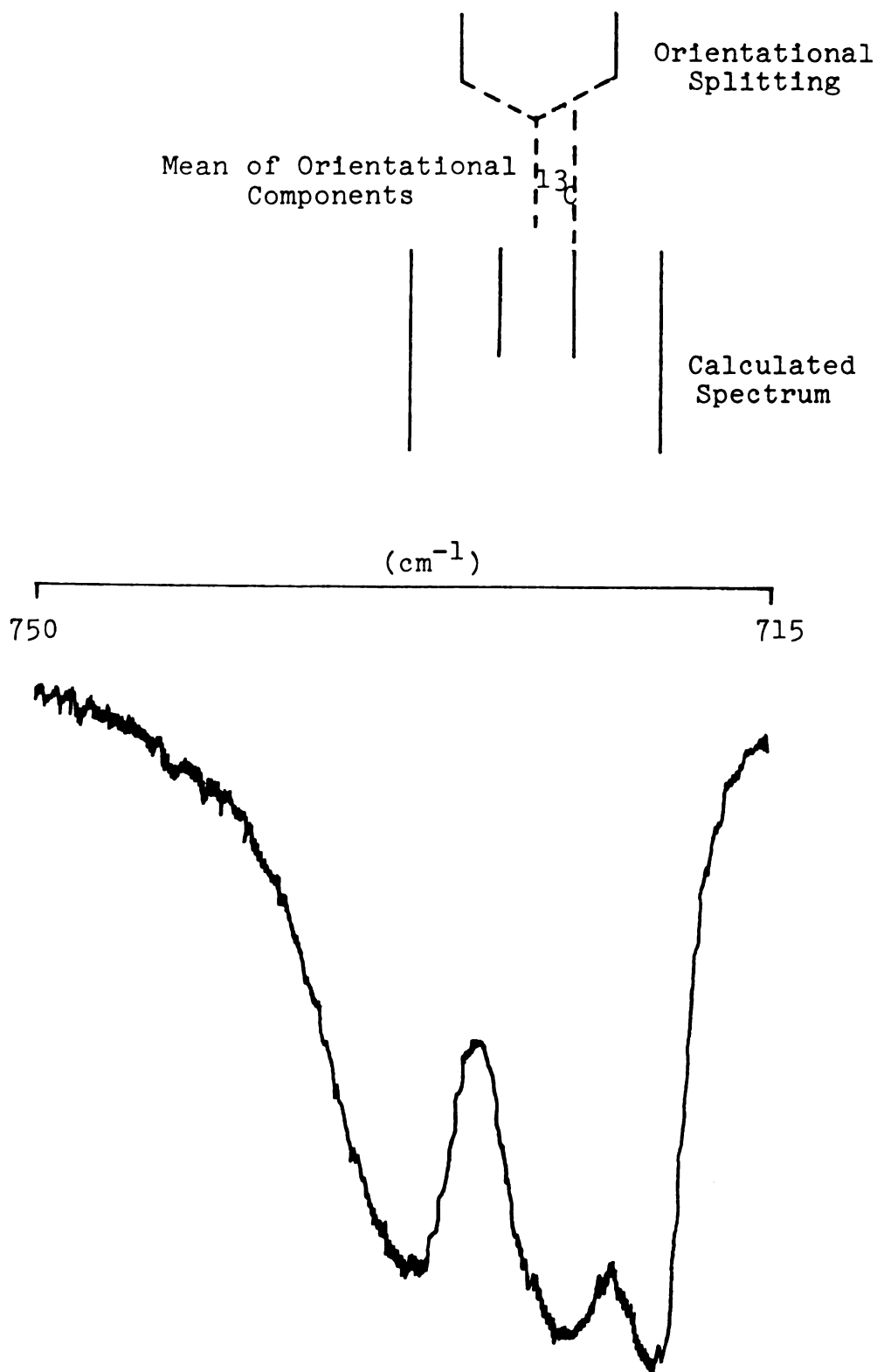


Figure 35. ν_7 , $\text{trans-C}_2\text{H}_2\text{D}_2$, calculated and observed infrared band.

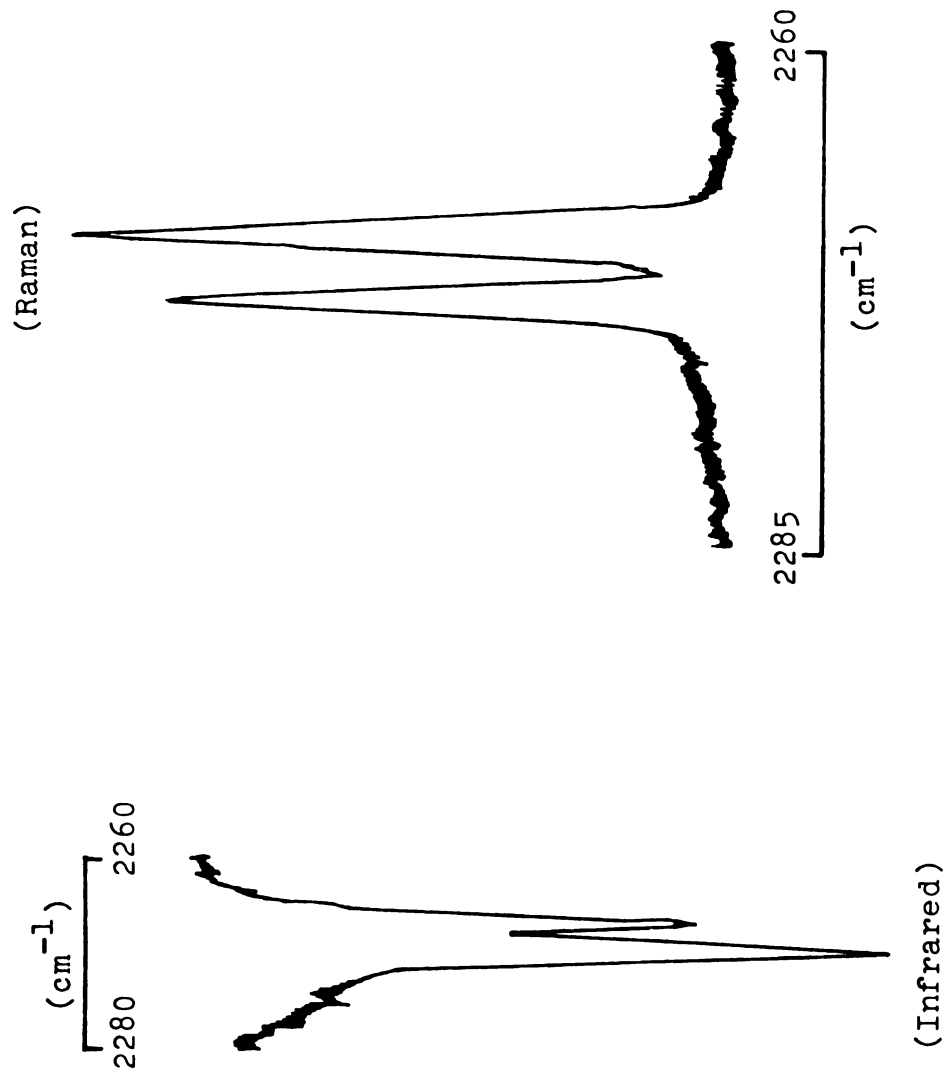


Figure 36. ν_1 region of C_2HD_3 in the infrared and Raman spectra.

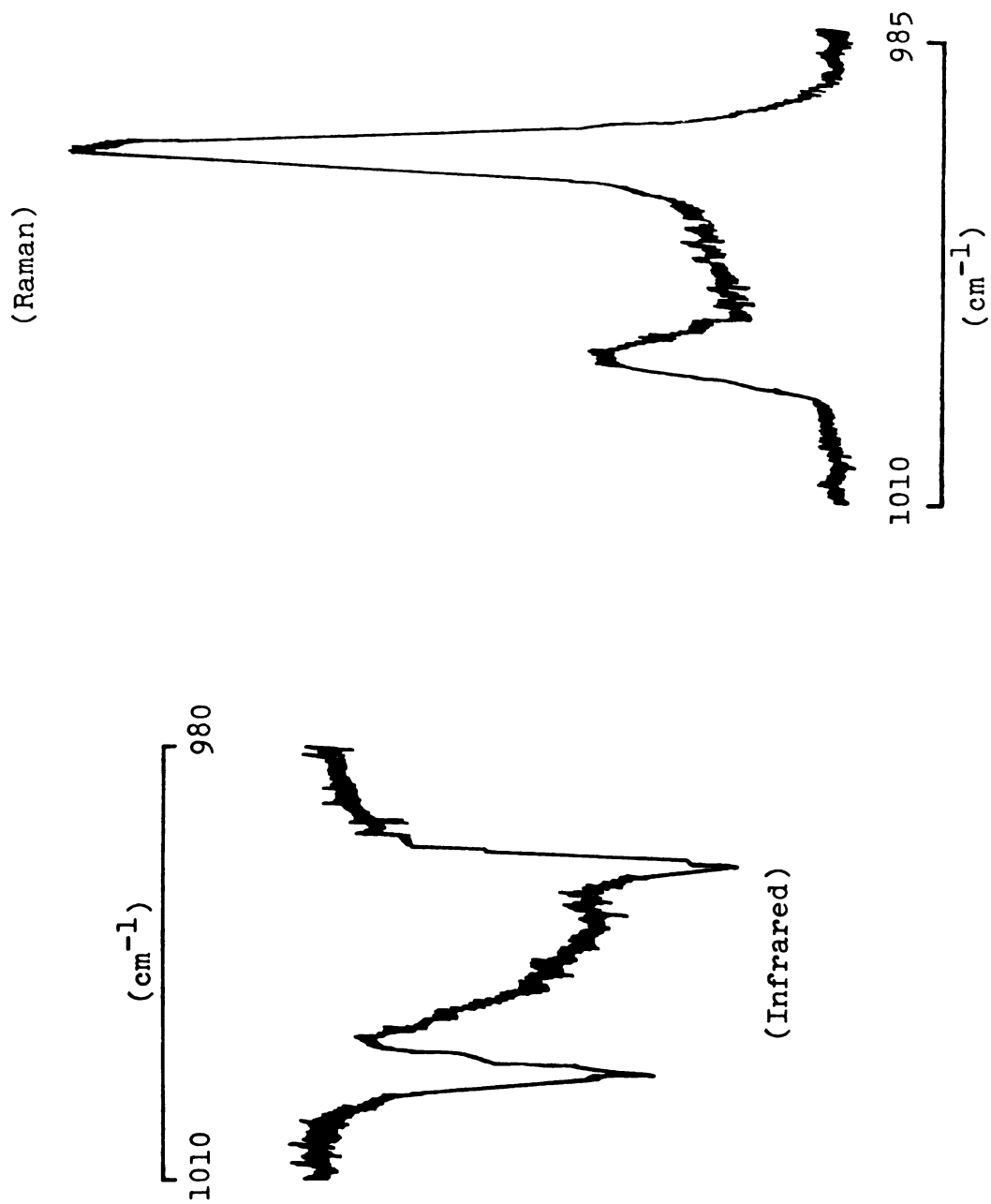


Figure 37. ν_6 region of C_2HD_3 in the infrared and Raman spectra.

orientational splitting is 1.2 cm^{-1} . If a bandwidth of 2.2 cm^{-1} is assumed for ν_{10} , the observed Davydov component positions for the band are calculated. Therefore, this band is in the amalgamation limit.

ν_3 and ν_{11} both show doublets in the neat crystal spectra (see Figure 31, for example). The observed orientational splittings are 2.4 cm^{-1} and 2.6 cm^{-1} , respectively. If the bandwidth of ν_3 is assumed to be 12.8 cm^{-1} the observed Davydov components are calculated; therefore ν_3 is amalgamated. The orientational splitting and energy difference of the observed pure crystal components of ν_{11} are approximately equal. Bands of this nature are either close to or in the separate-band limit and the bandwidth is best approximated by the full width at half height of one of the two components, since theoretically a quartet should be observed in this situation (see Figure 29). It is assumed that each experimental feature is an unresolved Davydov doublet. Unfortunately, the doublet observed for ν_{11} in both the infrared and Raman spectra is not resolved very well, so the bandwidth is approximated by one half the total width at half height of the entire ν_{11} band. The bandwidth approximated in this way is 2.6 cm^{-1} .

ν_5 and ν_7 have orientational splittings of 4.6 cm^{-1} and 3.3 cm^{-1} , respectively. ν_5 shows a relatively sharp doublet in the Raman spectrum of the pure crystal and

the observed splitting of this doublet is less than the orientational splitting. This band is then very similar to ν_{11} and is presumed to be in the separate-band limit. The bandwidth is approximated by the mean of the full widths at half height of the observed pure crystal components (1.4 cm^{-1}). ν_7 shows quite a broad band in both the infrared and Raman spectra. The two infrared components are barely resolved and a fit to these components leads to a calculated bandwidth of 0.8 cm^{-1} . Four components are predicted since with a width of 0.8 cm^{-1} the band is in the separate band limit. The two unobserved but calculated components are assumed to contribute to the broadness of this band.

ν_4 has the largest orientational splitting (8.0 cm^{-1}) of all the $\text{C}_2\text{H}_3\text{D}$ bands. A quartet is observed in the neat crystal infrared spectrum (Figure 31). However, attempts to calculate this observed spectrum using 8.0 cm^{-1} as the orientational splitting were unsuccessful. If the orientational splitting is assumed to be 11.0 cm^{-1} the observed splitting pattern can be calculated, if the bandwidth is taken as 5.2 cm^{-1} . The difference in the orientational splitting between pure $\text{C}_2\text{H}_3\text{D}$ and the C_2H_4 host could be due to a dependence of the orientational splitting on the nature of the host, a breakdown of the coherent potential approximation, or the assumption that the density of states of the band can be adequately described by a

one-dimensional model. The orientational splittings of the partially-deuterated ethylenes have been shown to be independent of the host (see Chapter V). Even where the guest modes are very close in energy to a host band, little change in the orientational splitting was observed. The cause of the difference in orientational splittings must therefore lie in the density of states function or the coherent-potential approximation. Assumption (5) (Appendix B) of the CPA states that the resonance interactions for each component and between the different components are equivalent. If this assumption breaks down, the effective-orientational splitting could increase due to resonance interaction between translationally-equivalent molecules (see Figure 2).

ν_6 , ν_8 and ν_9 were not observed in the C_2H_4 matrix; therefore it is difficult to classify these bands as either amalgamated or in the separate-band limit. ν_6 shows a rather weak band in both the infrared and Raman spectra. ν_8 shows a triplet in the Raman spectrum suggesting this band is in the separate-band limit. However, one of the shoulders on the high-frequency side of the 949.0 cm^{-1} component may be attributable to $H_2^{13}C=^{12}CHD$ which has a calculated C-13 shift of 0.2 cm^{-1} . ν_9 shows a doublet in the pure crystal spectrum so it could either be amalgamated or in the separate band limit, depending on the magnitude of the orientational splitting.

trans-C₂H₂D₂

ν_1 , ν_2 , ν_3 and ν_{10} have observed orientational splittings of 2.2 cm^{-1} , 1.7 cm^{-1} , 2.4 cm^{-1} and 2.2 cm^{-1} , respectively. ν_1 can be assumed to be near the separate-band limit since the orientational splitting is approximately equal to the energy difference between the observed pure crystal components (Figure 32). ν_2 is similar except that the high frequency neat crystal component is a weak shoulder rather than a component of near-equal intensity. ν_3 shows a triplet in the Raman spectrum for an orientational splitting of 2.4 cm^{-1} , a bandwidth of approximately 14.0 cm^{-1} is needed for the outer components to have the observed energy difference. However, with such a bandwidth the band is expected to be amalgamated and a doublet not a triplet, should be observed. The middle peak at 1282.3 cm^{-1} does not correspond to the calculated C-13 shift of 75 cm^{-1} , and a weak peak is observed at 1273.5 cm^{-1} which is shifted 7.6 cm^{-1} from the mean of the orientational components which agrees with the calculated shift. The weak intensity of the 1282.3 cm^{-1} peak suggests that the band is very close to being amalgamated. A doublet is observed for ν_{10} in the pure crystal. If a bandwidth of 2.0 cm^{-1} is assumed, four components are calculated for this band. If it is assumed that the two observed components are unresolved doublets, ν_{10} is in the separate-band limit.

ν_{12} has an orientational splitting of 3.5 cm^{-1} , and a quartet is observed in the infrared spectrum of the pure crystal (see Figure 32). The band is similar to ν_4 of $\text{C}_2\text{H}_3\text{D}$ in that the pure crystal pattern cannot be calculated using the observed orientational splitting. However, if the orientational splitting is assumed to be 5.2 cm^{-1} a bandwidth of 2.6 cm^{-1} gives the correct location of the four Davydov components.

ν_5 , ν_8 and ν_9 have orientational splittings of 4.7 cm^{-1} , 4.5 cm^{-1} and 4.5 cm^{-1} , respectively. ν_5 shows a triplet in the neat crystal spectrum (Figure 33); however, the energy difference between the outer components is nearly equal to the orientational splitting, suggesting that this band is near the separate band limit. The middle component might be due to C-13, although (as with ν_3) the calculated shift does not agree with the observed position and a weak peak at 3020.7 cm^{-1} which has a shift of 7.5 cm^{-1} from the mean of the orientational components is more likely the C-13 band. The calculated C-13 shift is 10 cm^{-1} . The calculated band splitting and intensity pattern for ν_8 , assuming a bandwidth of 5.0 cm^{-1} , is shown in Figure 34 along with the observed Raman scattering. A triplet is observed in the pure crystal and the middle component corresponds to one of the calculated center components. The other center component is assumed to be hidden by the 864.6 cm^{-1} band. This vibration

cannot be classified as amalgamated or in the separate-band limit since the orientational splitting is approximately equal to the bandwidth. It is of interest that the CPA seems to work quite well here. ν_9 also shows a triplet in the pure crystal infrared spectrum. However, the low frequency component is very weak, suggesting that it may be attributed to C-13; the calculated shift is 0.1 cm^{-1} . The energy difference between the two strong components is approximately equal to the orientational splitting which classifies this band near the separate band limit.

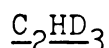
ν_4 shows a quartet in the infrared spectrum of the pure crystal (Figure 33), as did ν_4 of $\text{C}_2\text{H}_3\text{D}$. Again the orientational splitting must be increased - from 11.0 cm^{-1} to 18.7 cm^{-1} - to obtain calculated components near those of the observed band. The closest agreement was obtained assuming a bandwidth of 7.0 cm^{-1} .

ν_7 shows three strong components in the pure crystal spectrum. A quartet is calculated with CPA (Figure 35), to which three of the observed peaks correspond if the bandwidth is assumed to be 5.2 cm^{-1} . However, the center component in the spectrum also corresponds to the calculated C-13 shift from the mean of the Davydov components, so no definitive conclusion can be drawn.

ν_{11} shows only a single absorption in C_2H_4 , so the orientational splitting is assumed to be zero. A partially

resolved doublet is observed in the infrared of the pure crystal. Since the orientational splitting is zero, ν_{11} is in the amalgamation limit and the bandwidth can be closely approximated by the energy difference of the observed pure crystal components.

ν_6 was not observed in the matrix, making it difficult to classify this band. A triplet is observed in the Raman spectrum suggesting that ν_6 is in the separate band limit. However, the C-13 component was not observed and could be contributing to the triplet structure.



ν_2 , ν_4 and ν_{12} have orientational splittings of 2.3 cm^{-1} , 2.2 cm^{-1} and 2.5 cm^{-1} respectively. A strong doublet is observed in the pure crystal Raman spectrum for ν_2 . If a bandwidth of 1.2 cm^{-1} is assumed, the CPA predicts a quartet which would correspond to the observed doublet if each observed component is assumed to be an unresolved doublet. A similar situation exists for ν_4 if the bandwidth is assumed to be 1.6 cm^{-1} .

ν_{12} shows a very strong doublet in the pure crystal and the energy difference between these observed bands is nearly equivalent to the orientational splitting. Thus, this band is near the separate-band limit, and each component is an unresolved doublet.

ν_1 and ν_9 have orientational splittings of 3.5 cm^{-1} and 3.7 cm^{-1} , respectively. A strong doublet is observed

in the pure crystal spectrum for ν_1 (Figure 36), and the orientational splitting is approximately equal to the energy difference between the two bands of the observed doublet. Therefore ν_1 can be interpreted in the same fashion as ν_{12} . ν_9 is also quite similar, showing a strong doublet with a separation which is approximately equal to the orientational splitting. These bands are in the separate-band limit.

ν_7 and ν_8 have orientational splittings of 11.2 cm^{-1} and 9.6 cm^{-1} , respectively. ν_7 shows a strong triplet in the infrared spectrum of the pure crystal. If a bandwidth of 4.0 cm^{-1} is assumed a quartet is predicted in which three of the calculated components correspond to the observed absorptions. The fourth component is assumed to be hidden by the 735.3 cm^{-1} component although it does not appear to be appreciably broader. A very-strong doublet is observed for ν_8 in the infrared spectrum and a triplet is recorded in the Raman spectrum. The orientational splitting is nearly equivalent to the splitting of the infrared components and the outer components of the Raman triplet. Thus, this band is in or near the separate-band limit with each of the two components an unresolved doublet. The center component of the Raman triplet may correspond to $\text{HD}^{12}\text{C}=\text{C}^{13}\text{CD}_2$ which has a calculated C-13 shift of 0.5 cm^{-1} ; however, the observed shift from the mean of the orientational component is 2.8 cm^{-1} . The

difference in shifts may again be caused by Fermi resonance interaction.

ν_3 , ν_5 , ν_6 , ν_{10} and ν_{11} show no orientational splitting in the C_2H_4 matrix. ν_3 exhibits a triplet in the pure crystal Raman spectrum. This suggests that either the mode is in the separate-band limit, or that one of the triplet peaks is due to $HD^{12}C=^{13}CD_2$. ν_5 shows a strong singlet in the pure-crystal spectrum, which indicates that this band is likely amalgamated. ν_6 shows a triplet in both the infrared and Raman spectra (see Figure 37); however, no component corresponds to the calculated C-13 shift. This suggests that ν_6 is in the separate band limit or that Fermi resonance exists between the C-12 and C-13 molecules. ν_{10} also shows a triplet; however, here the center component at 626.8 cm^{-1} corresponds to the calculated position of $HD^{12}C=^{13}CD_2$. ν_{11} is a singlet like ν_5 ; therefore ν_{11} is probably in the amalgamation limit.

It is of interest to note that not nearly as many C-13 components are observed for the C_2H_3D , *trans*- $C_2H_2D_2$ and C_2HD_3 crystals as are observed for solid *cis*- $C_2H_2D_2$ and 1,1- $C_2H_2D_2$. This arises from the greater overall breadths of the C-12 bands of crystalline ethylene- d_1 , *trans*-ethylene- d_2 and C_2HD_3 , due to the orientational splitting. The full widths at half height of many of the C-12 components in these crystals are larger than those

of the corresponding $\text{cis-C}_2\text{H}_2\text{D}_2$ and $1,1\text{-C}_2\text{H}_2\text{D}_2$ fundamentals, but the larger widths are usually accompanied by unresolved bands in the separate band limit.

E. Comparison of the Internal Modes of the Polycrystalline Ethylenes

A comparison of the band structures of the ethylenes may reveal information regarding possible perturbations of fundamental vibrations by other fundamentals, overtones, combinations, or impurity vibrations of similar energy.^{24,26} However, it must be noted that the contributions of the various symmetry coordinates (that is, motions) to a particular fundamental vibration will change upon deuteration, so that a strict comparison is not possible. For example, a normal coordinate calculation using Shimanouchi's program LSMA⁶⁹ and Duncan's force field²⁴ for ethylene reveals ν_1 to be 99% a symmetric C-H stretching motion, while for $\text{trans-ethylene-d}_2$ ν_1 is comprised 49% of the symmetric C-H stretch and 44% of the asymmetric C-H stretch. These changes, however, are expected to have the most pronounced effect on the bandwidths of the vibrations which arise from dynamic interaction between the molecules, and less effect on the static interactions; that is, the orientational splittings and the A's - the gas to crystal field shifts - should be

less dependent on the potential energy distribution.

The orientational splittings of the partially-deuterated ethylenes are given in Table 26. The splittings appear to be relatively constant for ν_1 , ν_2 , ν_3 , ν_5 , ν_9 , ν_{10} and ν_{12} if only the cases where non-zero splittings are observed are compared. An experimental orientational splitting of zero may indicate poor-sample quality rather than an absence of an orientational-energy difference. This is supported by the pure-crystal bands, which do not appear to be amalgamated although no orientational splitting is observed. Therefore, it is considered reasonable to ignore the zeros in this comparison.

The largest deviations from the norm for a given band appear for ν_4 (C_2HD_3) and ν_7 (C_2H_3D), and a large difference exists for ν_8 (trans- $C_2H_2D_2$ and ν_8 (C_2HD_3)). The orientational splittings of ν_4 (C_2HD_3) and ν_8 (C_2HD_3) are 2.2 cm^{-1} and 9.6 cm^{-1} , respectively. If these assignments were switched the agreement between the orientational splittings of these C_2HD_3 bands and those of the corresponding vibrations of the other ethylenes would be more reasonable. The normal-coordinate calculation gives the potential-energy distribution of these modes listed in Table 30. The symmetry coordinates are taken from Kuchitsu, et al.⁷⁰ and the force field is that of Duncan.²⁴ S_4 is the out-of-plane twisting motion of the ethylene molecule, and S_7 and S_8 are the plus and minus

Table 30. Potential-energy distribution and calculated frequencies of the out-of-plane vibrations of C_2HD_3 .

Symmetry Coordinates	Calculated Frequencies (cm^{-1})		
	734	777	937
S_4	39%	24%	37%
S_7	61%	13%	26%
S_8	0	63%	37%

linear combinations of the out-of-plane wags, respectively. In C_2H_4 there is no mixing of these modes and ν_4 is purely the twisting motion while ν_7 is the motion arising from the plus linear combination of the wags and ν_8 is the minus linear combination. It can be seen from Table 30 that the 734 cm^{-1} band is 61% S_7 ; therefore this is ν_7 as it has been traditionally assigned. However, the 777 cm^{-1} and 937 cm^{-1} bands have been assigned previously as ν_4 and ν_8 , respectively by Arnett and Crawford,⁷¹ based on a less sophisticated force field calculation. The potential energy distribution given in Table 30 does not support these assignments. The mode at 777 cm^{-1} is 63% S_8 , and thus should be assigned as ν_8 , leaving the 937 cm^{-1} mode to be assigned as ν_4 . If the ν_4 and ν_8 assignments are switched the orientational splittings of C_2HD_3 agree more closely with those of the other ethylenes.

It is of interest to note here that the orientational splittings of the out-of-plane vibrations tend to be larger than those of the in-plane motions of the ethylenes. This is especially true for ν_4 and ν_7 . The same trend was observed for the benzenes by Bernstein.²⁶ This is believed to be caused by the large vibrational amplitudes of the out-of-plane motions; although not always larger than the in-plane-motions, the amplitudes of the out-of-plane vibrations are never substantially smaller than the in-plane amplitudes. The large orientational

splittings seem to indicate that the static field is probed more by the out-of-plane motions than the in-plane-motions.

A summary of the A's, the gas-to-mixed crystal shifts, for the ethylene is given in Table 31. A was calculated as $\epsilon_{\text{gas}} - \epsilon_{\text{mixed crystal}}$. The shifts of $\text{C}_2\text{H}_3\text{D}$, $\text{trans-C}_2\text{H}_2\text{D}_2$ and C_2HD_3 were obtained by taking the mean of the orientational components as the mixed crystal energy. ν_1 , ν_5 , ν_9 and ν_{11} are the C-H(D) stretching vibrations of the ethylenes. An examination of the A's for these vibrations reveals relatively large values ($13 \pm 3 \text{ cm}^{-1}$) and relatively constant shifts for all the stretches. The shifts of the stretches involving deuterium motion rather than hydrogen motion tend to be smaller; implying the deuteriums do not probe the crystal field as much as the hydrogens. This is supported by calculated vibrational amplitudes.

ν_3 , ν_6 , ν_{10} and ν_{12} are the C-H(D) bending vibrations of the ethylenes. The shifts of these vibrations are smaller, and not nearly as constant as those of the stretches, although the values remain relatively constant for each vibration. No comment can be made concerning the hydrogen versus deuterium motions except that the deuterium shifts appear to be a little smaller if the C_2H_4 and C_2D_4 shifts of ν_3 and ν_{12} are compared; however, this difference may not be real due to the experimental

Table 31. Gas-to-mixed crystal shifts of the ethylenes (cm⁻¹).^a

	C ₂ H ₄ ^b	C ₂ H ₃ D	cis-C ₂ H ₂ D ₂	1,1-C ₂ H ₂ D ₂	trans-C ₂ H ₂ D ₂	C ₂ HD ₃	C ₂ D ₄ ^a
ν ₁	30.1	-8.0(H)	13.9(D)	17.2(H)	14.2(D)	14.7(D)	14.3
ν ₂	5.0	10.0	7.3	5.8	6.4	1.9	7.9
ν ₃	4.5	5.9	5.3	-3.7	4.9	3.1	4.1
ν ₄	---	-6.9	---	---	-8.3	-4.0 ^c	-10.2
ν ₅	15.0	15.5(H)	16.8(H)	12.2(D)	16.8(H)	15.9(D)	6.7
ν ₆	---	---	---	---	---	3.6	11.1
ν ₇	---	-2.9	-11.4	-4.3	-2.6	-4.4	-6.3
ν ₈	1.9	---	---	---	-4.0	-7.2 ^c	3.1
ν ₉	15.9	---	15.1(H)	16.5(H)	15.7(H)	17.0(H)	16.8
ν ₁₀	---	-0.2	0.7	4.0	1.3	-17.5	-7.6
ν ₁₁	46.9	14.9(D)	12.2(D)	13.4(D)	6.4(D)	12.7(D)	10.7
ν ₁₂	5.8	6.4	7.0	3.7	5.5	5.1	5.2

^a(H) indicates a primarily protonic motion, (D) a deuterium motion.

^bFrom References 13, 17 and 24. ^cTraditional assignments.

uncertainty. The only other comparison that can be drawn is between ν_7 and ν_8 and no obvious pattern has appeared; however it should be noted that the A's of all the out-of-plane motions are negative. Again the agreement between the values of the other ethylenes, and ν_4 and ν_8 of C_2HD_3 is best if the assignment of these bands are switched.

A large deviation from a typical shift for a given vibration (if such a typical shift can be determined) usually indicates that the band in question is perturbed by Fermi resonance interaction with a nearby band. This is strikingly observed for ν_1 (C_2H_3D) and (1,1- $C_2H_2D_2$), which are known to be perturbed in the gas phase. A for these molecules are -8.0 cm^{-1} and 17.2 cm^{-1} , respectively, and these shifts deviate from the general ν_1 shift (14.0 cm^{-1}). Another example is ν_{11} (C_2H_4) which has the largest shift of the observed bands (46.9 cm^{-1}). Once again this is known to be a Fermi resonanting band.²⁴ The shift of ν_1 of C_2H_4 is 30.1 cm^{-1} , suggesting that this band is also Fermi perturbed. This agrees with Elliott and Leroi's intermolecular Fermi resonance argument for this band in a C_2D_4 host.¹³

Other bands which appear to have large deviations from typical A values include: ν_2 (C_2H_3D), ν_2 (C_2HD_3), ν_3 (1,1- $C_2H_2D_2$), ν_5 (C_2D_4), ν_7 (cis- $C_2H_2D_2$), ν_{10} (C_2HD_3), ν_{10} (C_2D_4), and ν_{11} (trans- $C_2H_2D_2$). The ν_{10} 's can be

eliminated from the preceding list because the uncertainty of the determined gas phase frequencies is quite high.²⁴ It is not obvious how the other bands are being perturbed. The only cases for which there is an obvious nearby band is ν_2 (C_2HD_3). $2\nu_4$ of C_2HD_3 is observed as a doublet at 1531.0 cm^{-1} and 1527.6 cm^{-1} (see Appendix A). The 1531.0 cm^{-1} component is strong while the 1527.6 cm^{-1} component is of moderate intensity. The unusual A value of ν_2 (C_2HD_3) and strong intensity of $2\nu_4$ indicates a Fermi resonance interaction between these vibrations. It should be remembered that the A's of the different isotopes are not strictly comparable because of the differing potential energy distributions. This may account for the deviations observed for the other above-mentioned vibrations.

The translational shifts of the ethylenes (C in Figure 2) are usually less than the experimental uncertainty, and therefore no other general comment can be made about them. The other resonance contribution to the exciton band structure is the bandwidth, that is, $2T$ in Figure 2.

The bandwidths of the ethylenes are given in Table 32. In the cases where the Davydov doublets were not resolved the bandwidths were approximated by the full width at half height of the observed singlet, or the bandwidth determined with the CPA; otherwise the spacing between the Davydov components is taken as the

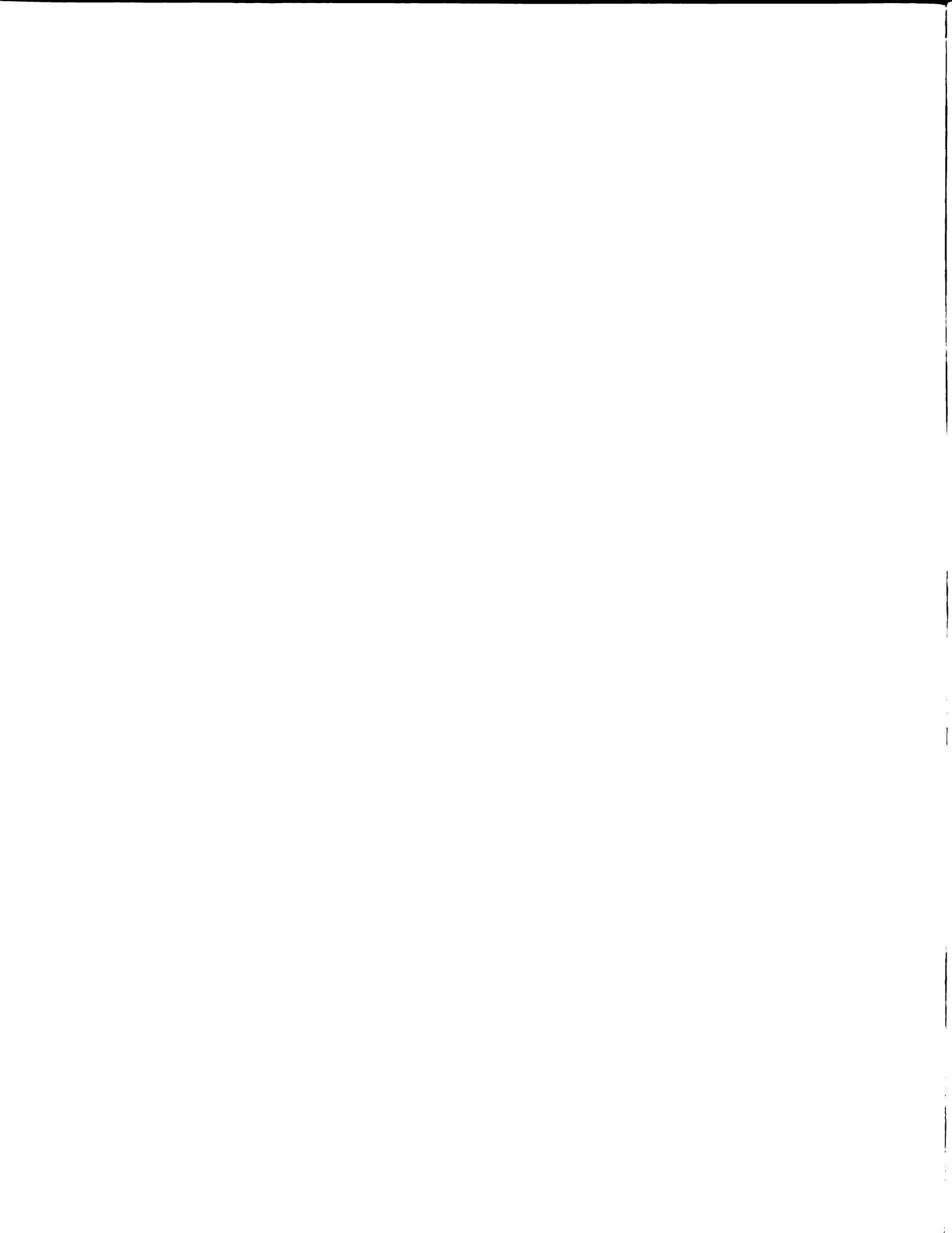


Table 32. Bandwidths of the ethylenes (cm^{-1}).

	$\text{C}_2\text{H}_4^{\text{a,c}}$	$\text{C}_2\text{H}_3\text{D}$	cis- $\text{C}_2\text{H}_2\text{D}_2$	1,1- $\text{C}_2\text{H}_2\text{D}_2$	trans- $\text{C}_2\text{H}_2\text{D}_2$	C_2HD_3	$\text{C}_2\text{D}_4^{\text{a,c}}$
ν_1	10.5	1.0 ^c	1.1 ^b	1.3 ^c	3.5 ^t	1.6 ^b	1.5
ν_2	7.1	0.7 ^b	3.4 ^c	0.8 ^b	2.2 ^b	1.2 ^d	2.2
ν_3	19.5	12.8 ^d	17.6 ^c	11.6 ^c	14.0 ^d	---	14.5
ν_4	5.3	5.2 ^d	4.8 ^b	3.8 ^c	7.0 ^d	1.6 ^d	4.9
ν_5	2.4	1.4 ^b	1.4 ^c	1.6 ^b	2.3 ^b	---	3.5
ν_6	4.3	---	3.7 ^c	4.2 ^c	---	---	5.2
ν_7	7.9	0.8 ^d	6.6 ^c	4.4 ^c	5.2 ^d	4.0 ^d	6.0
ν_8	9.9	---	5.6 ^b	7.6 ^c	5.0 ^d	4.8 ^b	5.4
ν_9	2.5	---	1.3 ^b	1.8 ^c	4.0 ^b	1.8 ^b	2.0
ν_{10}	5.6	2.2 ^d	4.7 ^c	5.0 ^c	2.0 ^d	---	4.1
ν_{11}	1.3	2.6 ^b	2.2 ^b	1.0 ^b	2.2 ^c	---	1.5
ν_{12}	3.9	3.0 ^c	3.6 ^c	6.8 ^c	2.6 ^d	2.3 ^b	2.8

^aFrom References 13, 17 and 24. ^bFull width at half height.^cSpacing between Davydov components. ^dCalculated, CPA.

bandwidth. It is of interest that the bandwidths of the partially-deuterated ethylenes tend to be nearer to the C_2D_4 values than to the C_2H_4 bandwidths except for ν_5 and ν_6 . However, the bandwidths of C_2D_4 are less than the C_2H_4 values except for ν_5 and ν_6 also. No general increase or decrease in the bandwidths is observed with the addition of more deuterium atoms, nor are the values of the three d_2 -compounds particularly similar. The random behavior of the bandwidths is believed to reflect the changes in the motions which take place upon deuteration.

F. Conclusions

The following conclusions can be drawn from the observation of the internal modes of the partially-deuterated ethylenes.

(a) $\tilde{k} = 0$ selection rules apply to the crystals of the partially-deuterated ethylenes. Thus the crystal bands of 1,1- $C_2H_2D_2$ and cis- $C_2H_2D_2$ are similar to the bands of C_2H_4 and C_2D_4 , and mutual exclusion was observed for the internal modes of trans- $C_2H_2D_2$.

(b) The internal fundamentals of the crystals of C_2H_3D , trans- $C_2H_2D_2$ and C_2HD_3 can be interpreted as mixed crystal bands.

(c) The coherent-potential approximation appears to work within the approximations used here for the

vibrational modes of the partially-deuterated ethylenes; although it may have failed for particular bands.

(d) The assignments of ν_4 and ν_8 of C_2HD_3 should be interchanged.

(e) The observed gas-to-crystal shifts support previously assigned Fermi resonances including the intermolecular Fermi resonance, assigned by Elliott and Leroi.¹³ A new Fermi resonance has been observed between $2\nu_4$ and ν_2 of C_2HD_3 .

CHAPTER VII

DISCUSSION AND SUGGESTIONS FOR FUTURE WORK

Probably the most interesting conclusion that can be drawn from this study is the existence of "effective" symmetry in the crystals of the partially-deuterated ethylenes. Although observed-lattice spectra of various isotopic mixed crystals have suggested the existence of "effective" symmetry in isotopically-disordered solids, no other study, of which this author is aware, has probed the site symmetry directly. This has been done by observing the orientational splitting of the partially-deuterated ethylenes in one another. The observed-lattice frequencies and mutual exclusion of the lattice modes of the partially-deuterated ethylenes suggests an "effective" C_1 site. This is confirmed by the observed orientational splittings and the mutual exclusion of the trans-ethylene- d_2 fundamental internal modes.

The lattice modes of the partially-deuterated ethylenes can be described in the virtual-crystal limit, implying that deuteration causes a purely mass effect on the observed energies. It would be of interest to study the lattice modes of mixed crystals of C_2H_4 in C_2D_4 , especially the 25%, 50% and 75% mixtures, and to compare these with the partially-deuterated ethylene lattice spectra. The

virtual crystal approximation predicts that these spectra would be the same as the ethylene-d₁, ethylene-d₂ and ethylene-d₃ spectra, respectively. It would also be quite valuable to confirm the observation of the third optically active translation of C₂H₄, and to observe the third optically active translation of C₂D₄. The translations of mixed molecular crystals have been observed in very few cases; thus it would also be of interest to observe to far-infrared spectra of the partially-deuterated ethylenes and mixed crystals of C₂H₄ in C₂D₄.

A better intermolecular interaction potential for ethylene is certainly required. In principle this can be obtained by a refinement of the potential parameters to the observed lattice frequencies, including both the librations and translations. In the same vein, the exciton splitting may be calculable with a refined potential; however, the intramolecular potential may need to be adjusted to suit the molecules in the crystal sites before this task is accomplished.

Unfortunately, little specific information was obtained about the ethylene crystals from the internal mode spectra. Again, a better intermolecular potential function may assist in giving more weight to the assignments of some of the bands of the partially-deuterated ethylenes; however an experimentally determined density of states function may be necessary to improve the assignments of

the C_2H_3D , $trans-C_2H_2D_2$ and C_2HD_3 internal fundamentals.

The coherent-potential approximation appears to have worked for the partially-deuterated ethylenes. However, one should be cautious in attempting to use this calculation for the vibrational bands of mixed crystals in general, since the wave functions of different isotopes may be different and this is not accounted for by the CPA. Certainly more testing of the CPA for application to the general-vibrational problem is necessary, but this should be done on systems with a density of states function and bandwidths which are known, and on bands which show behavior from the amalgamation to the separate-band limit.

Polarization studies of the internal modes of the partially-deuterated ethylenes may assist in a confirmation of the assignments made in this study and provide information concerning the symmetry of the internal modes. It would be of interest to establish what effect the "effective" crystal symmetry has on the symmetries of the internal modes. Obviously the observed activities gave little information concerning this problem, except possibly for the $trans$ -ethylene- d_2 .

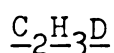
Mixed-crystal studies may also assist in the confirmation of the assignments of this study. For example, if a guest band is well isolated from a host band, the Davydov splitting of the guest band varies with the concentration of the host. If the crystal has a high concentration

of host molecules, the Davydov splitting is small, but it increases as the guest concentration is increased. Studies of this nature could undoubtedly distinguish C-12 Davydov components from C-13 impurity components.

APPENDICES

APPENDIX A

The following is a list of the observed frequencies (cm^{-1}) and relative intensities of the bands in the internal spectral region of the neat, partially-deuterated ethylene crystals.



Infrared	Raman	Assignment
3089.6 w		ν_9 (C_2H_4)
3080.1 vs	3080.4 sh	ν_9
3079.8 sh	3079.6 vs	
3069.1 w	3069.0 m	ν_9 ($\text{H}_2^{13}\text{C}=\text{C}^{12}\text{H}\text{D}$)
3048.0 s	3047.2 vs	
3045.1 s	3043.9 vs	ν_5
3037.5 vw	3037.3 vw	ν_5 ($\text{H}_2^{12}\text{C}=\text{C}^{13}\text{H}\text{D}$)
3034.0 vw	3033.4 vw	$2\nu_6+\nu_7$
3011.1 s	3010.8 sh	ν_1
	3009.8 vs	
	3004.9 vw	ν_1 ($\text{H}_2^{13}\text{C}=\text{C}^{12}\text{H}\text{D}$)
3000.6 vw		$\nu_{10}+\nu_{11}$
2999.1 vw	2999.9 vw	ν_1 (1,1- $\text{C}_2\text{H}_2\text{D}_2$)
	2996.5 vw	ν_1 (C_2H_4)
2974.1 m		ν_{11} (C_2H_4)
2961.2 s	2960.0 s	$\nu_2+\nu_{12}$

Infrared	Raman	Assignment
2870.9 vw	2870.1 w	$\nu_2 + \nu_3$
2869.0 vw		
2339.8 m		$\nu_8 + \nu_{12}$
2330.7 m	2332.5 m	
2262.6 s	2262.6 s	ν_{11}
2260.2 sh	2259.8 s	
2122.8 vw	2122.2 w	$\nu_4 + \nu_6, \nu_{10} + \nu_{12}$
2015.5 m		$\nu_3 + \nu_{10}$
1997.5 w, sp		$2\nu_4$
1955.5 w		$\nu_4 + \nu_8$
1907.9 s, asy		$2\nu_8, \nu_6 + \nu_7$
1848.0 w		$\nu_6 + \nu_{10}$
1818.2 m		$\nu_4 + \nu_7$
1764.0 w		$\nu_7 + \nu_8$
1620.0 m		$2\nu_7$
	1618.1	ν_2 (C_2H_4)
1597.2 s	1595.3 s	ν_2
1591.8 vw		ν_2 (^{13}C of C_2H_4)?
1580.1 w	1579.1 w	ν_2 ($H_2^{12}C=^{13}CHD$)
1572.9 w	1571.0 w	ν_2 ($H_2^{13}C=^{12}CHD$)
	1464.5 w	$2\nu_{10}$

Infrared	Raman	Assignment
1438.2 s		ν_{12} (C_2H_4)
1435.1 w		ν_{12} (^{13}C of C_2H_4)
1395.8 bd	1395.3 sh	ν_{12}
	1392.3 s	
1385.5 w	1385.4 vw	ν_{12} ($H_2^{12}C=^{13}CHD$)
	1338.1 w	ν_3 (C_2H_4)
	1292.1 s	
1285.0 m		ν_3
	1277.7 s	
1123.6 w	1120.8 m	ν_6
1090.8 bd, sh		
1017.6 w		ν_4
1012.8 w		
1006.2 m		
1002.2 m	1002.6 vw	
	957.3 sh	ν_8
950.2 s, sh	953.2 sh	
945.2 s, asy	949.0 s	
941.6 w, sh		ν_8 ($H_2^{12}C=^{13}CHD$)
809.6 bd	809.4 m	ν_7
805.8 asy		
755.0 w		ν_7 ($1,1-C_2H_2D_2$)
729.9 bd, asy	729.1 w	ν_{10}
726.6 m		

cis-C₂H₂D₂

Infrared	Raman	Assignment
	3126.5 vw	$\nu_1 + \nu_7$
3123.5 s	3121.2 s	$2\nu_2$
3085.5 w	3082.8 m	$\nu_{11} + \nu_7$
3081.5 m	3079.1 m	
3052.0 w		$\nu_1 + \nu_8$
	3047.5	ν_9, ν_5 (C ₂ H ₃ D)
3044.6 vs	3043.2 vs	
	3037.3 s, sh	ν_5
	3035.9 s	
3032.4 w	3032.3 w	ν_5 (¹³ C)
	3027.0 w	ν_9 (¹³ C)?
	3024.8 vw	
		ν_5 (trans-C ₂ H ₂ D ₂)
3011.2 vw	3010.5 w	ν_1 (C ₂ H ₃ D)
	3008.4 vw	$\nu_{11} + \nu_8$
	3001.0 vw	ν_1 (1,1-C ₂ H ₂ D ₂)
	2960.0 vw	$\nu_2 + \nu_{12}$ (C ₂ H ₃ D)
2961.4 vw	2950.5 vw	
		$\nu_1 + \nu_{10}$
2886.5 s	2885.6 m	$\nu_2 + \nu_{12}$
2665.0 w	2667.3 vw	$2\nu_{12}$

Infrared	Raman	Assignment
2595.9 w		$\nu_2 + \nu_6$
2555.9 vw		$\nu_2 + \nu_4$
	2541.3 w	$\nu_{12} + \nu_3$
2407.8 vw		ν_3 (C_2D_2)
2404.9 vw		
2373.2 vw	2372.7 w	$\nu_6 + \nu_{12}$
2339.1 vw		$\nu_2 + \nu_8$
2329.1 vw	2329.9 vw	$\nu_4 + \nu_{12}$
2286.2 vs	2287.1 vs	ν_1
2278.0 vw	2278.9 w	ν_1 (^{13}C)
	2277.8 w	$2\nu_{10} + \nu_4$
	2272.8 w	ν_1 (trans- $C_2H_2D_2$)
	2269.8 w	
2265.8 vw		ν_{11} (trans- $C_2H_2D_2$)
2263.0 vw		$\nu_3 + \nu_6$
	2261.8 w	ν_{11} (C_2H_3D)
	2259.3 w	
2242.1 s,asy	2241.7 s,asy	ν_{11}
2213.5 s	2213.5 s	$\nu_2 + \nu_{10}$
	2194.8 vw	$\nu_3 + \nu_4$
	2065.0 vw	$\nu_3 + \nu_7$
2020.9 vw		$\nu_6 + \nu_4$

Infrared	Raman	Assignment
1996.1 w,asy	1995.3 w	$\nu_{10}+\nu_{12}$
1965.4 w		$\nu_3+\nu_8$
	1958.4 w	$2\nu_4$
1906.0 w		$2\nu_8$ (C_2H_3D)?
1881.0 w		$\nu_6+\nu_7$
1868.6 vw		$\nu_3+\nu_{10}$
1831.5 s,asy		$\nu_4+\nu_7$
	1749.9 w	$\nu_4+\nu_8$
1700.4 vw		$2\nu_7$
1695.9 vw		$\nu_6+\nu_{10}$
1692.5 m	1691.7 w	
1685.0 vw		$\nu_4+\nu_{10}$?
1683.1 vw		
1612.1 m,asy		$\nu_7+\nu_8$
1597.8 w	1595.4 m	ν_2 (C_2H_3D)
	1589.3 vw	$2\nu_8$?
1564.0 m,asy	1563.7 vw	ν_2
	1560.3 vs	
	1541.6 w	ν_2 (^{13}C)
1438.0 vw		$\nu_8+\nu_{10}$
1396.8 s	1393.7 m	ν_{12} (C_2H_3D)

Infrared	Raman	Assignment
1386.0 vw		ν_{12} ($\text{H}_2^{12}\text{C}=\text{}^{13}\text{CHD}$)
1338.6 vs		
1335.0 vs		ν_{12}
1331.9 w,sh	1333.8 w	ν_{12} (^{13}C)
	1327.5 m	
	1325.7 m	$2\nu_{10}$
1295.9 m		
1292.2 m		ν_{12} (trans- $\text{C}_2\text{H}_2\text{D}_2$)
1286.1 w	1285.7 m	
1283.4 w	1282.8 m	ν_3 ($\text{C}_2\text{H}_3\text{D}$)
	1280.0 m	ν_3 (trans- $\text{C}_2\text{H}_2\text{D}_2$)
1218.0 w,bd	1219.6 vs	
1205.1 w,sp	1202.0 vs	ν_3
	1124.0	ν_6 ($\text{C}_2\text{H}_3\text{D}$)
1034.0 m,asy	1036.7 m	
	1033.0 m	ν_6
1026.9 w		ν_6 (^{13}C)
1011.1 m		
1003.9 m		ν_4 ($\text{C}_2\text{H}_3\text{D}$)
1001.9 m		ν_4 (trans- $\text{C}_2\text{H}_2\text{D}_2$)
	997.4 vw	?
991.5 m,asy	989.0 sh	
	985.3 s	ν_4
	982.2 s	

Infrared	Raman	Assignment
952.1 s	952.4 w	ν_8 (1,1- $C_2H_2D_2$), ν_8 (C_2H_3D)
887.0 vw		?
874.2 vw		?
849.4 vs 842.8 vs	850.8 vw	ν_7
812.8 m 809.6 m	810.2 vw	ν_7 (C_2H_3D)
766.6 m	761.8 m	ν_8
753.1 vw		ν_7 (1,1- $C_2H_2D_2$)
740.0 vw 735.8 vw		ν_5 (C_2H_2)
731.4 m 724.0 m		ν_7 (trans- $C_2H_2D_2$)
702.0 vw		ν_5 (C_2HD)
687.0 vw 6		?
668.0 vw		ν_{10} (trans- $C_2H_2D_2$)?
663.1 m 660.7		$\nu_{10}({}^{13}C) \} \nu_{10}$
658.4 s		
652.0 vw		?
556.4 w 546.2 w		ν_5 C_2D_2

trans-C₂H₂D₂

Infrared	Raman	Assignment
3140.0 w		$\nu_8 + \nu_{11}$
	3124.1 m	$2\nu_2$
	3121.2 m	
3081.0 vw		ν_9 (C ₂ H ₃ D)?
3052.1 s		ν_9
3048.0 s		
3042.9 w		$2\nu_7 + \nu_2, \nu_9$
	3049.8 w	
	3030.2 s	ν_5
	3026.9 m	
	3025.2 m	
	3020.7 w	ν_5 (¹³ C), $2\nu_7 + \nu_2$
	3013.6 w	$\nu_1 + \nu_7, 2\nu_8 + \nu_3$
	2876.8 w	$2\nu_6 + \nu_8$
2847.0 w		$\nu_2 + \nu_{12}$
	2836.0 w	$\nu_2 + \nu_3$
2562.2 vw		$\nu_2 + \nu_4$
	2553.6 w	$2\nu_3, \nu_2 + \nu_6$
2407.0 m		$2\nu_8 + \nu_{10}$
2402.0 w		
2395.0 w		?

Infrared	Raman	Assignment
2338.0 w		$2\nu_{10} + \nu_4$
	2325.0 w	ν_5 (1,1- $C_2H_2D_2$)
2294.2 m		$\nu_6 + \nu_{12}, \nu_2 + \nu_7$
2284.8 w, sh		
	2271.6 s	ν_1
	2268.9 s	
2265.9 s		ν_{11}
2263.6 sh		
2251.6 w	2252.8 w	$\nu_3 + \nu_4, \nu_3 + \nu_6$
2213.8 s		$\nu_2 + \nu_{10}$
2195.0 w		$\nu_2 + \nu_{10}$ (^{13}C), $3\nu_7$
	1961.8 w	$\nu_{10} + \nu_{12}$
1949.4 bd, asy		$\nu_3 + \nu_{10}$
1905.0 vw		?
1866.8 m		$\nu_6 + \nu_8, ?$
1860.3 w		?
1850.0 s		$\nu_4 + \nu_8$
	1748.2 w	$2\nu_8$
1662.0 w		$\nu_6 + \nu_{10}$
1597.1 m	1598.7 w	ν_2 (C_2H_3D)

Infrared	Raman	Assignment
	1563.8 vw,sh	ν_2
	1562.0 s	
	1541.3 w	ν_2 (^{13}C)
1396.8 m		ν_{12} ($\text{C}_2\text{H}_3\text{D}$)
1373.0 w,sh		?
	1348.9 w	$2\nu_{10}$
1298.0 s		
1296.0 s		ν_{12}
1292.4 s		
1290.6 s		
	1289.5 m	
	1282.3 w	ν_3
	1275.7 s	
	1273.5	ν_3 (^{13}C)
1274.0 w		ν_3 (^{13}C)?
1125.0 w		
1098.0 w		$\nu_4 + \nu_5$ (C_2D_2)-?
1060.0 w		
1006.5 sh		
1004.1 s		ν_4
991.0 s		
985.4 s		
	1005.7 m	
	1002.2 m	ν_6
	995.5 s	

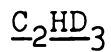
Infrared	Raman	Assignment
952.2 w		ν_8 (1,1- $C_2H_2D_2$), ν_8 (C_2H_3D)
	873.8 s	
	869.7 w	ν_8
	864.6 m	
	859.9 w	ν_8 (^{13}C)
813.0 w		ν_7 (C_2H_3D)
810.9 w		
732.9 s		
725.6 s		ν_7
721.1 s		
687.6 vw		?
671.6 s		
667.8 s		ν_{10}
565.0 w		
556.0 m		ν_5 (C_2D_2), ν_4 (C_2HD)
546.8 m		
<hr/>		
<u>1,1-$C_2H_2D_2$</u>		
	3160.7 sh	
3153.0 m	3151.0 m	$\nu_8 + \nu_{11}$, $2\nu_2$
3080.2 s	3078.3 vs	
3078.4 s		ν_9
3066.4 w	3067.8 vw	ν_9 ($H_2^{13}C=^{12}CD_2$)
3048.0 w	3047.4 w	
3044.8 w	3043.9 w	ν_5 (C_2H_3D)

Infrared	Raman	Assignment
3009.8 w	3011.1	ν_1 (C_2H_3D)
	3000.6 sh	ν_1
2998.9 s	2999.3 vs	
2993.2 w	2993.1 w	ν_1 ($H_2^{13}C=^{12}CD_2$)
2988.3 vw	2989.1 w	$\nu_7+\nu_{11}$
2973.6 vw		ν_{11} (C_2H_4)
2960.2 w	2960.9 w	$\nu_2+\nu_{12}$ (C_2H_3D)
2937.9 m	2938.9	$\nu_2+\nu_{12}$
2928.1 w	2929.2 w	$\nu_2+\nu_{12}$ (^{13}C), $2\nu_8+\nu_3$
2926.6 w		
2897.2 vw		$\nu_{10}+\nu_{12}$
2705.0 w	2706.0 vw	$\nu_2+\nu_6$
2555.8 vw		$\nu_2+\nu_8$
2512.0 vw		$\nu_6+\nu_{12}$
2406.3 vw		$\nu_3+\nu_{12}$
2340.6 w		$\nu_2+\nu_7$
2335.8 w		$\nu_8+\nu_{12}$
2328.1 vw		$2\nu_{10}+\nu_8$
2322.9 s	2322.6 vs	ν_5
2304.0 w	2305.7 w	ν_5 ($H_2^{12}C=^{13}CD_2$)
2276.8 vw		$2\nu_6$

Infrared	Raman	Assignment
2262.1 w 2260.2 w	2261.6 w	ν_{11} (C_2H_3D)
2251.2 m	2252.3 m	$\nu_2 + \nu_{10}$
2216.9 s 2204.8 w	2217.4 vs 2205.5 w	ν_{11} ν_{11} ($H_2^{12}C=^{13}CD_2$)
2066.8 vw	2068.1 vw	$2\nu_3$
2054.0 vw	2054.2 vw	$\nu_{10} + \nu_{12}$
2034.1 vw		$\nu_4 + \nu_6$
1906.8 s, bd		$2\nu_8$
1839.2 m	1838.0 vw	$\nu_4 + \nu_8$
1818.0 m		$\nu_6 + \nu_{10}$
	1748.0 vw	$\nu_3 + \nu_7$
1708.4 vw		$\nu_7 + \nu_8$
1596.9 w	1596.8 m	ν_2 (C_2H_3D)
1592.4 vw		$\nu_4 + \nu_{10}$
1577.9 m 1564.1 w 1552.5 w	1575.9 vs 1564.0 m 1552.4 m	ν_2 ν_2 ($H_2^{12}C=^{13}CD_2$) ν_2 ($H_2^{13}C=^{12}CD_2$)
1505.6 s		$2\nu_7$
1485.2 vw		$2\nu_7$ (^{13}C)
1437.4 m		ν_{12} (C_2H_4), $\nu_7 + \nu_{10}$

Infrared	Raman	Assignment
1396.8 s	1396.6 w	ν_{12} (C_2H_3D)
1379.8	1382.6 s	ν_{12}
	1375.8 vs	
1369.6 s	1371.0 m	ν_{12} ($H_2^{12}C=^{13}CD_2$)
	1368.9 m	$2\nu_{10}$
1335.8 w	1339.2 w	ν_{12} (cis- $C_2H_2D_2$)
1295.0 vw		ν_{12} (trans- $C_2H_2D_2$)
1291.6 vw		
1285.0 m	1285.5 m	ν_3 (C_2H_3D)
1282.8 m	1283.1 m	
1139.0 vw	1142.4 w	ν_6
	1138.2 w	
1024.9 s, bd	1029.1 vs	ν_3
	1017.5 vs	
1010.2 s		ν_4 (C_2H_3D)
1002.9 s		
989.6 w		ν_4 (trans- $C_2H_2D_2$)
946.0 vs, asy	955.3 sh	ν_8 ($H_2^{12}C=^{13}CD_2$) } ν_8
	951.5 sh	
	947.7 s	
921.9 w		?
905.4 vs		ν_4
901.6 vs		

Infrared	Raman	Assignment
852.4 m		ν_7 (cis-C ₂ H ₂ D ₂)
813.2 m	810.4 vw	ν_7 (C ₂ H ₃ D)
810.0 m		
753.5 vs	752.8 s,asy	ν_7
749.1 vs		
742.8 s		ν_7 (H ₂ ¹² C= ¹³ CD ₂)
730.9 vw		ν_{10} (C ₂ H ₃ D)
729.5 vw		
724.0 vw		ν_7 (trans-C ₂ H ₂ D ₂)
705.6 w		ν_5 (C ₂ HD)
701.6 w		
688.5 vw		?
685.1 m		
682.6 w		ν_{10} (H ₂ ¹³ C= ¹² CD ₂)
680.1 s		} ν_{10}
660.4 vw		ν_{10} (cis-C ₂ H ₂ D ₂)
656.2 vw		?
597.8 w		?
556.0 vw		
546.0 w		ν_5 (C ₂ D ₂) + ν_4 (C ₂ HD)
531.8 vw		
523.5 vw		



Infrared	Raman	Assignment
3205.0 vw		$\nu_6 + \nu_{11}$
3198.0 w		$\nu_1 + \nu_8$
3085.9 w	3088.4 m	$2\nu_2$
3081.8 s	3083.8 s	
3073.1 m	3076.0 s	$\nu_4 + \nu_5$
3068.2 m	3071.3 m	
3059.0 w	3060.9 vw	$\nu_5 + \nu_6$
3051.9 w		ν_9 (trans- $C_2H_2D_2$)
3046.9 vw		
3043.0 vw		ν_9 (cis- $C_2H_2D_2$)
3035.8 s	3036.6 s	ν_9
3032.1 s	3032.7 s	
2999.7 w		$\nu_1 + \nu_7, \nu_1$ (1,1- $C_2H_2D_2$)
2344.0 vw		$2\nu_7 + \nu_8$
2340.4 m		$\nu_3 + \nu_{12}$
2338.1 m		
2328.1 m		ν_9 (C_2D_4)
2320.2 s	2319.2 s	ν_5 ν_5 (HD $^{12}C=^{13}CD_2$)
2304.0 w	2303.1 w	
	2293.6 vw	$\nu_6 + \nu_{12}$
2285.8 vw	2287.0 vw	ν_1 (cis- $C_2H_2D_2$)

Infrared	Raman	Assignment
2269.2 s	2269.6 s	
2266.3 s	2266.3 s	ν_1
2255.5 vw	2255.3 w	ν_1 (HD ¹³ C= ¹² CD ₂)
	2247.6 m	$2\nu_{10}+\nu_6$
2241.5 vw	2242.6 vw	ν_{11} (cis-C ₂ H ₂ D ₂)
2216.6 w	2217.5 w	ν_{11} (1,1-C ₂ H ₂ D ₂), $\nu_8+\nu_{12}$
2210.1 vs	2211.4 s	ν_{11}
2199.0 w	2201.4 w	ν_{11} (HD ¹² C= ¹³ CD ₂)
2188.2 w		ν_{11} (C ₂ D ₄)
	2167.2 vw	$\nu_2+\nu_{10}$
2153.1 vw		$3\nu_7$
1916.0 w	1917.9 vw	$\nu_6+\nu_8$
1907.1 vw		$\nu_3+\nu_4$ (1,1-C ₂ H ₂ D ₂)
1890.8 vw		$3\nu_{10}$
1858.5 m		$2\nu_8$
1855.2 m		
1850.0 m		$\nu_8+\nu_4$ (trans-C ₂ H ₂ D ₂)
1836.8 s		$\nu_3+\nu_4$
1700.0 vw		$\nu_6+\nu_7$
1695.8 vw		

Infrared	Raman	Assignment
1688.2 vw		$\nu_4 + \nu_8$
1684.8 vw		
1663.0 m		$\nu_7 + \nu_8$
1657.0 m		
1635.9 vw		$\nu_7 + \nu_8$ (^{13}C)?
1623.9 sh		$\nu_6 + \nu_{10}$
1618.8 w		
	1582.2 vw	?
1578.4 w		ν_2 (1,1- $\text{C}_2\text{H}_2\text{D}_2$)
1543.3 vw	1546.1 s	ν_2
1542.6 w	1542.8 s	
1531.0 s	1530.8 m	$2\nu_4$
1527.6 m	1527.5 m	
	1522.8 vw	ν_2 (C_2D_4), $\nu_4 + \nu_7$
	1514.0 sh	
	1512.2 m	
1499.1 m		$2\nu_7$
1491.1 m		
1378.6 m	1381.3 w	ν_{12} (1,1- $\text{C}_2\text{H}_2\text{D}_2$)
1368.4 vw		$2\nu_{10}$ (1,1- $\text{C}_2\text{H}_2\text{D}_2$)
1336.1 m		ν_{12} (cis- $\text{C}_2\text{H}_2\text{D}_2$)
1295.1 m		ν_{12} (trans- $\text{C}_2\text{H}_2\text{D}_2$)
1292.2 m		
	1293.0 m	?

Infrared	Raman	Assignment
1286.0 vs	1287.1 s	ν_{12}
1283.0 vs	1284.3 s	
1277.5 w,sh		ν_{12} (^{13}C)?
1275.5 w		
1258.0 m	1262.6 vw	$2\nu_{10}$
	1217.5 vw	ν_3 (cis- $\text{C}_2\text{H}_2\text{D}_2$)
1073.0 m		ν_{12} (C_2D_4)
	1046.6 s	
	1041.4 s	ν_3
1039.2 vs	1039.8 s	
1032.8 w		ν_3 ($\text{HD}^{13}\text{C}=\text{}^{12}\text{CD}_2$)
1002.8 w	1002.4 m	
993.2 w,asy	996.5 w	ν_6
989.5 w,sp	991.5 s	
	982.3 vw	ν_3 (C_2D_4)
952.2 m	954.1 vw	ν_8 (1,1- $\text{C}_2\text{H}_2\text{D}_2$), ν_8 ($\text{C}_2\text{H}_3\text{D}$)
932.0 vs	933.3 m	
921.2 vs	923.4 sh	ν_8
	921.4 s	
916.1 w,sh		ν_8 ($\text{HD}^{13}\text{C}=\text{}^{12}\text{CD}_2$)
852.4 m		ν_7 (cis- $\text{C}_2\text{H}_2\text{D}_2$)
	781.9 vw	ν_8 (C_2D_4)
767.6 vs	769.5 sh	ν_4
	765.9 s	

Infrared	Raman	Assignment
754.4 m		ν_7 (1,1-C ₂ H ₂ D ₂)
735.3 s		
724.8 s		ν_7
720.8 s		
660.8 vw		ν_{10} (cis-C ₂ H ₂ D ₂)
628.8 w	627.5 w	
626.8 w		ν_{10}
624.6 s		

APPENDIX B

Hoshen and Jortner have applied the coherent potential approximation to the electronic states of substitutionally disordered molecular crystals.^{62,63} The following discussion follows their treatment.

The following assumptions are made for the binary mixed crystal:

Assumption (1). The sites of the perfect empty lattice are substituted by the two components without any change in molecular orientation.

Assumption (2). The tight-binding limit applies for the description of the excited states of the crystal; that is the excitations are localized.

Assumption (3). Crystal field mixing effects between different states of the crystal are negligible.

Assumption (4). The environmental shift terms, D^f , for the two components are equal and concentration independent.

Assumption (5). The intermolecular transfer matrix elements are invariant under isotopic substitution. (The $L_{\alpha\alpha}^f(\vec{k})$'s).

Assumption (6). The two components differ by only their gas-phase excitation energies and are characterized

by the same wave-functions.

Assumption (7). Molecule-Molecule spatial correlations are neglected. The properties of a configurationally averaged system are considered.

The Hamiltonian of the mixed crystal is written as:

$$H = H_0 + H_1, \quad (\text{B-1})$$

where

$$H_0 = \sum_n \sum_\alpha |n\alpha\rangle \bar{\epsilon} \langle n\alpha| + J. \quad (\text{B-2})$$

H_0 is the virtual crystal Hamiltonian, where the excitation energy, $\bar{\epsilon}$, is a weighted mean of the excitation energies of the pure crystals:

$$\bar{\epsilon} = C_A (\Delta\epsilon_A^f + D^f) + C_B (\Delta\epsilon_B^f + D^f) \equiv C_A \epsilon_A + C_B \epsilon_B. \quad (\text{B-3})$$

Here C_A and C_B are the concentrations of components A and B, which have gas-phase excitation energies $\Delta\epsilon_A^f$ and $\Delta\epsilon_B^f$, respectively. n and α designate the unit cell and the molecule in the unit cell, respectively, and the $|n\alpha\rangle$ represent the wave functions in the tight-binding limit. J accounts for the intermolecular excitation transfer.

H_1 expresses the deviation of the crystal from the

virtual crystal as follows:

$$H_1 = \Delta \sum_n \sum_{\alpha} |n\alpha\rangle \xi_{n\alpha} \langle n\alpha|. \quad (\text{B-4})$$

$\xi_{n\alpha}$ is a random variable that equals $-C_A$ when site $n\alpha$ is occupied by component B, and equals C_B when site $n\alpha$ is occupied by component A, if Δ is defined as follows:

$$\Delta = \epsilon_A - \epsilon_B. \quad (\text{B-5})$$

The pertinent physical information (spectroscopic information) is contained in the Green's function:

$$G(z) = 1/(z-H). \quad (\text{B-6})$$

Now, theoretically one should solve the problem for a fixed configuration of the crystal and then average over all possible configurations. However, this is mathematically unmanageable. Therefore assuming molecule-molecule spatial correlations can be neglected, the physical properties of the mixed crystal can be described by the configurationally averaged Green's function:

$$\langle G(z) \rangle = \langle 1/(z-H) \rangle = 1/(z-H_{\text{eff}}(z)) \quad (\text{B-7})$$

The above equation defines an effective Hamiltonian,

H_{eff} , which characterizes the properties of the configurationally-averaged crystal. The effective Hamiltonian can be expressed in terms of the virtual crystal Hamiltonian and the complex self energy, $\Sigma(z)$, with respect to the virtual crystal:

$$H_{\text{eff}}(z) = H_0 + \Sigma(z). \quad (\text{B-8})$$

$\Sigma(z)$ expresses the deviation of the mixed crystal from the virtual crystal; it describes the shift and broadening of the states of the virtual crystal. The poles of $(z - H_{\text{eff}}(z))^{-1}$ determine the widths and positions of the configurationally averaged crystal states.

It is now assumed that the local nature of the self-energy operator can be approximated as:

$$\langle n\alpha | \hat{\Sigma}(z) | m\beta \rangle = \sigma_\alpha(z) \delta_{nm} \delta_{\alpha\beta}, \quad (\text{B-9})$$

where $\sigma_\alpha(z)$ is the self-energy at site α . If the sites are interchange equivalent,

$$\sigma_\alpha(z) = \sigma(z) \quad (\text{B-10})$$

for all α .

V expresses the generalized perturbation resulting from the deviation of the mixed crystal from its

configurational averaged behavior as follows:

$$V = H-H_{\text{eff}} = \sum_{n\alpha} V_{n\alpha}, \quad (\text{B-11})$$

where the $V_{n\alpha}$ are the local perturbations. Excitation scattering due to this deviation can be expressed as:

$$T = V + V\langle G(z)\rangle T, \quad (\text{B-12})$$

and the relation between the mixed crystal Green's function $G(z)$ and the configurationally averaged Green's function $\langle G(z)\rangle$ is given by:

$$G(z) = \langle G(z)\rangle + \langle G(z)\rangle T \langle G(z)\rangle. \quad (\text{B-13})$$

The exact condition for ignoring molecule-molecule spatial correlations is:

$$\langle T(z)\rangle = 0. \quad (\text{B-14})$$

This makes the coherent potential approximation self-consistent. If multiple scattering contributions to T can be neglected then Equation (B-14) can be approximated by:

$$\langle t_{n\alpha}(z)\rangle = 0, \quad (\text{B-15})$$

where $t_{n\alpha}$ is a molecular scattering matrix associated with site $n\alpha$, given by:

$$t_{n\alpha} = (1 - V_{n\alpha}(z)) \langle G(z) \rangle^{-1} V_{n\alpha}(z). \quad (\text{B-16})$$

Thus, for a binary mixed crystal,

$$\begin{aligned} C_A t_A + C_B t_B &= C_A (1 - V_A \langle G(z) \rangle)^{-1} V_A \\ &+ C_B (1 - V_B \langle G(z) \rangle)^{-1} V_B = 0, \end{aligned} \quad (\text{B-17})$$

where

$$V_A = (\Delta C_A - \sigma) |n\alpha\rangle \langle n\alpha|$$

and

$$V_B = (-\Delta C_B - \sigma) |n\alpha\rangle \langle n\alpha|;$$

(B-18)

This development leads to the relation,

$$C_A V_A + C_B V_B = V_A \langle G \rangle V_B. \quad (\text{B-19})$$

Therefore,

$$\sigma(z) = (\Delta C_B - \sigma(z)) f^0(z - \bar{\epsilon} - \sigma(z)) (\Delta C_A + \sigma(z)), \quad (\text{B-20})$$

where $f(z)$ is a complex function such that the density of

states is given as follows:

$$\rho(E) = \pi^{-1} \text{Im}f(E-i0^{-1}), \quad (\text{B-21})$$

$f(z)$ is given by:

$$f(z) = (N\sigma_p)^{-1} \text{Tr}\langle G(z) \rangle = \int_{-\infty}^{\infty} \frac{dE'}{z-E'} \rho(E'). \quad (\text{B-22})$$

The superscript zero in Equation (B-20) indicates the complex function is related to the pure crystal density of states.

The spectral density, which can be considered to express the \underline{k} components of the density of states and thus is intimately connected to the optical properties of the crystals, may be expressed as:

$$S(\underline{k}, j, E) = \pi^{-1} \text{Im}\langle \underline{k}, j | G(E-i0^+) | \underline{k}, j \rangle, \quad (\text{B-23})$$

where j labels the Davydov components. In terms of the self-energy, $\sigma(z)$, the spectral density becomes:

$$S(\underline{k}, j, E) = (\pi^{-1}) \frac{\text{Im}\sigma(E-i0^+)}{[E-\bar{\epsilon}-t_j-\text{Re}\sigma(E-i0^+)]^2 + [\text{Im}\sigma(E-i0^+)]^2}, \quad (\text{B-24})$$

where t_j is the energy of the j^{th} Davydov component of the pure crystal.

A plot of $S(0, j, E)$ versus E reveals the absorption

pattern for the band of the binary-mixed crystal.

The CPA is attractive because it does not have the limitations of the virtual crystal approximation and the average T-matrix approximation, and it requires a knowledge of only the pure crystal density of states function and the position of the Davydov components of the pure crystal in order to calculate the mixed-crystal spectrum.

APPENDIX C

The following is a listing of program MIX:

```

PROGRAM MIX(INPUT,OUTPUT,TAPE5=INPUT,TAPE6=OUTPUT)
REAL INCR, IMSIG
DATA D/1H,1H+,1HO/
1000 FORMAT(7F10.2)
11  FORMAT('1CA=', F5.2,5X,'DEL=',F10.1,5X,'T='F10.1/'0')
1   READ(5,1000)CA,T,DEL,Z1,ZN,INCR,EPS
    IF(EOF(5)) 2000,2
2   WRITE(6,11)CA,DEL,T
    X=1./3.
    I=0
    CB=1.0-CA
    P1=T**2+(CA*DEL)**2-4.*CA*CB*DEL**2
    Q1=CA*CB*(CB-CA)*(DEL**3)*2.
    R1=(CA*CB*(DEL**2))**2
10  P2=2*(Z1+CA*DEL)
    IF(P2.EQ.0.) GO TO 5
    P=(P1-Z1**2-2*Z1*CB*DEL)/P2
    Q=Q1/P2
    R=R1/P2
    A=(3.*Q-P**2)/3.
    B=(2.*(P**3)-9.*P*Q+27.*R)/27.
    CK=B*B/4.+(A**3)/27.
    IF(CK.GT.0.0)GO TO 100
5   I = I+1
    E(I)=Z1
    SPEC(I)=0.0
    Z1=Z1+INCR
    IF(Z1.GT.ZN) GO TO 201
    GO TO 10

```

```
100  A1=-B/2.+SQRT(CK)
      B1=-B/2.-SQRT(CK)
      IF(A1.LT.0.)AA=-(ABS(A1)**X)
      IF(B1.LT.0.)BB=-(ABS(B1)**X)
      IF(A1.GT.0.)AA=A1**X
      IF(B1.GT.0.)BB=B1**X
      IF(A1.EQ.0.)AA=0.
      IF(B1.EQ.0.)BB=0.
      RESIG=0(AA+BB)/2.-P/3.
      IMSIG=ABS((AA-BB)*1.73205/2.)
      I=I+1
      ALPHAXX=IMSIG/((Z1-EPS-T-RESIG)**2+IMSIG**2)/3.14159
      BETAXXX=IMSIG/((Z1-EPS+T-RESIG)**2+IMSIG**2)/3.14159
      SPEC(I)=ALPHAXX+BETAXXX
      F(I)=Z1
      IF(I.GE.1000) GO TO 101
      Z1=Z1+INCR
      GO TO 10
50   FORMAT ('E=',F10.1,5X,'SPECTRAL DENSITY=',E10.3)
201  IF(I.EQ.0) GO TO 1
101  DO 51 J=1,I
      WRITE (6,50)E(J),SPEC(J)
51   CONTINUE
      EMIN=E(1)
      YMAX=SPEC(1)
      DO 3 J=2,I
      IF(SPEC(J).LT.YMAX) GO TO 3
      YMAX=SPEC(J)
3    CONTINUE
      WRITE (6,104)YMAX
104  FORMAT(19H1 THE MAX Y VALUE IS, 2X,E15.7//)
      DO 52 J=1,I
      DO 4 KK=1,121
4    YP(KK)=D(1)
      YP(1)=D(2)
```

```
YC=(SPEC(J)/YMAX)*120.+5
NC=IFIX(YC)
NP=NC+1
YP(NP)=D(3)
WRITE (6,105) E(J), (YP(K),K=1,121)
105  FORMAT (1H,F6.2,2X,121A1)
52   CONTINUE
     GO TO 1
2000 STOP
     END
```

REFERENCES

REFERENCES

1. G. Turrell, Infrared and Raman Spectra of Crystals, (Academic Press, New York, 1972).
2. P. M. A. Sherwood, The Vibrational Spectroscopy of Solids, (Cambridge University Press, Cambridge, 1972).
3. M. M. Sushchinskii, Raman Spectra of Molecules and Crystals, (Israel Program for Scientific Translations, New York, 1972).
4. D. F. Hornig, J. Chem. Phys. 16, 1063 (1948).
5. H. Winston and R. S. Halford, J. Chem. Phys. 17, 607 (1949).
6. D. A. Dows, J. Chem. Phys. 36, 2836 (1962).
7. D. A. Dows, Physics and Chemistry of the Organic Solid State, Vol. I, Ed. D. Fox, M. M. Labes and A. Weissberger, (Interscience, New York, 1963).
8. O. Schnepp, Advances in Atomic and Molecular Physics, Vol. 5, Ed. D. R. Bates and I. Estermann, (Academic Press, New York, 1969).
9. R. T. Bailey, Transfer and Storage of Energy by Molecules, Vol. 4, Ed. G. M. Burnett, A. M. North and J. N. Sherwood, (Wiley-Interscience, New York, 1974).
10. G. S. Pawley, Transfer and Storage of Energy by Molecules, Vol. 4, Ed. G. M. Burnett, A. M. North and J. N. Sherwood, (Wiley-Interscience, New York, 1974).
11. O. Schwepp and N. Jacobi, Dynamical Properties of Solids, Vol. 2, Ed. G. K. Horton and A. A. Maradudin, (North-Holland Publishing Company, Amsterdam, 1975).
12. M. Ito, T. Yokoyama and M. Suzuki, Spectrochim. Acta 26A, 695 (1970).
13. G. R. Elliott and G. E. Leroi, J. Chem. Phys. 59, 1217 (1973).
14. S. B. Tejada and D. E. Eggers, Jr., Spectrochim. Acta 32A, 1557 (1976).

15. E. R. Bernstein, S. D. Colson, R. Kopelman and G. W. Robinson, *J. Chem. Phys.* 48, 5596 (1968).
16. N. Rich and D. A. Dows, *Mol. Crystals, Liquid Crystals* 5, 111 (1968).
17. D. A. Dows, *J. Chem. Phys.* 36, 2833 (1962).
18. M. Brith and A. Ron, *J. Chem. Phys.* 50, 3053 (1969).
19. Y. A. Schwartz, A. Ron and S. Kimel, *J. Chem. Phys.* 54, 99 (1971)
20. S. M. Blumenfeld, S. P. Reddy and H. L. Welsh, *Can. J. Phys.* 48, 513 (1970).
21. G. J. H. vanNes and A. Vos, *Acta Cryst.* B33, 1653 (1977).
22. W. Press and J. Eckert, *J. Chem. Phys.* 65, 4362 (1976).
23. F. A. S. Ligthart, Thesis, University of Amsterdam (1975).
24. J. L. Duncan, D. C. McKean and P. D. Mallinson, *J. Mol. Spectrosc.* 45, 221 (1973).
25. E. R. Bernstein and G. W. Robinson, *J. Chem. Phys.* 49, 4962 (1968).
26. E. R. Bernstein, *J. Chem. Phys.* 50, 4842 (1969).
27. E. R. Bernstein, *J. Chem. Phys.* 52, 4701 (1970).
28. S. Bhagavantam and T. Venkatarayudu, Theory of Groups and its Application to Physical Problems, (Academic Press, New York, 1969).
29. W. G. Fateley, N. T. McDevitt and F. F. Bentley, *Appl. Spectrosc.* 25, 155 (1971).
30. J. L. Duncan, *Mol. Phys.* 28, 1177 (1974).
31. C. W. Bunn, *Trans. Faraday Soc.* 40, 23 (1944).
32. G. Taddei, H. Bonadeo, M. P. Marzocchi and S. Califano, *J. Chem. Phys.* 58, 966 (1973).
33. R. Kopelman, Excited States, Vol. 2, Ed. E. C. Lim, (Academic Press, New York, 1975).

34. A. S. Davydov, Theory of Molecular Excitons, (Plenum Press, New York, 1971).
35. N. Neto, G. Taddei, S. Califano and S. H. Walmsley, *Mol. Phys.* 31, 457 (1976).
36. N. Neto, G. Taddei, S. Califano and S. H. Walmsley, in Molecular Spectroscopy of Dense Phase, (Elsevier, New York, 1975).
37. R. Kopelman, *J. Chem. Phys.* 47, 2631 (1967).
38. I. M. Lifshitz, *J. Phys. USSR* 7, 215, 249 (1948),
8, 89 (1944).
39. R. J. Elliott, J. A. Krumhansl and P. L. Leath, *Rev. Mod. Phys.* 46, 465 (1974).
40. A. S. Baker, Jr. and A. J. Sievers, *Rev. Mod. Phys.* 47, 52 (1975).
41. P. N. Prasad and R. Kopelman, *J. Chem. Phys.* 57, 863 (1972).
42. P. N. Prasad and R. Kopelman, *J. Chem. Phys.* 58, 126 (1973).
43. H. K. Hong and R. Kopelman, *J. Chem. Phys.* 58, 384 (1973).
44. Y. Onodera and Y. Toyozawa, *J. Phys. Soc. Japan* 24, 341 (1968).
45. B. Velicky, S. Kirkpatrick and H. Ehrenreich, *Phys. Rev.* 175, 747 (1968).
46. J. C. Bellows and P. N. Prasad, *J. Chem. Phys.* 66, 625 (1977).
47. H. K. Hong and R. Kopelman, *J. Chem. Phys.* 58, 2557 (1973).
48. D. Hall and D. E. Williams, *Acta Cryst.* A31, 56 (1975).
49. D. E. Williams, *J. Chem. Phys.* 45, 3770 (1966).
50. D. E. Williams, *J. Chem. Phys.* 47, 4680 (1967).
51. A. I. Kitaigorodsky, *J. Chim. Phys.* 63, 6 (1966).
52. D. E. Williams, *Trans. Amer. Cryst. Assoc.* 6, 21 (1970).

53. G. Herzberg, Molecular Spectra and Molecular Structure, Vol. 2 (VanNostrand Reinhold Company, New York, 1945).
54. J. L. Duncan, private communication.
55. E. B. Wilson, J. C. Decius, and P. C. Cross, Molecular Vibrations, (McGraw-Hill Book Company, Inc., New York, 1955).
56. P. N. Prasad and R. Kopelman, J. Chem. Phys. 57, 856 (1972).
57. G. N. Zhizhin, M. A. Moskaleva and E. B. Perminov, Opt. Spectrosc. 30, 562 (1971).
58. M. A. Moskaleva and G. N. Zhizhin, Opt. Spectrosc. 36, 535 (1974).
59. G. N. Zhizhin and M. A. Moskaleva, Opt. Spectrosc. 37, 52 (1974).
60. H. K. Hong and G. W. Robinson, J. Chem. Phys. 52, 825 (1970).
61. H. K. Hong and G. W. Robinson, J. Chem. Phys. 54, 1369 (1971).
62. J. Hoshen and J. Jortner, J. Chem. Phys. 56, 933 (1972).
63. J. Hoshen and J. Jortner, J. Chem. Phys. 56, 5550 (1972).
64. R. J. Elliott and D. W. Taylor, Proc. Roy. Soc. (London) A296, 161 (1967).
65. P. Soven, Phys. Rev. 156, 809 (1967).
66. D. W. Taylor, Phys. Rev. 156, 1017 (1967).
67. L. Schwartz, F. Brovers, A. V. Vedyayev and H. Ehrenreich, Phys. Rev. B4, 3383 (1971).
68. S. D. Woodruff and R. Kopelman, private communication.
69. T. Shimanouchi, Computer Programs for Normal Coordinate Treatment of Polyatomic Molecules, Tokyo: Univ. of Tokyo (1968).
70. K. Kuchitsu, T. Oka and Y. Morino, J. Mol. Spectrosc. 15, 51 (1965).
71. R. L. Arnett and B. L. Crawford, Jr., J. Chem. Phys. 18, 118 (1950).



MICHIGAN STATE UNIVERSITY LIBRARIES



3 1293 03178 5706